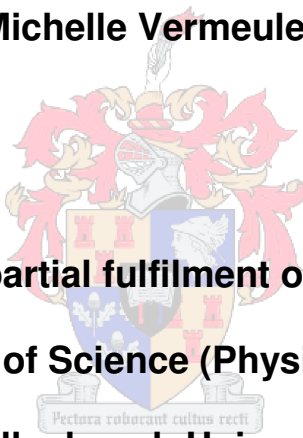


**The role of MKP-1 in autophagy,
apoptosis and necrosis during
ischaemia/reperfusion injury in the heart**

By

Michelle Vermeulen



**Thesis presented in partial fulfilment of the requirements for
the degree of Master of Science (Physiological Sciences) at
Stellenbosch University**

Supervisor: Prof Anna-Mart Engelbrecht

Co-supervisors: Prof Amanda Lochner and Dr Ben Loos

December 2010

Declaration

By submitting this thesis, I declare that the entirety of the work contained therein is my own, original work, that I am the owner of the copyright thereof (unless to the extent explicitly otherwise stated) and that I have not previously in its entirety or in part submitted it for obtaining any qualification.

Signature

Date

ABSTRACT

Introduction:

Ischaemic heart disease is a leading cause of death worldwide and is also largely contributing to deaths in Africa. Better treatment or even prevention of ischaemia/reperfusion injury in the heart, necessitates a better understanding of the molecular pathways and mechanisms of cell death. Three types of cell death can occur in the diseased myocardium. Type I, better known as apoptotic cell death, is characterised by cell shrinkage and chromatin condensation, type II, known as autophagic cell death, is characterised by intracellular accumulation of double membranes vacuoles and type III, necrotic cell death, is characterised by cellular swelling and loss of membrane integrity. Many signaling pathways are activated during ischaemia/reperfusion injury which include the mitogen activated protein kinases (MAPKs), such as extracellular signal-regulated protein kinase (ERK), c-Jun NH₂-terminal protein kinase (JNK) and p38 MAPK. These kinases are dephosphorylated by appropriate phosphatases. MAPK phosphatase-1 (MKP-1), a dual specificity phosphatase, inactivates the MAPKs by dephosphorylating specific Thr/Tyr residues. Upregulation of MKP-1 during ischaemia/reperfusion injury has been shown to be cardioprotective, however no knowledge regarding a role of MKP-1 in autophagy exists. Therefore the aim of this study is to investigate the role of MKP-1 in autophagy, apoptosis and necrosis during simulated ischaemia/reperfusion injury in the heart.

Methods:

H9C2 cells (rat cardiomyocytes) were cultured under standard conditions. Upon reaching 75-80% confluency, cells were treated for 30 min during normoxic conditions with dexamethasone, to induce MKP-1 expression, or sanguinarine, to inhibit MKP-1 induction. Thereafter, they were exposed to 3 hrs simulated ischaemia (induced by an ischaemic buffer and 5% CO₂/1% O₂) in the presence of the above mentioned treatments. Cells were then allowed to reperfuse for 30 min in the presence of dexamethasone or sanguinarine. Samples were analysed after simulated ischaemia and after reperfusion. Cell viability was measured by MTT assay. Propidium iodide and Hoechst staining were used to assess morphological markers of apoptosis and necrosis. LDH release during reperfusion was assessed as indicator of necrotic cell death. LysoTracker[®]Red was used to visualise the autophagic flux occurring during ischaemia/reperfusion in the cell. Flow cytometry was used to quantify cells stained with acridine orange as indicator for autophagy. Autophagic and apoptotic protein markers as well as MAPK and MKP-1 activity were analysed by Western Blotting.

Results and discussion:

Our results indicate a clear relationship between MKP-1 induction, autophagy and cell survival during simulated ischaemia/reperfusion (SI/R). MKP-1 inhibition during SI/R resulted in decreased autophagy activity accompanied by significant apoptotic and necrotic cell death. Increased

MKP-1 induction, on the other hand, during SI/R resulted in increased levels of autophagy activity and subsequent attenuation of apoptotic and necrotic cell death. p38 MAPK phosphorylation was significantly higher while MKP-1 was inhibited and significantly lower while MKP-1 was induced. This strongly indicates that upregulation of MKP-1, known to attenuate ischaemia/reperfusion injury, has an important role in cell survival during ischaemia/reperfusion injury in the heart, through its involvement in the regulation of autophagic activity as a stress response against apoptotic or necrotic cell death.

OPSOMMING

Inleiding:

Iskemiese hartsiekte is een van die grootste oorsake van sterftes wêreldwyd en dra ook beduidend by tot sterftes in Afrika. Om iskemiese hartsiektes te behandel of selfs te voorkom, is 'n goeie begrip van die molekulêre paaie wat betrokke is tydens iskemie/herperfusie, noodsaaklik. Drie tipes seldood kom tydens patologiese toestande in die hart voor. Tipe I, ook bekend as apoptotiese seldood, word gekenmerk deur selkrimpings en kromatien kondensasie, tipe II, ook bekend as autofagiese seldood word gekenmerk deur intrasellulêre opeenhoping van dubbelmembraan vakuole en tipe III, bekend as nekrotiese seldood, word deur sellulêre swelling en verlies van membraan integriteit gekenmerk. Iskemie/herperfusie lei tot die aktivering van seintransduksiepaaie wat die MAPKs, soos p38, ERK en JNK insluit. Hierdie kinases word deur die gepaste fosfatases gedefosforileer. MKP-1, 'n dubbele spesifieke fosfatase, deaktiveer MAPKs deur hul Thr/Tyr eenhede te defosforileer. Alhoewel daar al voorheen getoon is dat verhoogte MKP-1 'n beskermende funksie in die hart tydens iskemie/herperfusie het, is daar nog geen bewyse vir 'n rol van MKP-1 tydens autofagie nie. Die doel van hierdie studie is dus om die rol van MKP-1 in autofagie, apoptose en nekrose te ondersoek tydens gesimuleerde iskemie/herperfusie in die hart.

Metodes:

H9C2 selle (rot ventrikulêre hartselle) is onder standaard toestande gekweek. Wanneer die selle 75-80% konfluensie bereik het, is dit behandel met dexametasone of sanguinarine onder standaard toestande vir 30 min. Daarna is selle blootgestel aan 3 ure iskemie, in die teenwoordigheid van dexametasone of sanguinarine. Selle is dan toegelaat om vir 30 min te herperfuseer, weer in die teenwoordigheid van dexametasone of sanguinarine. Monsters is na iskemie en herperfusie geneem vir analise. Selvatbaarheid is gekwantifiseer deur 'n MTT bepaling. Morfologiese merkers van seldood is bepaal met behulp van propidium iodide en Hoechst kleuringsmetodes. Laktaatdehidrogenase (LDH) vrystelling tydens herperfusie is as merker van nekrose gebruik. Autofagie is gevisualiseer deur gebruik te maak van LysoTracker[®]Red kleuring tydens iskemie en herperfusie. Akridienoranje is gebruik om suur kompartemente te kleur. Vloesitometrie is as kwantifiseringstegniek vir autofagie gebruik. Western Blotting is gebruik om uitdrukking van merkerproteïene van autofagie en apoptose sowel as MAPK en MKP-1 aktiwiteit tydens iskemie/reperfusie te bepaal.

Resultate en bespreking:

Ons resultate toon 'n verband tussen MKP-1 induksie, autofagie en seloorlewing gedurende gesimuleerde iskemie/herperfusie (SI/R) aan. MKP-1 inhibisie gedurende SI/R het tot 'n afname in autofagie gelei tesame met 'n

beduidende toename in apoptotiese en nekrotiese seldood. Verhoogde MKP-1 induksie gedurende SI/R, daarteenoor, het autofagiese aktiwiteit verhoog, gepaardgaande met 'n verlaging in apoptose en nekrose. p38 MAPK fosforilasie was beduidend hoër tydens MKP-1 inhibisie en laer met MKP-1 induksie. Hierdie resultate toon dat MKP-1 'n belangrike rol in seloorlewing speel tydens iskemie/herperfusiesskade in die hart, deur sy deelname in die regulering van autofagiese aktiwiteit as 'n stres reaksie teen apoptotiese en nekrotiese seldood.

ZUSAMMENFASSUNG

Einführung

Die ischämisch bedingte Herzkrankheit stellt weltweit eine der Haupttodesursachen dar und trägt zunehmend zur Mortalität in Südafrika bei. Um verbesserte Behandlungsmethoden zu erreichen und eine Ischämie/Reperfusionsschädigung des Gewebes zu verhindern, ist ein umfangreiches Verständnis der molekularen Signalpfadwege und des Zelltodmechanismus erforderlich. Drei verschiedene Arten von Zelltod werden im erkrankten Myokard unterschieden. Dies sind Typ I Apoptose, gekennzeichnet durch Zellschrumpfung und Chromatinverdichtung, Typ II Autophagie, charakterisiert durch die Bildung von Autophagosomen und Typ III, Nekrose, gekennzeichnet durch den Verlust der Zellmembranintegrität. Zelltod mit Autophagie, Apoptose und Nekrose sind vor allem in die Ischämie/Reperfusionsschädigung involviert. Mehrere Signalpfadwege sind während dieses Vorgangs aktiviert und induzieren die Mitogen-aktivierten Proteinkinasen (MAPKs), wie zum Beispiel die extrazellulär signal-regulierte Proteinkinase (ERK), die c-Jun-Nh2-terminale Proteinkinase (JNK) und die p38-MAPK. Diese Kinasen werden durch entsprechende Phosphatasen dephosphoryliert. Die MAPK-Phosphatase-I-(MKP-I), eine dualspezifische Phosphatase, inaktiviert MAPKs durch spezifische Dephosphorylierung von Thr/Tyr-Abschnitten. Eine Erhöhung der MKP-I-Aktivität während Ischämie-Reperfusionsschädigung hat eine schützende Wirkung auf das Herz, jedoch ist das gegenwärtige Wissen über die Rolle von MKP-I in der Autophagie limitiert. Ziel dieser Studie ist daher, die Rolle von MKP-I in Autophagie,

Apoptose und Nekrose im Zusammenhang mit Ischämie/Reperfusionverletzung des Myokards zu erforschen.

Methodik

H9c-2-Herzmyoblastzellen wurden in Dulbecco's Modified Eagle's Medium (DMEM) und 10% fötalem bovinem Serum (FBS) unter 5 % CO₂ inkubiert. Bei Erreichen einer Konfluenz von 75% - 80% wurden die Zellen unter sauerstoffreichen Bedingungen entweder für 30 Minuten mit Dexamethasone behandelt, um MKP-1 zu induzieren, oder mit Sanguinarine, um MKP-1 zu hemmen. Im Anschluss wurden die Zellen einer dreistündigen simulierten Ischämie unter Anwesenheit von Dexamethasone und Sanguinarine ausgesetzt. Die Proben wurden je nach der Ischämie- und nach der Reperusionsphase untersucht. Relative Zellvitabilität wurde durch das MTT-Verfahren bestimmt. Propidium Jodid und Höchst wurden verwendet, um morphologische Erscheinungen für Apoptose und Nekrose zu untersuchen. Das LDH-Verfahren wurde angewandt, um den Nekrose bedingten LDH-Verlust nach Reperfusion zu bestimmen. Lysotracker-Rot wurde eingesetzt, um Autophagie und deren zelluläre Aktivität zu bestimmen. Durchflusszytometrie wurde benutzt, um Akridine-orange-gefärbte Zellen, eine Indikation für Autophagie, zu quantifizieren. Proteinmarker für Apoptose und Autophagie wurden des Weiteren unter Verwendung der Western-Blot-Technik bestimmt. MAP-Kinase- und MKP-1-Aktivität wurden ebenfalls mittels Western-Blot bestimmt.

Ergebnisse und Schlussfolgerung

Unsere Ergebnisse deuten auf eine Beziehung zwischen MKP-1-Induktion und Zelltod während simulierter Ischämie/Reperfusion (SI/R) hin. Während SI/R führte MKP-1-Hemmung zu einer Verminderung der Autophagie und gleichzeitig zu einer Zunahme von Apoptose und Nekrose. Eine erhöhte MKP-1-Expression während SI/R resultierte in erhöhter Autophagieaktivität und in vermindertem apoptotischen oder nekrotischen Zelltod. Unter MKP-1-Hemmung war P38-MAPK-Phosphorylierung signifikant erhöht und verringert unter MKP-1-Induktion. Dieses Ergebnis weist sehr deutlich darauf hin, dass MKP-1, welche bekannt ist für eine gewebesetzende Wirkung, eine wichtige Rolle im zellulären Schutz gegen myokardiale Ischämie spielt. Dieser Schutz wird durch die Regulation von Autophagie hervorgerufen, welche als Stressantwort gegen Zelltod durch Apoptose und Nekrose agiert.

ACKNOWLEDGEMENTS

First and foremost I thank my Lord and Shepherd for providing me with a backbone of supportive and loving people and the privilege and perseverance to finish this degree.

I would like to thank the following people to whom I will be forever grateful:

My supervisor, Prof Anna-Mart Engelbrecht, for her guidance and patience during this study. Ben who was always there with a helping hand and guidance and especially for translating my abstract to German. Mark who I always knew I could turn to for great advice and brainstorming. DSG, thanks so much for the encouragement, continuous support, advice and friendship.

I also want to thank and acknowledge my Tygerberg Physiology family for being not only colleagues, but also great friends! Prof. Amanda Lochner, for providing me with the foundation on which I can forever base my research. Thank you for the support and continuous interest in my work.

The NRF for financial support, and so allowing me to pursue my studies.

Last but certainly not least, I would like to thank my family and friends, in particular AJ and my Mom who are my pillars of strength. Thank you all for being my support system and my encouragement. I love you all!

ABBREVIATIONS

AIF	Apoptosis-inducing factor
AMP	Adenosine monophosphate
AMPK	AMP-activated protein kinase
ANOVA	Analysis of variance
APS	Ammonium persulphate
ATG	Autophagy regulated genes
BSA	Bovine serum albumin
CAD	Caspase-activated deoxyribonuclease
CD	Cardiovascular disease
cGMP	Cyclic guanosine monophosphate
Con	Control
DD	Death domain
DED	Death effector domain
DISC	Death-inducing signaling complex
DMEM	Dulbecco's modified Eagle medium
DMSO	Dimethyl sulfoxide

Dex	Dexamethasone
ECL	Enhanced chemiluminescence
EDTA	Ethylene diamine tetra-acetic acid
eEF2	Eukaryotic elongation factor-2
EGTA	Ethylene glycol-bis (β -aminoethyl ether)-N, N, N', N'-tetraacetic acid
eNOS	Endothelial nitric oxide synthase
ERK	Extracellular signal-regulated protein kinase
FADD	Fas-associated death domain
FBS	Fetal bovine serum
GC	Guanylyl cyclase
HEPES	4-(2-Hydroxyethyl)-1-piperazineethanesulfonic acid
ID	Intermediate domain
IHD	Ischaemic heart disease
Ins	Insulin
JNK	c-Jun NH ₂ -terminal protein kinase
LC3	Microtubule-associated protein 1 light chain 3

LDH	Lactate dehydrogenase
MAPK	Mitogen activated protein kinase
MAPKK/MKK	MAPK kinase
MAPKKK	MAPK kinase kinase
MAPKK1	First isoform of MAPKK
MAPKK2	Second isoform of MAPKK
MAPKK3	Third isoform of MAPKK
MKP-1	Mitogen activated protein kinase phosphatase-1
MPTP	Mitochondrial permeability transition pores
mTOR	Mammalian form of target of rapamycin
MTT	3-[4, 5-dimethylthiazol-2-yl]-2, 5-diphenyl tetrazolium bromide
NAD	Nicotinamide adenine dinucleotide
NADH	Nicotinamide adenine dinucleotide plus hydrogen
NAM	Nitric acid monohydrate
NO	Nitric oxide
Norm	Normoxic

PARP	Poly (ADP-ribose) polymerase
PBS	Phosphate buffered saline
PCD	Programmed cell death
PI	Propidium iodide
PI3K	Phosphoinositide 3-kinase
PMSF	Phenylmethylsulfonyl fluoride
PVDF	Polyvinylidene fluoride
RIP	Receptor interacting protein
RIPA	Radioimmunoprecipitation assay
SAPK	Stress activated protein kinase
SC	Sanguinarine
SDS-PAGE	Sodium dodecyl sulphate polyacrylamide gel electrophoresis
SEM	Standard error of the mean
SI	Simulated ischaemia
SI/R	Simulated ischaemia/reperfusion
TBS-T	Tris buffered saline-Tween20

TNF	Tumor necrosis factor
TRADD	TNFR1-associated death domain
TRAFs	TNF receptor-associated factors
TRAIL	TNF-related apoptosis-inducing ligand
T25	25 cm ² culture flask
T75	75 cm ² culture flask
2DG	2-deoxy- <i>D</i> -glucose

LIST OF FIGURES

CHAPTER 1

Figure 2.1: MAPK activation signaling cascade	9
Figure 2.2: MKP-1 signal transduction	15
Figure 2.3: Autophagy signaling	21
Figure 2.4: Apoptosis	31

CHAPTER 3

Figure 3.1: Treatment protocol for simulated ischaemic treated groups	43
Figure 3.2: Treatment protocol for SI/R treated groups	43
Figure 3.3: Fluorescence micrograph showing normal and pyknotic nuclei of H9c2 cells	48
Figure 3.4: Fluorescence micrograph showing late pyknotic nuclei of H9c2 cells	48
Figure 3.5: Fluorescence micrograph showing normal and PI positive nuclei of H9c2 cells	48

CHAPTER 4

Figure 4.1: MKP-1 activity after 3 hrs simulated ischaemia	57
Figure 4.2: p38 MAPK phosphorylation after 3 hrs simulated ischaemia	58
Figure 4.3: ERK 1 and 2 phosphorylation after 3 hrs simulated Ischaemia	59
Figure 4.4: JNK phosphorylation after 3 hrs simulated ischaemia	60
Figure 4.5: MKP-1 induction after simulated ischaemia/reperfusion	63
Figure 4.6: p38 MAPK phosphorylation after simulated ischaemia/reperfusion	64
Figure 4.7: ERK 1 and 2 phosphorylation after simulated ischaemia/reperfusion	65
Figure 4.8: JNK phosphorylation after simulated ischaemia/reperfusion	66
Figure 4.9: LysoTracker Red dye and Hoechst micrographs after 3 hrs simulated ischaemia	68
Figure 4.10: Cell sample selected and analysed during flow cytometry	69
Figure 4.11: Percentage red fluorescence intensity indicating acidic vacuoles, using acridine orange in flow cytometry	71

Figure 4.12: Beclin-1 activity after 3 hrs simulated ischaemia	73
Figure 4.13: LC3-II activity after 3 hrs simulated ischaemia	74
Figure 4.14: LysoTracker Red dye and Hoechst micrographs after simulated ischaemia/reperfusion	76
Figure 4.15: Cell sample selected and analysed during flow cytometry	77
Figure 4.16: Percentage red fluorescence intensity indicating acidic vacuoles	78
Figure 4.17: Beclin-1 activity after simulated ischaemia/reperfusion	80
Figure 4.18: LC3-II activity after simulated ischaemia/reperfusion	81
Figure 4.19: Relative viability based of MTT reduction after simulated ischaemia	83
Figure 4.20: Fluorescent micrographs showing nuclear DNA using Hoechst 33342 and karyorhexis using PI	86
Figure 4.21: Percentage pyknosis after simulated ischaemia	87
Figure 4.22: Percentage late pyknosis after simulated ischaemia	88
Figure 4.23: Percentage PI positive cells after simulated ischaemia	89
Figure 4.24: Caspase-3 cleavage after simulated ischaemia	91
Figure 4.25: PARP cleavage after simulated ischaemia	92

Figure 4.26: Relative viability based of MTT reduction, after simulated ischaemia/reperfusion	94
Figure 4.27: Fluorescent micrographs showing nuclear DNA using Hoechst 33342 (blue) and karyorhexis using PI	96
Figure 4.28: Percentage pyknosis after simulated ischaemia/reperfusion	97
Figure 4.29: Percentage late pyknosis after simulated ischaemia/reperfusion	98
Figure 4.30: Percentage PI positive cells after simulated ischaemia/reperfusion	99
Figure 4.31: Relative viability based on LDH release after simulated ischaemia/reperfusion	101
Figure 4.32: Caspase-3 cleavage after simulated ischaemia/reperfusion	103
Figure 4.33: PARP cleavage after simulated ischaemia/reperfusion	104

CHAPTER 8

Figure 8.1: Esumi and Esumi supplemented with 2DG groups treated for 3 h and 4 h	119
--	-----

Fig 8.2: Relative viability based of MTT reduction, triptolide concentration curve	121
Fig 8.3: Percentage pyknosis after SI/R	123
Figure 8.4 Lysotracker Red dye and Hoechst micrographs after simulated ischaemia/reperfusion	125
Fig 8.5: MKP-1 activity after triptolide or insulin treatment	126
Fig 8.6: Relative viability based of MTT reduction, sanguinarine concentration determination curve	128
Figure 8.7: MKP-1 activity after insulin or sanguinarine treatment	129
Figure 8.8: MKP-1 activity after SI	130
Figure 8.9: Phosphorylated p38 MAPK after SI	131
Figure 8.10: Phosphorylated ERK after SI	132
Figure 8.11: Phosphorylated JNK after SI	133
Figure 8.12: MKP-1 induction after SI/R	134
Figure 8.13: Phosphorylated p38 MAPK after SI/R	135
Figure 8.14: Phosphorylated ERK after SI/R	136
Figure 8.15: Phosphorylated JNK after SI/R	137
Figure 8.16: Percentage red fluorescence intensity after SI	138

Figure 8.17: LC3-II induction after SI	139
Figure 8.18: Beclin-1 induction after SI	140
Figure 8.19: Percentage red fluorescence intensity after SI/R	141
Figure 8.20: LC3-II induction after SI/R	142
Figure 8.21: Beclin-1 induction after SI/R	143
Figure 8.22: Relative viability based of MTT reduction after SI	144
Figure 8.23: Percentage pyknosis after SI	145
Figure 8.24: Percentage late pyknosis after SI	146
Figure 8.25: Percentage PI positive cells after SI	147
Figure 8.26: Caspase-3 cleavage after SI	148
Figure 8.27: PARP cleavage after SI	149
Figure 8.28: Relative viability based of MTT reduction after SI/R	150
Figure 8.29: Percentage pyknosis after SI/R	151
Figure 8.30: Percentage late pyknotic cells after SI/R	152
Figure 8.31: Percentage PI positive cells after SI/R	153
Figure 8.32: Relative viability based on LDH release	154
Figure 8.33: PARP cleavage after SI/R	155

Figure 8.34: Relative viability based of MTT reduction, modified Esumi buffer vs. modified Esumi supplemented with 2DG buffer	157
Figure 8.35: Glucose uptake in H9C2 cells	159
Figure 8.36: Glucose uptake in isolated adult rat myocytes	160
Figure 8.37: MKP-1 activity after 1 hour treatment; dexamethasone concentration curve	162

TABLE OF CONTENTS

CHAPTER 1 INTRODUCTION	1
1.1 Motivation for study	1
CHAPTER 2 LITERATURE REVIEW	4
2.1 Ischaemic heart disease	4
2.1.1 Introduction	4
2.1.2 Ischaemia/reperfusion injury	5
2.2 Signaling pathways and cell death	7
2.2.1 Introduction	7
2.2.2 MAPK signaling pathways	7
2.2.3 MKP-1 signaling	11
2.2.4 Activation of MKP-1	16
2.2.4.1 Insulin	16
2.2.4.2 Dexamethasone	17
2.2.5 Inhibition of MKP-1	18
2.2.5.1 Sanguinarine	18

2.2.5.2 Triptolide	18
2.3 Cell death, ischaemia/reperfusion injury and MKP-1	19
2.3.1 Introduction	19
2.3.2 Autophagy	19
2.3.2.1 Autophagy and ischaemia/reperfusion	23
2.3.2.2. Autophagy and MKP-1 signaling	25
2.3.3 Apoptosis	26
2.3.3.1 Apoptosis and ischaemia/reperfusion	32
2.3.3.2 Apoptosis and MKP-1 signaling	33
2.3.4 Necrosis	34
2.3.4.1 Necrosis and ischaemia/reperfusion	36
2.3.4.2 Necrosis and MKP-1 signaling	37
2.3.5 Cross-talk between autophagic, apoptotic and necrotic signaling pathways	37
CHAPTER 3 MATERIALS AND METHODS	40
3.1 Cell culture	40

3.2 Experimental protocol	40
3.2.1 Normoxic groups	40
3.2.2 Ischaemic groups	41
3.3 Western blot analysis	44
3.4 Cell viability analysis	45
3.4.1 MTT assay	45
3.4.2 LDH assay	46
3.4.3 Propidium iodide (PI) and Hoechst staining	47
3.4.4 LysoTracker [®] Red labelling	49
3.4.5 Flow cytometry	49
3.5 Determination of 2-deoxy-D-³[H] glucose uptake	50
3.6 Statistical analysis	51
CHAPTER 4 RESULTS	52
Pilot studies	52
A. Simulated ischaemic conditions	52
B. MKP-1 inhibition	53

C. MKP-1 induction	54
4.1 MKP-1 and MAPK signaling after 3 hrs simulated ischaemia	55
4.2 MKP-1 and MAPK signaling after 3 hrs simulated ischaemia/reperfusion	61
4.3 Autophagic activity after 3 hrs simulated ischaemia	67
4.3.1 LysoTracker [®] Red labelling	67
4.3.2 Flow cytometry	69
4.3.3 Beclin-1 and LC3-II	72
4.4 Autophagic activity after simulated ischaemia/reperfusion	75
4.4.1 Lysotracker [®] Red labelling	75
4.4.2 Flow cytometry	77
4.4.3 Beclin-1 and LC3-II	78
4.5 Cell viability after 3 hrs simulated ischaemia	81
4.5.1 MTT	81
4.5.2 PI/Hoechst	84
4.5.3 Cleaved caspase-3 and cleaved PARP	90
4.6 Cell viability after simulated ischaemia/reperfusion	93

4.6.1 MTT	93
4.6.2 PI/Hoechst	95
4.6.3 LDH assay	100
4.6.4 Cleaved caspase-3 and cleaved PARP	102
CHAPTER 5 DISCUSSION	105
5.1 Experimental model	105
5.2 Induction and inhibition of MKP-1 expression and subsequent influence on MAPK activity, during ischaemia/reperfusion	107
5.3 Role of MKP-1 in autophagy during simulated ischaemia/reperfusion	109
5.4 Role of MKP- in apoptosis and necrosis during simulated ischaemia/reperfusion	111
CHAPTER 6 SUMMARY	115
CHAPTER 7 FUTURE DIRECTIONS	117

CHAPTER 8 PILOT STUDIES	118
8.1 Determination of simulated ischaemia conditions	118
8.2 MKP-1 inhibition	120
8.2.1 Triptolide	121
8.2.2 Sanguinarine	127
8.3 Western blots: insulin	120
8.4 Investigating insulin induced MKP-1 induction	156
8.5 Dexamethasone concentration determination	161
REFERENCES	162
Appendix A	193
Appendix B	204
Appendix C	211

CHAPTER 1

Introduction

1.1 Motivation for study

It has been suggested that mitogen activated protein kinase phosphatase -1 (MKP-1) attenuates myocardial ischaemia/reperfusion injury (Engelbrecht *et al.*, 2005; Fan *et al.*, 2009). For example, it has been demonstrated that transgenic mice overexpressing myocardial MKP-1 were protected from ischaemia/reperfusion injury, while knockout mice were more sensitive to this phenomenon (Kaiser *et al.*, 2004; Boutros *et al.*, 2008b). MKP-1, found predominantly in the nucleus, is a dual specificity phosphatase which dephosphorylates phosphotyrosine and phosphothreonine-containing protein kinases, such as the mitogen activated protein kinases (MAPKs). MAPKs are known to be involved in intracellular signaling pathways that regulate gene expression in response to a variety of extracellular signals. The three major classes of MAPK include the extracellular signal-regulated protein kinase (ERK)/p42/44, c-Jun NH₂-terminal protein kinase (JNK)/stress activated protein kinase (SAPK) and p38 MAPK (Begum *et al.*, 1998; Cowan & Storey, 2003). MAPKs are activated during ischaemia/reperfusion, which in turn leads to MKP-1 activation. Upon activation MKP-1 dephosphorylates and deactivates MAPKs (Bogoyevitch *et al.*, 1996; Hutter *et al.*, 2000; Pearson *et al.*, 2001).

ERK, JNK and p38 MAPKs have been shown to be involved in autophagic, apoptotic and necrotic responses to cellular stressors (Lee *et al.*, 1997; Khan *et al.*, 2004; Lee *et al.*, 2004; Codogno & Meijer, 2005; Park *et al.*, 2009; Yang *et al.*, 2009). Autophagy is foremost a survival mechanism which is activated in cells subjected to nutrient or growth factor deprivation. However, when cellular stress continues, cell death may occur either by autophagy, or becomes associated with features of apoptotic or necrotic cell death (Maiuri *et al.*, 2007). Apoptosis is essential for removal of specifically targeted cells, through the process of apoptotic body formation and phagocytosis (Peter *et al.*, 2008). Necrosis is a pathological cellular response requiring no ATP. Necrotic cells are morphologically characterised by disrupted membranes, cytoplasm and mitochondrial swelling, disintegration of organelles and complete cell lysis, followed by DNA fragmentation (Zong & Thompson, 2006). Cell death following ischaemia/reperfusion injury, is thought to be a mixture of apoptotic, necrotic and autophagic cell death (Murphy & Steenbergen, 2008).

MKP-1 has been shown to be involved in the regulation of apoptosis (Morisco *et al.*, 2007) and very recently it was also demonstrated that MKP-1 may lead to autophagy induction in cancer cells (Lu *et al.*, 2010). Currently, to our knowledge, there is no evidence for a role for MKP-1 in autophagy during ischaemia/reperfusion injury in the heart.

In view of this we hypothesize that during ischaemia/reperfusion, MKP-1 induction leads to increased MAPK dephosphorylation, followed by increased autophagic activity and a subsequent attenuation of myocardial cell death.

Using cultured H9c2 adult rat heart cardiomyocytes as experimental model, the aims of the present study were to determine:

- whether autophagy, apoptosis and necrosis are upregulated during ischaemia as well as during reperfusion following ischaemia,
- how inhibition of the dual-specificity phosphatase family member, MKP-1, affects autophagy, apoptosis and necrosis,
- how upregulation of MKP-1 affects autophagy, apoptosis and necrosis,
- if MAPK regulation is affected and where it is involved.

In order to do a thorough study of the above mentioned aims, extensive knowledge and understanding of the concepts and processes involved, are required. Therefore the phenomenon of ischaemia/reperfusion, MKP-1 and MAPK signaling and their involvement in the autophagic, apoptotic and necrotic signaling processes will be discussed in the literature review.

CHAPTER 2

Literature review

2.1 Ischaemic heart disease

2.1.1 Introduction

Ischaemic heart disease (IHD) has become one of the leading causes of death worldwide. The prevalence is predicted to increase by alarming rates with up to 23.3 million global cardiovascular disease deaths estimated to occur in the year 2030 (Mathers & Loncar, 2006). IHD is also prevalent in South Africa. In 2002 it was the fourth largest contributor to South African deaths; resulting in 4% of the mortality rate (WHO, 2006).

Morbidity and mortality in the western nations are largely attributed to myocardial cell death caused by ischaemia/reperfusion (Murphy & Steenbergen, 2008). As South Africans are adopting the lifestyle associated with western nations, this is an alarming notion. Over the past few decades numerous researchers have investigated the pathways involved in ischaemia/reperfusion injury as well as the mechanisms of cell death. Knowledge of these events will contribute to development of interventions and drugs aimed at salvage of damaged tissues.

2.1.2 Ischaemia/reperfusion injury

Rudolf Virchow first used the term ischaemia in 1858. It is derived from the Greek terms “ischein”, which means to restrain, and “haima”, which means blood (Virchow, 1858). Ischaemia can be defined as an imbalance between the amount of oxygen, glucose (a major fuel for the heart) and other substrates needed by and supplied to the heart (Dennis *et al.*, 1991; Zong & Thompson, 2006). This leads to anaerobic metabolism and reduced contractile function. A biochemical imbalance occurs as the maintenance of the metabolism cannot be kept at a steady state due to inadequate coronary flow. A reduction in metabolite clearance also occurs during ischaemia and intracellular pH levels drop as the acid by-products of glycolysis accumulate.

In the heart the severity of the ischaemic injury depends on the duration of ischaemia and subsequent reperfusion (Dennis *et al.*, 1991; Zong & Thompson, 2006). If, however, ischaemia is maintained, reversible injury gradually transitions to irreversible injury and a myocardial infarct develops. Reperfusion with its reinforced oxygen and substrate availability is thus a prerequisite for myocardial salvage (Zong & Thompson, 2006). However, reperfusion after an ischaemic period causes generation of free radicals and is associated with detrimental changes such as enzyme release, arrhythmias and intramyocardial haemorrhage which are known as reperfusion injuries (Murry *et al.*, 1986).

Cardiomyocytes are highly dependent on a continuous supply of oxygen. During ischaemia, cardiomyocyte capacity to generate sufficient ATP and creatine phosphate, becomes depleted; only two ATP moles are produced

for every mole of glucose instead of the thirty-eight moles that are generated during aerobic metabolism. Multiple adaptive processes occur in response to these hypoxic environments created during ischaemia. To reduce oxygen consumption, oxidative phosphorylation is limited and glycolysis is stimulated. This aids in ATP production, even under low oxygen supply (Nishida *et al.*, 2009).

Prolonged ischaemia leads to cardiac failure which is characterized by the progressive death of myocytes (Olivetti *et al.*, 1997). Three major morphologies of cell death have been described: apoptosis (type I), cell death associated with autophagy (type II) and necrosis (type III). Apoptosis, also known as programmed cell death, can be described as the cytological changes that can be observed during cellular self-destruction (Kerr, 1971; Kerr *et al.*, 1972; Elmore, 2007). Apoptosis is essential for removal of specifically targeted cells in multicellular organisms, through the process of apoptotic body formation and phagocytosis (Peter *et al.*, 2008). Cells undergoing death associated with autophagy are characterised by the presence of double membrane autophagic vacuoles. Autophagy is foremost a survival mechanism which is activated in cells subjected to nutrient or growth factor deprivation. However, when cellular stress continues, cell death may occur by autophagy alone, or often becomes associated with features of apoptotic or necrotic cell death (Maiuri *et al.*, 2007). Necrosis is a pathological cellular response requiring no ATP. Necrotic cells are morphologically characterised by disrupted membrane, cytoplasm and mitochondrial swelling, disintegration of organelles and complete cell lysis, followed by DNA fragmentation (Zong & Thompson, 2006).

It has been suggested that apoptosis contributes greatly to cardiomyocyte loss in pathophysiological conditions, such as acute myocardial infarction and heart failure (Suzuki *et al.*, 2001). In experimental models apoptosis, autophagic cell death and necrosis, contribute differentially to cell death and may depend on the model; i.e. adult vs. neonatal, cultured cells vs. *in vivo*. However, it appears that cell death following ischaemia/reperfusion injury, is a mixture of apoptotic, necrotic and autophagic cell death (Murphy & Steenbergen, 2008).

2.2 Signaling pathways and cell death

2.2.1 Introduction

Great efforts have been made to disentangle the intricate relationships between signaling pathways and the different modes of cell death. Analysis is complicated due to the fact that several pathways can be activated simultaneously with differential effects on cell death. It has become evident that the mitogen activated protein kinase (MAPK) signaling pathway is a major regulator of cell death in the heart.

2.2.2 MAPK signaling pathways

Three major classes of MAPK, which include the extracellular signal-regulated protein kinase (ERK)/p42/44, c-Jun NH₂-terminal protein kinase

(JNK)/stress activated protein kinase (SAPK) and p38 MAPK families have been identified (Begum *et al.*, 1998; Cowan & Storey, 2003). The ERK pathway has been depicted the pro-survival pathway and is activated by a variety of mitogens and phorbol esters (Marczin *et al.*, 2003; Junttila *et al.*, 2008). The JNK and p38 MAPK pathways are regarded as the pro-apoptotic pathways and are activated mainly by environmental stress and inflammatory cytokines (Pearson *et al.*, 2001; Weston & Davis, 2007; Junttila *et al.*, 2008). MAPK activity is regulated by phosphorylation cascades (Pearson *et al.*, 2001). Activation and inactivation signals, influenced by negative feedback triggered by activation signals upstream from the MAPK, determine the duration and amplitude of MAPK activity (Pearson *et al.*, 2001).

MAPK activation results from activation of upstream kinases due to mitogens (Fig 2.1). MAPK kinase kinases (MAPKKK) phosphorylate dual specificity MAPK kinases (MAPKK/MKK) after receiving signals from stimulus-activated receptors on the cell surface by GTP-binding protein interactions (Cowan & Storey, 2003). MKK, a dual-specific kinase, in turn, phosphorylates hydroxyl side chains of tyrosine and serine/threonine residues (Seeger & Krebs, 1995; Begum *et al.*, 1998; Pearson *et al.*, 2001; Cowan & Storey, 2003; Avitzour *et al.*, 2007; Junttila *et al.*, 2008). ERKs are activated by MKK 1 and MKK 2, JNK is activated by MKK 4 and MKK 7, and p38 MAPK is activated by MKK 3 and MKK 6 (Robinson & Cobb, 1997; Zhang & Liu, 2002; Avitzour *et al.*, 2007; Junttila *et al.*, 2008). After activation by mitogens in the cytoplasm or nucleus, these MAPKs modulate the function of target transcription factors through serine/threonine phosphorylation (Pearson *et al.*, 2001; Weston & Davis, 2007; Junttila *et al.*, 2008).

A number of downstream target exist for the MAPKs. ERKs are known to be involved in meiosis and mitosis regulation, and also in postmitotic functions of differentiated cells. A three-kinase phospho-relay system for ERK includes MKKK c-Raf1, B-Raf or A-raf, activated by *Ras*. A downstream target for ERK1 is 90-kD ribosomal protein S6 kinase (p90RSK). JNK is known to phosphorylate DNA binding protein, c-Jun, which increases its transcriptional activity. c-Jun is also a component in the AP-1 transcription complex involved in the control of cytokine genes. p38 MAPK is known to regulate cytokine expression and also plays an important role in the activation of the immune response. MAPK-interacting kinase 1 (MNK1) is known to be downstream target of p38 MAPK (Brondello *et al.*, 1997; Johnson & Lapadat, 2002).

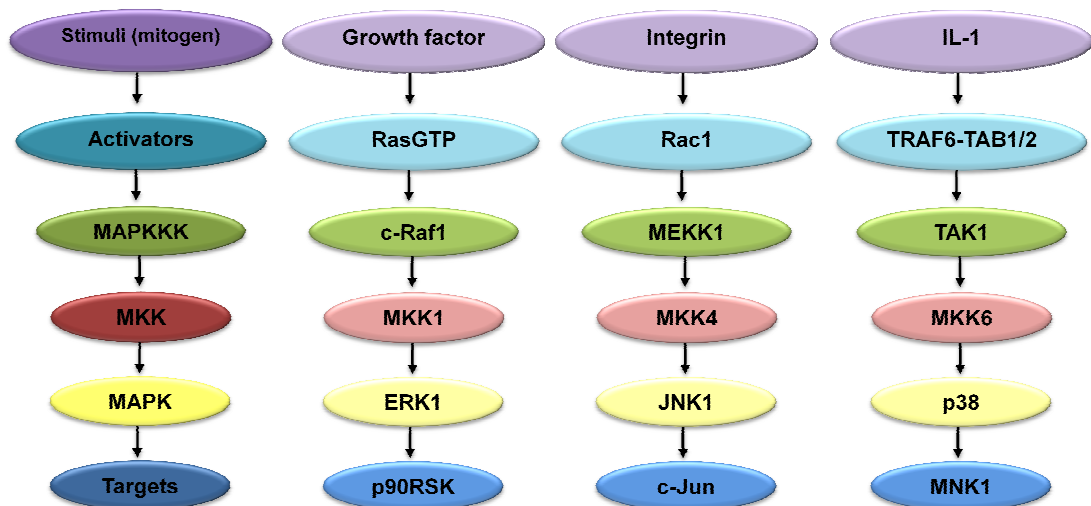


Figure 2.1: MAPK activation signaling cascade (modified from Johnson & Lapadat, 2002)

The p38 MAPK pathway can be activated in response to inflammatory cytokines, mitogens, pathogens and environmental stressors such as osmotic stress and hypoxia (Avitzour *et al.*, 2007; Junttila *et al.*, 2008). The p38 MAPK protein is known to have 4 main isoforms; p38 α , p38 β , p38 γ and p38 δ , which are coexpressed and coactivated in the same cells (Avitzour *et al.*, 2007; Junttila *et al.*, 2008). Dual phosphorylation of threonine and tyrosine residues, within the threonine-glycine-tyrosine sequence, in the activation domain of the sequence is required for the activation of all the isoforms (Cowan & Storey, 2003; Avitzour *et al.*, 2007; Junttila *et al.*, 2008). The isoforms are differentially activated by MKK. MKK 3 can activate p38 α , p38 γ and p38 δ . MKK 4 can activate p38 α , and p38 δ in specific cell types (Avitzour *et al.*, 2007) and MKK 6 can phosphorylate all four isoforms (Avitzour *et al.*, 2007). The p38 α isoform is known to be proapoptotic (Pearson *et al.*, 2001).

There is some discrepancy regarding the time points at which MAPKs are activated during ischaemia/reperfusion. It has been shown that JNK and ERK are activated during reperfusion and p38 MAPK is active during both ischaemia and reperfusion (Bogoyevitch *et al.*, 1996). ERK has however also been shown to be activated during ischaemia, while JNK activation was shown to occur only during early reperfusion (Engelbrecht *et al.*, 2004). ERK activation during reperfusion has been shown to increase cardiac functional recovery, while p38 MAPK activation has been related to myocardial dysfunction during reperfusion (Khan *et al.*, 2004). However, Engelbrecht *et al.* (2004) found that ERK inhibition did not affect apoptosis during ischaemia/reperfusion.

2.2.3 MKP-1 signaling

MAPK are activated by phosphorylation, but the dephosphorylation process via phosphatases is a key element in MAPK control. Dephosphorylation of MAPKs results in conformational changes rendering them inactive until they are again phosphorylated by upstream kinases (Cowan & Storey, 2003). The three phosphatase families which are involved in MAPK dephosphorylation include the serine/threonine phosphatases, the tyrosine phosphatases and the dual specificity phosphatases. The latter is able to dephosphorylate protein substrates on serine, threonine and tyrosine residues.

Dephosphorylation of MAPKs is largely attributed to the dual-specificity phosphatase subfamily known as MAPK phosphatases (MKPs). MAPK activation leads to increased expression of MKPs. Regions within the amino terminus of the MKP then binds to the MAPKs which trigger the activation of the catalytic domain of the phosphatase. The bound MAPKs are then subsequently dephosphorylated by the MKP. The MAPK then dissociates and leaves the phosphatase free to bind and dephosphorylate other MAPKs. Three main groups of MKPs are known to exist; those which are mainly found in the nucleus and are encoded by growth factor or stress-inducible genes, those which are located in the cytosol and not transcriptionally regulated and those localized in both the nucleus and cytosol (Pearson *et al.*, 2001). Three MKPs are known; MKP-1 and MKP-2, which dephosphorylates all three MAPK family members, and MKP-3, which is specific for ERK1 and -2 (Chu *et al.*, 1996; Muda *et al.*, 1996; Cowan & Storey, 2003).

MKP-1 (CL100, Erp, 3CH134, hVH-1) is a dual specificity protein phosphatase, found predominantly in the nucleus (Cowan & Storey, 2003) and is ubiquitously expressed in various tissues. The mechanism of MKP-1 regulation occurs via transcriptional and post-translational pathways (Yang & Wu, 2004; Lornejad-Schafer *et al.*, 2005). MKP1 is known to be transcriptionally induced through ERK, p53 and Jak2 (Brondello *et al.*, 1997; Li *et al.*, 2003a; Sandberg *et al.*, 2004).

As is the case with many genes coding for regulatory proteins, MKP-1 mRNA levels are upregulated by many factors in a variety of cell types, which include dexamethasone in human mammary epithelial cells (Wu *et al.*, 2004), insulin in a rat hepatoma cell line H4IIE-C3 (Lornejad-Schafer *et al.*, 2005) and arachidonic acid in rat aortic vascular smooth muscle cells (Metzler *et al.*, 1998). The MKP-1 transcript is also modulated by various stressful conditions such as ischaemia in the rat forebrain (Takano *et al.*, 1995), hypoxia in neonatal rat tissue (Bernaudin *et al.*, 2002) and osmotic shock in rat hepatoma cells (Lornejad-Schafer *et al.*, 2003).

MKP-1 is not only regulated during transcription but protein expression is also increased in various cell types by different factors. This has been shown in many models such as in insulin-treated rat smooth muscle cells (Lornejad-Schafer *et al.*, 2003) and dexamethasone treated human breast epithelial cell lines, MCF-7 and MDA-MB-231 (Wu *et al.*, 2004). It is important to note that it is not known whether the increase in protein levels is due to de novo synthesis or increased stabilization, as MKP-1 has a half-life which varies from 40 minutes to 2 hours (Boutros *et al.*, 2008a). This may be due to the

various mechanisms available for MKP-1 protein modulation. The treatments known to modulate MKP-1 protein expression are also not specific for MKP-1 regulation and may target many effectors.

The three-dimensional structure of MKP-1 is unknown and as a result no “tailor-made” inhibitors for this phosphatase are available. It has however been shown that compounds such as benzofuran block MKP-1 protein function (Lazo *et al.*, 2006). A plant alkaloid, Sanguinarine (Vogt *et al.*, 2005; Garcia *et al.*, 2006), has been shown to selectively inhibit MKP-1 activity (Vogt *et al.*, 2005). MKP-1 transcription has also been shown to be blocked by a vine root extract known as triptolide (Wang *et al.*, 2006) (Fig 2.2).

MKP-1 has dual catalytic activity towards phosphotyrosine- and phosphothreonine-containing proteins (Holt *et al.*, 1996; Junttila *et al.*, 2008). Upon binding to an active MAPK, MKP-1 is phosphorylated after which it dephosphorylates the MAPK it was bound to (Hutter *et al.*, 2000; Farooq & Zhou, 2004). MKP-mediated dephosphorylation is a two-step process which involves firstly the binding of MAPK to MKP-1, targeting the phospho-tyrosine residue which is the first to be dephosphorylated, followed by the release of the MKP-MAPK complex. Secondly, MAPK binds to MKP-1, the phospho-threonine residue is dephosphorylated and both proteins are released (Boutros *et al.*, 2008a). MKP-1 is known to dephosphorylate and inactivate p38 MAPK and JNK in the nucleus (Franklin & Kraft, 1997; Franklin *et al.*, 1998; Wu, 2004; Avitzour *et al.*, 2007). This phosphatase also dephosphorylates ERKs but to a much lesser extent. MKP-1 thus dephosphorylates MAPKs in a rank order of p38 MAPK > JNK > ERK2 >

ERK1 (Chu *et al.*, 1996; Franklin & Kraft, 1997; Franklin *et al.*, 1998; Li *et al.*, 1999; Boutros *et al.*, 2008a). MKP-1 dephosphorylation activity is restricted to the nucleus (Boutros *et al.*, 2008a).

The cell lineage may influence the regulatory mechanisms involved in the MAPK/MKP-1 interactions. MKP-1 is activated by ERK, JNK and p38 MAPK in vascular smooth muscle cells, mesangial cells and U937 cells. However, in NIH3T3 cells only JNK but not ERK cause MKP-1 upregulation. In H4IIE hepatoma cells only p38 MAPK activation results in the upregulation of MKP-1 (Bokemeyer *et al.*, 1996; Bokemeyer *et al.*, 1997; Franklin & Kraft, 1997; Li *et al.*, 1999).

As stated previously, MKP-1 is induced by a number of stress inducing factors which include hypoxia, ischaemia/reperfusion, osmotic shock, heat shock, UV light and growth factors. MKP-1 is involved in cell survival by attenuation of stress-responsive MAPK-mediated apoptosis. MKP-1 has also been found to be implicated in the regulation of various physiological processes such as apoptosis and cell growth (Camps *et al.*, 2000; Keyse, 2000). It is however not known if MKP-1 is an essential regulator in these processes.

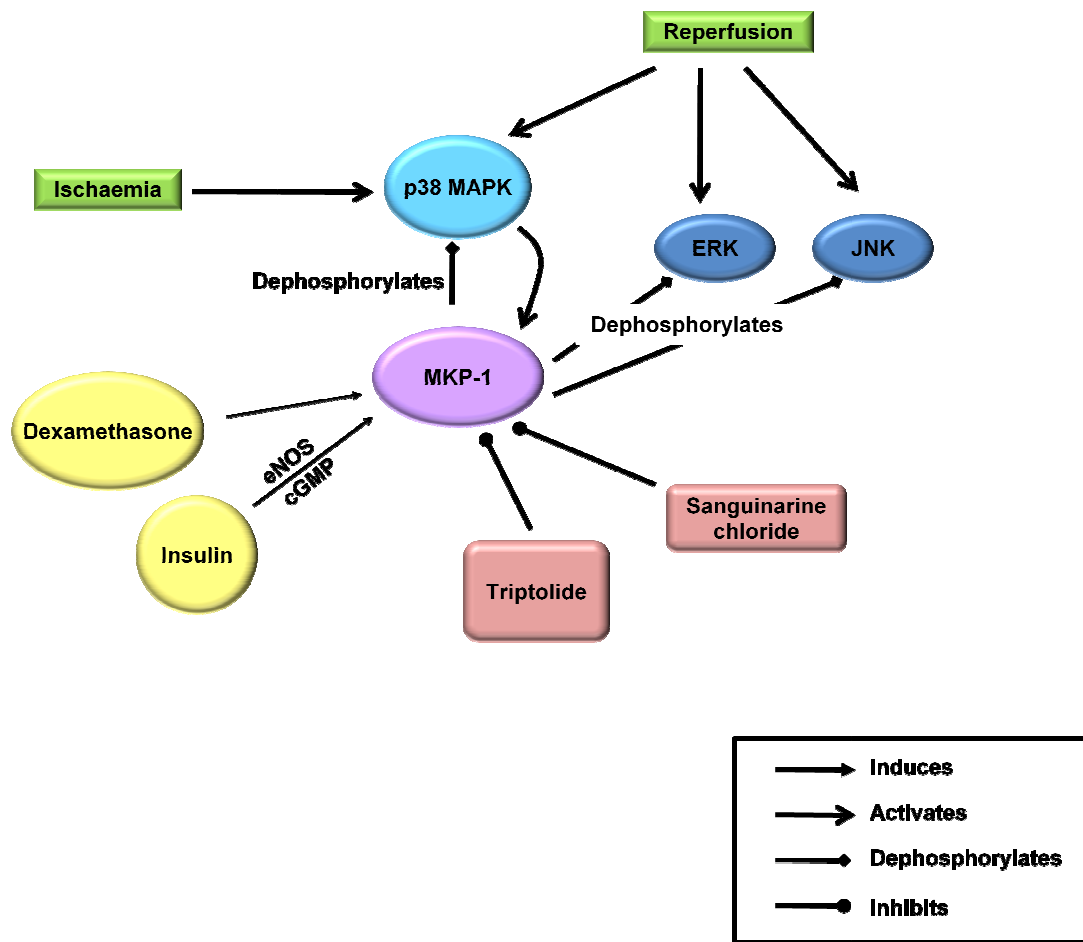


Figure 2.2: MKP-1 signal transduction

MKP-1 degradation has been shown to be attenuated by inhibitors of the ubiquitin-directed proteasome complex. MKP-1 phosphorylation by ERK at Ser³⁵⁹ and Ser³⁶⁴ in its carboxy-terminal region has also been shown to inhibit MKP-1 degradation through the ubiquitin pathway (Brondello *et al.*, 1999). Furthermore, it has been shown that hyperosmolarity in H4IIE cells, resulted in increased p38 MAPK and JNK expression, which subsequently promoted MKP-1 expression. The hyperosmolarity also produced an increase in proteosomal proteolysis; however despite this, the MKP-1 expression levels did not decrease during the period of hyperosmolarity

(Lornejad-Schafer *et al.*, 2005). These and other findings (Kim *et al.*, 2005; Choi *et al.*, 2006) suggest that MKP-1 is indeed degraded by the ubiquitin proteasome complex, however during activation by ERKs (and possibly other MAPKs), which is evident during ischaemia, MKP-1 degradation is inhibited.

2.2.4 Activation of MKP-1

2.2.4.1 Insulin

Insulin is a pleiotropic hormone involved in the regulation of several biological processes which include glucose and amino acid transport (Kusari *et al.*, 1997; Morisco *et al.*, 2007).

Insulin is well known to modify reperfusion conditions to reduce in-hospital mortality risks in patients with acute myocardial infarction (Abdallah & Schafer, 2006). Glucose-insulin-potassium (GIK) cocktail is often used in the clinical setting of post-myocardial ischaemia (Sack & Yellon, 2003), which is a concept first introduced by Sodi-Pallares in 1962 (Sodi-Pallares *et al.*, 1962). In a study on Sprague-Dawley rats it was seen that insulin plays a critical role in the myocardial protection elicited by the GIK treatment as rats treated with merely a GK cocktail shows no signs of cardiac protection (Gao *et al.*, 2003).

Reperfusion induced cell death was shown to be reduced by insulin through pathways comprising phosphoinositide 3-kinase (PI3K) and endothelial nitric oxide synthase (eNOS). NO activates the enzyme guanylyl cyclase (GC)

which in turn activates cyclic guanosine monophosphate (cGMP)-dependent signaling. Nitric oxide (NO) has been found to reduce infarct size (Wang *et al.*, 2005). Furthermore, it has been shown that agents which act via cGMP-dependent pathways, during reperfusion, reduced infarct size (Padilla *et al.*, 2001). It has also been shown, in vascular studies, that insulin induced an upregulation of MKP-1 via NO and cGMP (Jacob *et al.*, 2002). Unpublished data from our lab also confirmed this in cardiac tissue. It has recently been shown that insulin regulates MKP-1 expression via ERK, JNK MAPK and the PI3K pathway (Morisco *et al.*, 2007).

2.2.4.2 Dexamethasone

Expression of the MKP-1 gene, at promoter level, and the attenuation of proteosomal degradation of MKP-1 has been shown to be increased in the presence of dexamethasone (Kassel *et al.*, 2001). Dexamethasone is an anti-inflammatory glucocorticoid which has been shown to cause induction of MKP-1 and associated inhibition of p38 MAPK phosphorylation in HeLa cells (Lasa *et al.*, 2002). Increased post-ischaemic cardiac functional recovery and reduced infarct size, associated with increased MKP-1 expression and decreased p38 MAPK phosphorylation, has been shown in the presence of dexamethasone, in a isolated rat heart perfusion model (Fan *et al.*, 2009).

2.2.5 Inhibition of MKP-1

2.2.5.1 Sanguinarine

Sanguinarine, an alkaloid from the plant *Chelidonium majus* (Vogt *et al.*, 2005; Garcia *et al.*, 2006), has been shown to selectively inhibit MKP-1 activity (Vogt *et al.*, 2005). As a result of this inhibition, phospho-JNK and phospho-ERK levels have been shown to increase after 30 min treatment in a human pancreatic cancer cell line, PANC1 (Vogt *et al.*, 2005). Sanguinarine is known for its antibacterial, antiviral and even antitumour activity (Vogt *et al.*, 2005; Vollmer, 2006). It has also been reported to have multiple other cellular activities which include the inhibition of both nuclear factor κ B (NF κ B) and vascular endothelial growth factor-induced angiogenesis (Vogt *et al.*, 2005). MKP-1 has however been the only reported primary cellular target identified. A direct link between sanguinarine induced cell death and inhibition of MKP-1 activity is still required (Boutros *et al.*, 2008a).

2.2.5.2 Triptolide

Triptolide is a diterpene triepoxide isolated from the Chinese medicinal vine, *Trypterygium wilfordii hook f.* (Chang *et al.*, 2001). This vine has been used for centuries in Chinese medicine to treat rheumatoid arthritis, fever and edema (Wang *et al.*, 2006). An extract preparation of this vine has been shown to exhibit anti-inflammatory, immunosuppressive and antitumour

activities (Li & Wang, 2005). Triptolide is an active root extract from the vine and able to block the transcription of MKP-1 (Wang *et al.*, 2006).

2.3 Cell death, ischaemia/reperfusion injury and MKP-1

2.3.1 Introduction

The induction of cell death pathways is complex and depends on the reception of multiple extracellular and intracellular signals, integration and amplification of these signals by second messengers and finally, activation of death effector pathways. Defects in control of these pathways may contribute to a variety of diseases, including coronary heart disease.

2.3.2 Autophagy

Autophagic cell death, already mentioned earlier, was first described in 1966 by De Duve and Wattiaux (De Duve & Wattiaux, 1966) and more recently reviewed by Clarke in 1990 (Clarke, 1990; Gozuacik & Kimchi, 2007). The most prominent feature of this type of cell death is the appearance of double or multiple membrane enclosed vesicles. These vesicles engulf cytoplasm, long-lived proteins and organelles and then fuse with lysosomes to allow lysosomal enzymes to degrade the vesicles and their contents. This process is known as macroautophagy (Codogno & Meijer, 2005; Gozuacik & Kimchi, 2007). Two other mechanisms of autophagy known as microautophagy and

chaperone-mediated autophagy also exist (Codogno & Meijer, 2005). Microautophagy involves the sequestration of cytoplasmic portions by invaginations of lysosomal membranes followed by subsequent degradation. In chaperone-mediated autophagy, cytoplasmic proteins are selectively delivered to the lysosome. This process is dependent on the recognition of lysosomal receptors of a sequence motif in cytosolic proteins (Marino & Lopez-Otin, 2004). However, for the purpose of this thesis, we will only focus on macroautophagy which will be referred to as autophagy from here on.

Activation of the autophagy pathway starts with the formation of the autophagosome and involves a series of steps. The induction step involves isolation of a small membrane, the phagophore, to which necessary proteins are recruited to form the autophagosome. This process is regulated by a system of highly conserved evolutionary proteins, known as autophagy regulated genes (Atg) proteins. Atg6, also known as beclin-1, forms part of a PI3-K complex and plays an important role during the initial steps of autophagosome formation by mediating the localization of other Atg proteins to the isolation membrane (Kihara *et al.*, 2001).

In addition, the synthesis of the autophagosome requires two ubiquitin-like conjugation systems, one involving the conjugation of Atg12 to Atg5 with the help of Atg7 and -10. Once Atg12 and Atg5 have conjugated, it interacts with Atg16 to form an Atg12-Atg5-Atg16 conjugate which is involved in the elongation of the isolation membranes, to form the phagophore (Marino & Lopez-Otin, 2004). The other ubiquitin-like conjugation system involves the conjugation of phosphatidylethanolamine to Atg8 (microtubule-associated

protein 1 light chain 3 (LC3), the mammalian orthologue of Atg8) with the help of Atg4, -7 and -3. This conjugation then leads to the conversion of LC3-I to LC3-II, which is also used as an autophagy marker (Klionsky & Emr, 2000; Kunz *et al.*, 2004; Levine & Klionsky, 2004; Yang *et al.*, 2005; Yorimitsu & Klionsky, 2005; Dice, 2007; Ferraro & Cecconi, 2007; Maiuri *et al.*, 2007; Nishida *et al.*, 2009). The autophagosome is formed when the phagophore closes, resulting in a double-membrane vesicle. The autophagosome is targeted towards the lysosome, resulting in the fusion of the outer membrane of the autophagosome with the lysosome. A single membrane vesicle known as the autophagic body is released into the lysosomal compartment. This generates the autolysosome. Lysosomal hydrolases then degrade the sequestered contents (Fass *et al.*, 2006).

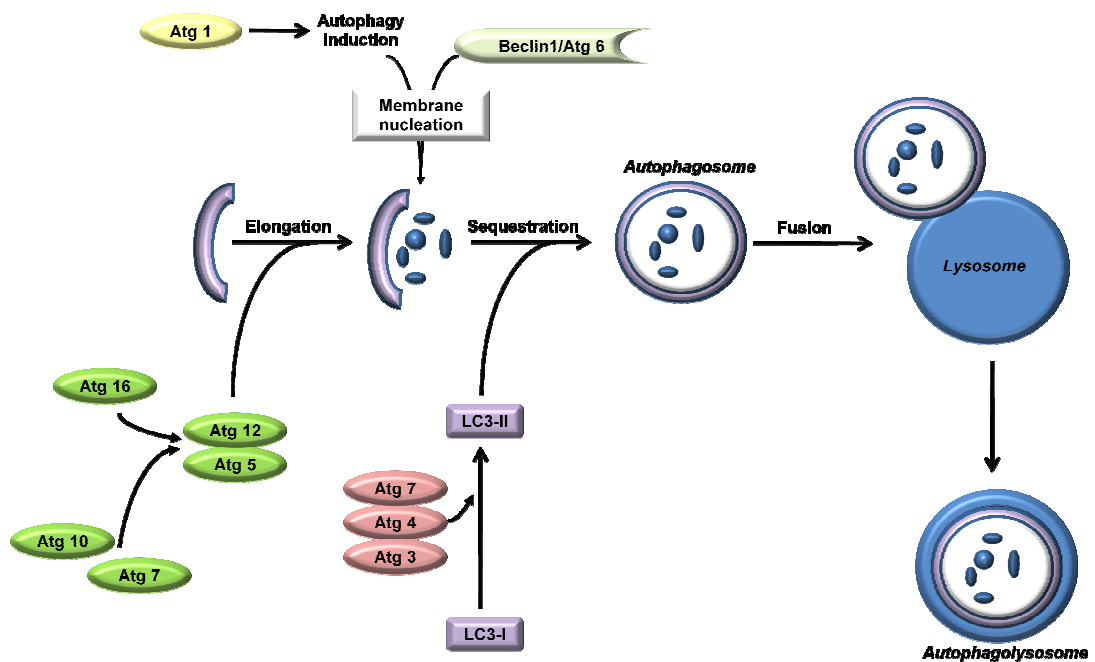


Figure 2.3: Autophagy signaling

(adopted from www.cellsignal.com/reference/pathway/Autophagy.html)

Autophagy is active at basal levels; it is involved in regulation of the turn-over of long-lived proteins and the removal of damaged structures (Matsui *et al.*, 2007). Damaged mitochondria are also removed by autophagy, which acts as a cytoprotective mechanism against apoptosis, as damaged mitochondria release proapoptotic factors such as cytochrome *c* (Nishida *et al.*, 2009). Various stressors can also result in the activation of autophagy, such as nutrient deprivation, myocardial ischaemia/reperfusion and heart failure (Codogno & Meijer, 2005; Nishida *et al.*, 2009). Autophagy is activated during nutrient deprivation, to generate free fatty acids and amino acids required to maintain function during nutrient limiting conditions. The mammalian target of rapamycin (mTOR) is the nutrient sensor of the cell and serves as a key regulator of autophagy (Codogno & Meijer, 2005). Autophagosome formation is favoured when mTOR is not stimulated by nutrients or is inhibited by rapamycin (Neufeld, 2007). Furthermore, cells can be prevented from undergoing apoptosis, by autophagy. This is achieved as autophagy maintains the intracellular substrate supply, during these nutrient deprived situations.

The stimulus, the amplitude and the duration of the induced stress determines whether autophagy results in cell death, either via autophagic cell death or concurrently with apoptosis (Codogno & Meijer, 2005; Gozuacik & Kimchi, 2007), or if it plays a role in cell survival, as seen during nutrient depletion (Codogno & Meijer, 2005; Nishida *et al.*, 2009). The latest school of thought is that autophagy is a stress response to promote cell survival. Cell death by autophagy is a rare scenario (Bergmann, 2007).

2.3.2.1 Autophagy and ischaemia/reperfusion

Autophagy plays an important role in the heart, not only during basal conditions but also during ischaemia and reperfusion. It is induced during ischaemia, and even more so by reperfusion (Matsui *et al.*, 2007). It was found that the enhancement of autophagy during ischaemia/reperfusion preserved cell viability and reduced apoptosis (Hamacher-Brady *et al.*, 2006). The onset of protection has been correlated with increased Beclin1 expression in the heart in an *in vivo* model of myocardial stunning (Yan *et al.*, 2005). In severe cases when cells die during reperfusion, it is however a question of whether cells die “with autophagy” or “by autophagy” (Matsui *et al.*, 2007; Nishida *et al.*, 2009).

Autophagy is stimulated during myocardial ischaemia as a result of glucose deprivation and low oxygen supply (Codogno & Meijer, 2005; Matsui *et al.*, 2007; Nishida *et al.*, 2009). However, during periods of severe ischaemia, when ATP is profoundly depleted, autophagy may be limited. This may also severely limit the protective effects of autophagy during ischaemia. In the case of myocardial infarction, autophagy may only occur at the border zones of the infarcts where the myocardium could obtain oxygen from adjacent areas through diffusion (Nishida *et al.*, 2009).

Autophagosomes are present during both ischaemia and reperfusion. An explanation for this might be that autophagy is present during ischaemic conditions to replenish the energy production and then during reperfusion switch to clearing up damaged organelles which accumulated during ischaemia (Matsui *et al.*, 2007; Takagi *et al.*, 2007). This clearance of or

eliminating damaged organelles during reperfusion may be beneficial as these organelles could result in increased oxidative stress and cellular dysfunction (Nishida *et al.*, 2009).

Autophagosomes have been found to contain mitochondria during ischaemia, suggesting that a large cytosolic fraction and many organelles can be destroyed during excessive autophagy, under severe stress. These autophagosomes were also found to release pro-apoptotic factors which lead to apoptotic cell death (Nishida *et al.*, 2009). A calcium-activated protease, calpain, has also been found to be involved in autophagy during ischaemia as it cleaves Atg5, which translocates to the mitochondria, binds to Bcl-2 and induces apoptosis (Murphy & Steenbergen, 2008).

As a result of glucose deprivation, during ischaemia, ATP pools are depleted, causing inhibition of mTOR, by activation of adenosine monophosphate (AMP)-activated protein kinase (AMPK) and subsequent autophagy stimulation. However, in the heart, AMPK also causes phosphorylation of eukaryotic elongation factor-2 (eEF2) by eEF2 kinase, resulting in autophagy stimulation (Matsui *et al.*, 2007; Nishida *et al.*, 2009). The work of Matsui *et al.* also suggests that in the heart, ischaemia stimulates autophagy through an AMPK-dependent mechanism, whereas ischaemia/reperfusion stimulates autophagy through Beclin-1 but AMPK-independent mechanism (Matsui *et al.*, 2007).

However, it has been shown that cell death during reperfusion was significantly decreased in the presence of the autophagy inhibitor, 3-methyladenine, or knockdown of beclin1, *in vitro*. During both ischaemia and

reperfusion, beclin1 expression has been found to increase. Beclin1 is known to be partially responsible for autophagy upregulation. This suggests that autophagy may very well be detrimental during myocardial ischaemia/reperfusion (Nishida *et al.*, 2009). Increased beclin-1 expression observed during reperfusion is thus associated with upregulation of autophagy and detrimental to the cardiac myocytes during these conditions.

2.3.2.2. Autophagy and MKP-1 signaling

Evidence is emerging for a role for the MAPKs in autophagy. In colorectal cancer cell lines, proapoptotic p38 α MAPK inhibition resulted in autophagic cell death (Comes *et al.*, 2007). p38 MAPK activity is involved in the negative control of autophagy in the human liver, in response to cellular hydration (vom Dahl *et al.*, 2001).

It has been shown that JNK activation is needed for endoplasmic reticulum (ER) stress induced autophagy. The results in this particular study indicated that JNK activation in the early phase of ER stress was needed to activate autophagy, although it did not lead to apoptosis. Sustained activation of JNK for 24 h by ER stress was required to cause apoptosis (Ogata *et al.*, 2006). More recently, it was shown that JNK activation leads to autophagic cell death in HCT116 cells. This occurred as JNK resulted in upregulation of Beclin-1 expression and caused induction of Bcl-2 and p53 phosphorylation, with subsequent autophagic cell death (Park *et al.*, 2009). It has also been shown that in an initial response to nutrient starvation in HeLa cells, lower

levels of Bcl-2 phosphorylation associated with lower JNK activity occur to promote cell survival by Bcl-2/Beclin-1 complex disruption, resulting in autophagy. However, after prolonged starvation, increased JNK activity is associated with higher levels of Bcl-2 phosphorylation, subsequent Bcl-2/Bax complex disruption, resulting in apoptosis (Wei *et al.*, 2008).

Evidence exists for a role of ERK activation in autophagy stimulation. In human colon cancer HT-29 cells, it was seen that ERK activation stimulates autophagy (Ogier-Denis *et al.*, 2000; Pattingre *et al.*, 2003). It was shown that cytoplasmic sequestration of ERK can promote autophagy in human ovarian cancer cells (Bartholomeusz *et al.*, 2008). ERK has been associated with autophagy and autophagic cell death in response to a variety of stresses such as amino acid depletion in human colorectal cancer cell line (HT29) (Ogier-Denis *et al.*, 2000), cadmium in the mesengial MES-13 cell line (Wang *et al.*, 2008; Yang *et al.*, 2009) and tumor necrosis factor (TNF)- α treatment in the breast cancer MCF-7 cell line (Sivaprasad & Basu, 2008; Cagnol & Chambard, 2010).

Not much is known about the role of MKP-1 in autophagy. To our knowledge, the only direct link found between MKP-1 and autophagy was discovered recently when it was observed that an areca nut extract (ANE), a carcinogen and addictive substance often used in Asia, causes induction of autophagy, which was mediated through p38 MAPK and MKP-1 activation, in oral cancer cells. ANE-induced autophagy inhibited apoptosis in this scenario (Lu *et al.*, 2010).

2.3.3 Apoptosis

Apoptosis, or Type I cell death, was first introduced by Kerr (1971) but was termed “shrinkage necrosis”, as necrosis was the only type of cell death known at the time (Kerr, 1971; Kerr *et al.*, 1972). The cytological changes which are observed during the process of cellular self-destruction are defined as apoptosis. Apoptosis has also been termed “programmed cell death” (PCD) as it requires controlled gene activation. This process can therefore be regulated by gene expression alteration (Elmore, 2007). Control of the apoptotic process is tightly linked to the progression of cells through the cell cycle.

The earliest morphological changes that take place in a cell undergoing apoptosis have been identified by light and electron microscopy (Hacker, 2000). During early apoptotic processes, cell shrinkage and pyknosis are visible (Kerr *et al.*, 1972). Chromatin is condensed as a result of pyknosis, organelles are tightly packed and the cells are visibly smaller during cell shrinkage. Cell surface changes, plasma membrane blebbing and the disappearance of the nucleolus can also be observed (Kanduc *et al.*, 2002; Elmore, 2007; Gozuacik & Kimchi, 2007; Vandenabeele *et al.*, 2008). DNA is then fragmented by a variety of nucleases into high molecular weight fragments and later on into fragments, the size of nucleosomes. Cells eventually are broken into apoptotic bodies which are phagocytosed by macrophages (Elmore, 2007). Inflammation does not occur because intracellular contents of the apoptotic cell are not released and apoptotic

bodies are quickly phagocytised preventing secondary necrosis from occurring (Savill, 2000; Kurosaka *et al.*, 2003) .

Two pathways of apoptosis have been characterised; the **extrinsic pathway**, i.e. the receptor mediated pathway (Ashkenazi & Dixit, 1998) and the **intrinsic pathway** also known as the mitochondria mediated pathway (Green & Reed, 1998). These two pathways are not separated from one another but are known to share cross-talk.

A key phenomenon of apoptotic cell death is the activation of a unique class of aspartate-specific proteases known as caspases. Three classes of caspases are known, of which 2 classes play important roles in apoptosis. These two classes are the initiator caspases -2, -8, -9 and -10 and the executioner caspases -3, -6 and -7. The third class are inflammatory caspases -1, -4, -5, -11 and -12. Initiator caspases are activated by autocleavage and then in turn cleave executioner caspases to activate them. The activated executioner caspases in turn cleave other substrates such as cytokeratins and poly (ADP-ribose) polymerase (PARP) (Slee *et al.*, 2001). Both intrinsic and extrinsic pathways merge at the activation of the executioner caspases-3, -6 and -7.

The **extrinsic pathway** involves transmembrane receptor-mediated interactions involving death receptors which are members of the TNF receptor gene superfamily, and include the Fas/CD95 and the TNF-related apoptosis-inducing ligand (TRAIL) receptors (Locksley *et al.*, 2001; Vicencio *et al.*, 2008). The cytoplasmic sequence divides the TNF receptor gene superfamily into two main subgroups of receptors that either possess or lack

a death domain (DD) (Tartaglia *et al.*, 1993). The death receptors interact via their DD with intracellular DD-containing adaptors, such as Fas associating protein with DD (FADD) and TNF receptor-associated death domain (TRADD), and recruit these adaptors to the cell membrane. Thus, binding of Fas ligand to Fas receptor leads to clustering of the Fas receptors DD. The adaptor, FADD, then binds through its own DD to the cluster receptor DD. FADD also contains a death effector domain (DED). Dimerization of the death effector domain then results in the association between FADD and procaspase-8. The death-inducing signaling complex (DISC) is then formed. DISC formation allows procaspase-8 to be activated by auto-catalytic activation to caspase-8 (Kischkel *et al.*, 1995).

The **intrinsic pathway** produces intracellular signals aimed toward intracellular targets and mitochondrial-initiated events. These mitochondrial events are regulated by the Bcl-2 protein family which governs mitochondrial membrane permeability. Members of the Bcl-2 family include both anti-apoptotic proteins, such as Bcl-2, Bcl-x_L, Bcl-1 and Bcl-w, and pro-apoptotic proteins such as Bax, Bad, Bid or Bim (Cory & Adams, 2002; Elmore, 2007). The Bcl-2 family, in turn is regulated by the tumour suppressor protein, p53 (Schuler & Green, 2001). During mitochondrial apoptosis, opening of the mitochondrial permeability transition pore (MPTP), resulting from changes in the inner mitochondrial membrane, occurs. Two of the pro-apoptotic protein groups which are released from the intermembrane space into the cytosol (Saelens *et al.*, 2004), include cytochrome *c* and Smac/DIABLO. Cytochrome *c* is involved in the formation of the apoptosome when it binds to and activates Apaf-1 and procaspase-9 (Chinnaiyan, 1999) which leads to

activation of caspase-9. The other group of pro-apoptotic proteins, which includes the apoptosis inducing factor (AIF), endonuclease G and caspase-activated deoxyribonuclease (CAD), are released from the mitochondria when the cell has undergone a death commitment, and are involved in chromatin condensation. After cleavage by caspase-3, CAD leads to DNA fragmentation and advanced chromatin condensation (Elmore, 2007). Apoptotic events are also regulated by AIPs which act as apoptotic inhibitors. The regulation by the Bcl-2 family of proteins and AIPs result in a controlled network of protein-protein interactions which ensure accuracy of the cell-death machinery.

The extrinsic and intrinsic pathways are interrelated and have points of cross-talk. The receptor-mediated pathway is connected to the mitochondrial pathway via Bid. Proteolytic cleavage of Bid to generate truncated Bid (tBid) by caspase-8 lead to the translocation of tBid to the mitochondria where it mediates membrane permeabilization (Korsmeyer *et al.*, 2000).

Another hallmark of apoptosis is PARP cleavage by the caspases. In response to DNA fragmentation PARP binds to DNA fragments and catalyzes poly(ADP)-ribosylation of many proteins by conversion of nicotinamide adenine dinucleotide (NAD) to nitric acid monohydrate (NAM) and ADP-ribose (Zong & Thompson, 2006). PARP preferentially depletes cytosolic NAD during this process, as cytosolic and mitochondrial NAD do not freely exchange across the inner mitochondrial membrane. This NAD depletion results in glucose catabolism which prevents glucose-dependent ATP production (Berger *et al.*, 1983), a situation which can be worsened

under ischaemic conditions. In case of inhibition of glucose breakdown, the activation of PARP could induce necrosis, unless NAD pools are replenished (Zong & Thompson, 2006). Cleavage of PARP by caspases thus prevents energy depletion and induction of necrosis. Caspases are thus not only important in apoptotic regulation but also in necrotic inhibition (Zong *et al.*, 2004; Zong & Thompson, 2006).

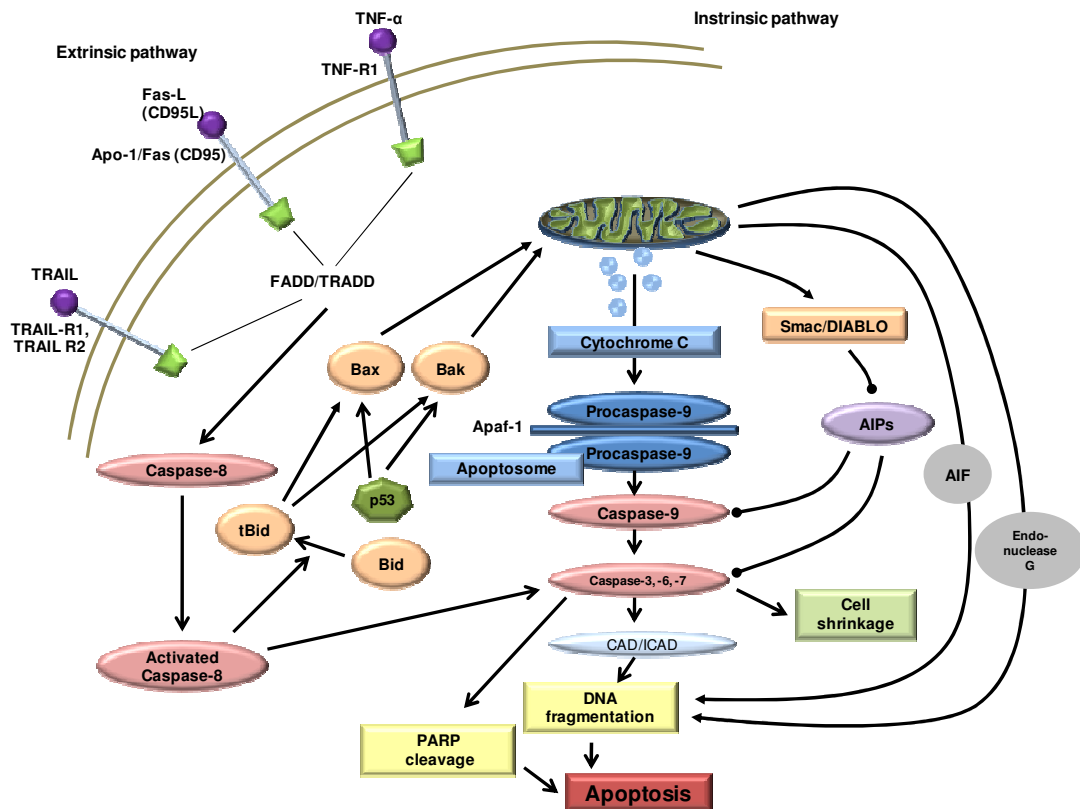


Figure 2.4: Apoptosis

(modified from www.cellsignal.com/reference/pathway/Apoptosis_Overview.html)

Apoptosis is essential for removal of target cells in multicellular organisms through the process of apoptotic body formation and phagocytosis (Peter *et*

al., 2008). Apoptosis occurs in a variety of processes, such as development and function of the immune system, embryonic development and normal cell turnover (Elmore, 2007). It is even known to contribute to morphological generation of the heart, during embryogenesis. After birth apoptosis is also involved in the morphological generation of the heart's conduction system, which includes the sinus node, the AV node and the bundle of His (James, 1994). In healthy multicellular organisms, cell proliferation and death occur in equilibrium, however, if this is not the case it may lead to subsequent developmental abnormalities and cancer cell growth. Abnormalities in apoptotic processes may be a result of many conditions which include ischaemic damage or cancer (Takemura & Fujiwara, 2006; Elmore, 2007).

2.3.3.1 Apoptosis and ischaemia/reperfusion

Myocardial ischaemia may lead to cardiomyocyte death which has been associated with apoptosis (Kajstura *et al.*, 1996). *In vivo* apoptosis in cardiomyocytes exposed to ischaemia/reperfusion, was first shown in rabbit hearts by Gottlieb *et al.* (Gottlieb *et al.*, 1994). Since then many other studies have investigated the relationship between apoptosis and myocardial ischaemia.

Although ischaemia may lead to initiation of apoptosis, prolonged ischaemia results in necrotic cardiomyocyte death (Freude *et al.*, 2000; Elmore, 2007). If ATP is restored during reperfusion, it allows for apoptotic processes, initiated by ischaemia, to proceed (Freude *et al.*, 2000).

It has been shown that deletion of proapoptotic proteins or increased expression of antiapoptotic proteins lead to reduced ischaemia/reperfusion mediated cell death. It is also interesting to note that it is likely that antiapoptotic proteins can not only reduce apoptotic cell death but also reduce necrotic and autophagic cell death (Murphy & Steenbergen, 2008). Caspase cleavage is thought to be an important mechanism and marker of apoptotic cell death. The majority of studies have found that infarct size was reduced during ischaemia/reperfusion, in the presence of caspase inhibitors (Okamura *et al.*, 2000; Mersmann *et al.*, 2008).

2.3.3.2 Apoptosis and MKP-1 signaling

As MKP-1 is known to dephosphorylate the MAPKs, it is therefore expected to also play a role in ischaemia/reperfusion injury and apoptosis. MKPs act in opposition of MAPKs by dephosphorylation and inactivating them, thus regulating the physiological outcome of signaling to induce cell survival or cell death. However, the relationships between the MAPK pathways involved in the induction of MKP-1 and those that regulate cell survival or cell death are less clear.

Increased JNK activation mediates cell death in MKP-1^{-/-} cells exposed to cisplatin, while inhibition of p38 MAPK prevents cell death after serum starvation and anisomycin treatment (Wu & Bennett, 2005). Furthermore, it is also known that caspase-3 cleavage and thus apoptosis can be induced via a p38 MAPK dependent pathway. It has been found that insulin stimulated

MKP-1 expression, inhibits caspase-3 cleavage, as MKP-1 dephosphorylates p38 MAPK. MKP-1 induction by insulin thus exerts a cardioprotective effect and also protects the heart from p38 MAPK induced injury (Morisco *et al.*, 2007).

2.3.4 Necrosis

Necrosis, also known as Type III cell death, is a pathological cellular response resulting from stressful stimuli such as ischaemia or UV radiation. It is a passive process requiring no ATP. Necrotic cells are morphologically characterised by disrupted membrane, cytoplasmic and mitochondrial swelling, disintegration of organelles and complete cell lysis, followed by DNA fragmentation (Zong & Thompson, 2006). Unlike apoptosis, necrosis results in inflammation, as these severely damaged cells do not form membrane-bound vesicles.

Until recently it has been accepted that necrosis is an uncontrolled, accidental process of cell death (Zong & Thompson, 2006). It is however becoming more evident that cells can initiate their own necrotic death, and in doing so, initiate inflammatory and reparative responses. This idea of programmed necrotic cell death can be seen as a way in which tissue integrity can be maintained (Zong & Thompson, 2006). It is evident that an increasing number of signal transduction pathways are involved in the execution of necrotic cell death (Festjens *et al.*, 2006; Zong & Thompson, 2006; Golstein & Kroemer, 2007). In the presence of caspase inhibitors or

the absence of FADD, an important adaptor protein involved in caspase-8 activation, it has been shown that necrotic cell death can be induced. This induction was shown to occur via TNF, TNF-related apoptosis-inducing ligand (TRAIL) and Fas ligand, using receptor interacting protein (RIP) as an effector molecule (Holler *et al.*, 2000). RIP is a family of serine/threonine kinases which act as sensors of cellular stressors such as inflammation, DNA damage and T-cell receptor stimulation. Upon exposure to such stressor signals, RIP1 kinase is involved in the important life or death decisions. These stressors all result in the activation of similar responses such as the activation of nuclear factor- κ B (Holler *et al.*, 2000; Vandenabeele *et al.*, 2008). RIP1 holds a C-terminal DD which belongs to the superfamily DD, and is important for binding to death receptors like TNF-receptor-1 and TRAIL-receptor 1. It has also been shown to be important for binding to DD-containing adaptor proteins such as TRADD and FADD (Vandenabeele *et al.*, 2008).

RIP1 is cleaved by caspase-8 during apoptotic signal transduction. This may explain why cells only undergo necrosis when apoptosis is blocked (Lin *et al.*, 1999; Vandenabeele *et al.*, 2008).

Secondary necrosis, resulting from apoptotic cells failing to be phagocytosed, can also give rise to cell death (Majno & Joris, 1995; Zong & Thompson, 2006). This form of necrotic cell death is usually observed *in vitro* in cultured cells where there is an absence of phagocytic cells. These cultured cells then lose their membrane integrity and release their cellular content. Secondary necrosis *in vivo* usually occurs when the clearance of

apoptotic cells is impaired, i.e. if phagocytic cells are unable to cope with the apoptotic load (Aderem & Underhill, 1999; Silva *et al.*, 2008).

2.3.4.1 Necrosis and ischaemia/reperfusion

During a cardiac ischaemic event, the supply of oxygen and nutrients is reduced as a result of decreased blood flow to a certain area. These conditions eventually contribute to necrotic cell death (Neumar, 2000; Zong & Thompson, 2006). Under these ischaemic conditions cells may switch from oxidative phosphorylation to glycolysis to maintain ATP production (Holt, 1983; Briddon *et al.*, 2004; Zong & Thompson, 2006). Inhibition of glycolysis in such circumstances by introduction of 2-deoxyglucose (2DG) induces necrosis (Zong & Thompson, 2006). As stated previously (see p. 34) necrosis results in an inflammatory response, which is an important component of ischaemia/reperfusion. Cell death by necrosis is largely dependent on energy depletion and membrane disruption. Calcium ions enter the cell once membrane damage has developed beyond a certain point, leading to irreversible damage. The extent of necrotic damage depends foremost on the pre-existing collateral flow but also on the number and severity of the coronary artery occlusions, the degree of reperfusion and the overall metabolic state of the organism (Opie, 1991).

2.3.4.2 Necrosis and MKP-1 signaling

It has been shown that RIP1 interacts with and recruits many proteins, such as MEKK1 and MEKK3 through its intermediate domain (ID) (Vandenabeele *et al.*, 2008). RIP1 and TNF receptor-associated factors (TRAF)-2 are known to interact with p38 MAPK, JNK and ERK (Lee *et al.*, 1997; Lee *et al.*, 2003). It has also been seen that RIP1 kinase activity has implications in ERK activation (Devin *et al.*, 2003). RIP1 has not been found to be important in other MAPK activation (Lee *et al.*, 2004). To our knowledge no direct link between MKP-1 and necrosis has been shown.

2.3.5 Cross-talk between autophagic, apoptotic and necrotic signaling pathways

Autophagy, apoptosis and necrosis do not occur as isolated pathways, but instead interact through extensive cross-talk to ensure that a balance exists in the cell's death decision making processes. Cross-talk between apoptosis, autophagy and necrosis controls whether a cell lives or dies. Perturbation of the cross-talk between cell death mechanisms may determine the amount and characteristics of cell death (Thorburn, 2008).

The relationship between apoptosis and autophagy is complex. Autophagy may represent a stress adaptation to avoid cell death and thus suppress apoptosis. On the other hand, it may act as an alternative cell-death pathway. Autophagy and apoptosis may also be triggered by common

upstream signals, which may result in combined autophagy and apoptosis which may induce cell death in a coordinated fashion. Autophagy may also precede apoptosis leading to apoptotic cell death without resulting in death itself or thirdly, apoptosis may precede autophagy (Maiuri *et al.*, 2007).

Reactive oxygen species trigger apoptotic and autophagic activity (Yamaguchi *et al.*, 2003; Scherz-Shouval *et al.*, 2007). p53 is also known to regulate both apoptosis and autophagy. Apoptosis is induced through expression of p53-upregulated modulator of apoptosis (PUMA) which leads to cytochrome c release from the mitochondria and autophagy, by targeting damage-regulated autophagy modulator (DRAM) and participating in autophagolysosome formation. DRAM is required for p53-induced apoptosis, which suggests that DRAM is upstream from apoptosis (Crichton *et al.*, 2006; Green & Chipuk, 2006). Autophagy was found to be involved in the caspase-independent apoptotic pathway and regulated by components of the caspase-dependent apoptotic pathway. Anti-apoptotic proteins Bcl-2 and Bcl-x_L, have an interaction with Beclin1 and are so linked to the autophagic pathway, where Bcl-2 inhibits Beclin-1 dependent autophagy (Hamacher-Brady *et al.*, 2006; Nishida *et al.*, 2008).

Necrosis can be induced by the inhibition of both apoptosis and autophagy (Golstein & Kroemer, 2007). It has also been suggested that necrosis may occur as a result of an unsuccessful autophagic survival response (Maruyama *et al.*, 2008). RIP1, known to be involved in necrosis regulation, is required for the autophagic response induced by caspase-8 inhibition (Xu *et al.*, 2006; Yu *et al.*, 2006). In *C. Elegans* it was shown that autophagy is

induced early on in necrotic cell death and that inhibition of autophagy results in necrosis suppression (Samara *et al.*, 2008). Autophagy is needed for induction of necrosis in response to endoplasmic reticulum stress in *Bax*^{-/-}/*bak*^{-/-} mouse embryonic fibroblasts which are unable to activate apoptosis (Ullman *et al.*, 2008).

In general, suppression of one of the cell death pathways results in the activation of another, with no significant improvements on long term cell survival (Galluzzi *et al.*, 2008).

CHAPTER 3

Materials and methods

3.1 Cell culture

H9c2 rat heart myoblasts from the European Collection of Cell Cultures (ECACC) was selected as experimental model. H9c2 cells were cultured in an incubator maintained at 37°C and 95% humidified atmosphere of 5% CO₂ and 21% O₂, in growth medium. Growth medium consisted of Dulbecco's modified Eagle medium (DMEM), supplemented with 10% fetal bovine serum (FBS), 1% L-glutamine and 1% penicillin/streptomycin. When cultures were 70-80% confluent, they were passaged. Cells were not passaged higher than passage 11. Cells were rinsed with phosphate buffered saline (PBS) (Sigma-Aldrich, South Africa) and trypsinised (0.25% Trypsin – ethylene diamine tetra-acetic acid (EDTA) (Sigma-Aldrich, South Africa). Cells were then centrifuged at 1500 rpm for 3 minutes. Appropriate numbers of cells were seeded in fresh warm growth medium in appropriate sized flasks.

3.2 Experimental protocol

3.2.1 Normoxic groups

Normoxic conditions created for cells were 5% CO₂/21% O₂ at 37°C in 95% humidified air. Three normoxic groups (norm) were used. One was used as a control (con); one was treated with 10 µM dexamethasone (dex) (Fan *et al.*,

2009) and the other with 10 μ M sanguinarine (sc) (Vogt *et al.*, 2005). Both dexamethasone and sanguinarine were suspended in warm growth medium.

The growth medium that the cells were cultured in was removed and the appropriate growth medium; with or without treatment, was added to the respective culture plates. Cells were treated for the duration of the protocol in normoxic conditions.

3.2.2 Ischaemic groups

Ischaemic conditions were created by exposing cells to 5% CO₂/1% O₂ at 37°C in 95% humidified air, in an ischaemic buffer, pH 6.4, containing (in mM): 137 NaCl, 12 KCl, 0.5 MgCl₂, 0.9 CaCl₂, 20 HEPES and 20 2-deoxyglucose (2DG) (Sigma-Aldrich, South Africa). Three ischaemic groups were created, one untreated, control group, a dexamethasone treated group and a sanguinarine treated group.

The growth medium was removed from the cells and replaced with fresh growth medium for the control group and medium with 10 μ M dexamethasone and the other with 10 μ M sanguinarine for the treatment groups. Cells were treated for 30 min in normoxic conditions. The growth medium was then removed and replaced with ischaemic buffer supplemented with 2DG, again containing dexamethasone or sanguinarine in the appropriate groups. The cells were then exposed to ischaemic conditions for 3 hours. Thereafter ischaemic buffer was removed and replaced with fresh growth medium, with dexamethasone or sanguinarine. Cells were then

allowed to reperfuse for 30 min, where after they were analysed. Samples were analysed at two time points; after simulated ischaemia and after reperfusion.

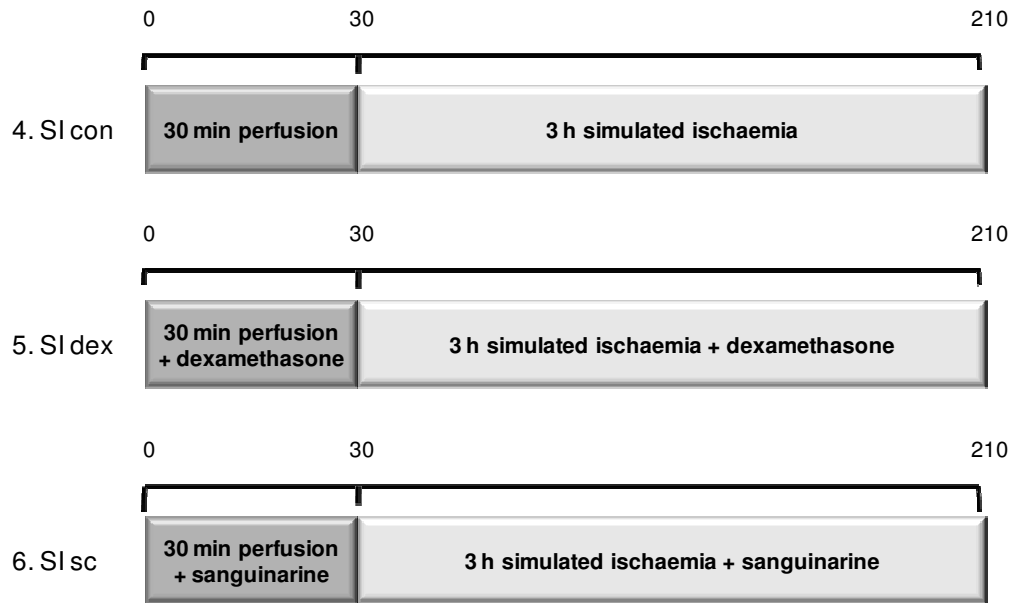


Figure 3.1: Treatment protocol for simulated ischemic treated groups: 4. Simulated ischaemia control (SI con), 5. Simulated ischaemia dexamethasone (SI dex), 6. Simulated ischaemia sanguinarine (SI sc).

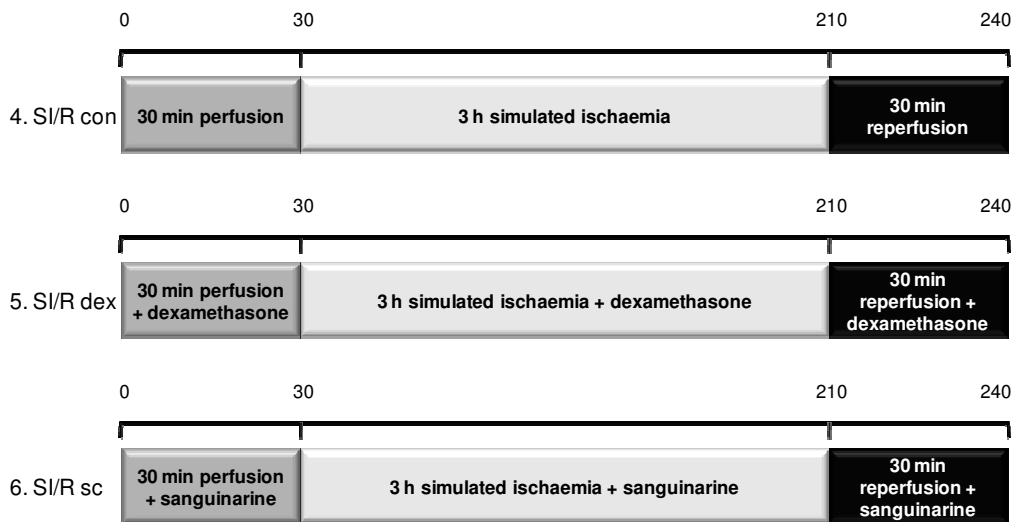


Figure 3.2: Treatment protocol for SI/R treated groups: 4. Simulated ischaemia/reperfusion control (SI/R con), 5. Simulated ischaemia/reperfusion dexamethasone (SI/R dex), 6. Simulated ischaemia/reperfusion sanguinarine (SI/R sc).

3.3 Western blot analysis

After treatment, cells were immediately placed on ice. Treatment medium was removed and cells were washed with cold PBS. Protein was extracted with lysis buffer (modified radioimmunoprecipitation (RIPA) buffer (see appendix B, P207). When MKP-1 induction was evaluated, MKP-1 lysis buffer was used instead of RIPA buffer (see appendix B, P206).

Eppendorfs containing cell lysates were centrifuged in a pre-cooled (0-4°C) centrifuge, at 8000 rpm for 10 minutes. The supernatant containing the cell contents were decanted into new eppendorfs that have been on ice. Protein concentrations of the supernatant were determined by the Bradford assay (Bradford, 1976) (see Appendix A, P195). The supernatant was used for Western blotting. Lysates were diluted in Laemmli sample buffer, pH 6.8, containing: Tris 0.5 M, 10% SDS, 2.5 ml glycerol, 0.2 ml 0.5% bromophenyl blue and deionized water. Samples were then boiled for 5 min and centrifuged at 5000 rpm for 20 seconds.

Proteins were separated with sodium dodecyl sulphate polyacrylamide gel electrophoresis (SDS-PAGE) (10% or 12% polyacrylamide gels were used, depending on the molecular weight of the protein being probed for). The Mini-Protean BIO RAD system was used. Proteins were then transferred to polyvinylidene fluoride (PVDF) membranes (Immobilon, Millipore, USA). Membranes were blocked in 5% (w/v) non-fat dried milk powder in Tris Buffered Saline-Tween20 (TBS-T, 0.05%) for 1 to 2 hours at room temperature. This prevents non-specific binding of proteins. Membranes were incubated with primary antibodies overnight at 4°C, against the desired

proteins (see appendix A, P201). Membranes were then incubated at room temperature, in anti-rabbit horseradish peroxidase-conjugated secondary antibody (Amersham Biosciences) for 1 hour. An enhanced chemiluminescence (ECL) kit (Amersham Biosciences) was used to detect antibodies. Protein bands were visualised with x-ray film (Hyperfilm, Amersham Biosciences). Exposure times differed between antibodies used (table A5). Bands were then quantified with the use of densitometry using the UN-SCAN-IT® program (Silk Scientific Corporation, Utah, USA).

For the Western blotting protocol, see Appendix A, P197.

3.4 Cell viability analysis

3.4.1 MTT assay

Modification of the 3-[4, 5-dimethylthiazol-2-yl]-2, 5-diphenyl tetrazolium bromide (MTT) assay (Goodwin *et al.*, 1995) was used to assess mitochondrial reductive capacity. This assay is based on cells' capacity to reduce MTT into blue formazan pigments, mainly by mitochondrial enzymes of viable cells.

Treatment medium was removed from cells. 1.5 ml PBS and 500 µl MTT solution was slowly added to each well to prevent detachment of cells. The plate was covered with foil and incubated for 2 hours. 2 ml Isopropanol/Triton solution was added to each well. The plates were then put on a shaker to allow the cells to loosen and to allow cell membranes to lyse and release

formazan pigments. The contents of each well were centrifuged for 2 minutes at 1400 rpm. The absorbance values of the supernatant were read at 540 nm using a spectrophotometer. The Isopropanol/Triton solution was used as a blank.

For the MTT assay protocol, see Appendix A, P202.

3.4.2 LDH assay

The assay is based on the conversion of pyruvate to lactate and simultaneous reduced nicotinamide adenine dinucleotide (NADH) oxidation to NAD. The lactate dehydrogenase (LDH) activity is directly proportional to the rate of NADH decrease, and is a good indicator of necrosis. Spontaneous LDH release was subtracted from treatment groups to measure LDH released from membranes that lost integrity. Cells were grown in 96-well plates and subjected to treatments as described in 3.2.2. The appropriate cell concentration was determined by following the Cytotoxicity Detection Kit^{PLUS} (LDH) (Roche) protocol. After treatment LDH release was determined by using the Cytotoxicity Detection Kit^{PLUS} (LDH). The protocol was followed as indicated by the manufacturer's protocol. Thereafter the plates were read using an ELISA plate reader and the percentage cytotoxicity determined.

3.4.3 Propidium iodide (PI) and Hoechst staining

Necrotic cell death can be indicated by the loss of membrane integrity (Festjens *et al.*, 2006). Propidium iodide (PI) (Sigma) is a DNA intercalating dye which only enters cells whose membranes are not intact. Thus, when a cell's nucleus is stained with PI it is a well established indicator of cells which have lost their membrane integrity (PI positive).

Nuclear condensation (pyknosis) has been described as a morphological marker for apoptosis (Kajstura *et al.*, 1996). Hoechst (Hoechst 33342, Sigma), a DNA intercalating dye, diffuses through intact cellular membranes and allows one to distinguish between apoptotic nuclear morphology (bright, condensed nuclei) and normal nuclear morphology.

Hoechst 33342 and PI were dissolved in warm sterile 0.1 M PBS to a 1:200 working solution, ensuring final concentrations of 50 µg/ml and 1 µg/ml, respectively. Treatment medium was removed from cells. Cells were incubated with PI/Hoechst solution for 5 minutes. Finally, they were visualised and random fields of view were acquired using the automatic stage setting (Olympus Cell^R Soft Imaging Systems). Images were excited with the 360nm and 572 nm excitation filter, using a Xenon-Arc burner (Olympus Biosystems GMBH) as light source and emission was collected using a UBG triplebandpass emission filter cube (Chroma).

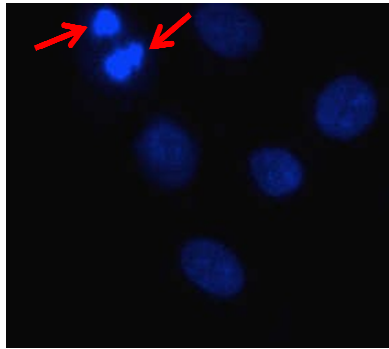


Figure 3.3: Fluorescence micrograph showing normal and pyknotic (arrows) nuclei of H9c2 cells.

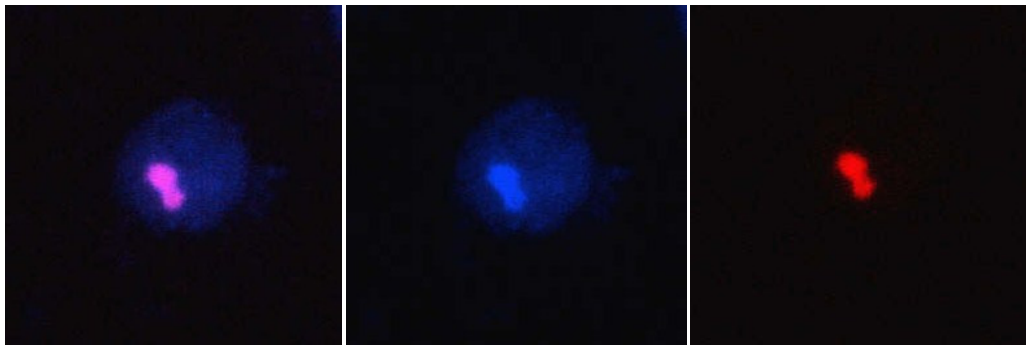


Figure 3.4: Fluorescence micrograph showing late pyknotic nuclei of H9c2 cells.

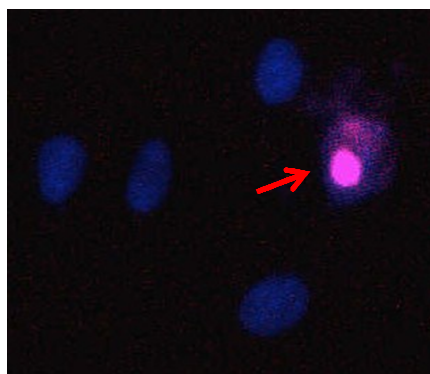


Figure 3.5: Fluorescence micrograph showing normal (PI negative) and PI positive (arrow) nuclei of H9c2 cells.

3.4.4 LysoTracker[®] Red labelling

LysoTracker Red DND-99 is a cationic red-fluorescent dye that accumulates in acidic lysosomal compartments in live cells. In cell culture the amount of dye taken up by the cells can be used as an indicator of lysosome content, which in turn is an indirect measure for the autophagic activity in the cell (Stern *et al.*, 2008).

After treatment LysoTracker (1 mM) and Hoechst 33342 (a 1/200 dilution, from 5 µM stock), suspended in warm PBS, was added to each well and allowed to incubate for 5 min. Cells were then visualised and images acquired.

3.4.5 Flow cytometry

To confirm the observations obtained from the lysotracker labelled cells, cells were incubated with acridine orange and analysed by flow cytometry. Acridine orange is DNA intercalating dye, which fluoresces green (510-530 nm), and also binds to acidic compartments such as lysosomes, where it fluoresces red (>650 nm). Acidic vesicles are known to develop during autophagy and acridine orange has been used to detect and quantify these (Paglin *et al.*, 2001).

After treatment, cells were washed with warm PBS and trypsinised. Thereafter, warm growth media, equal to double the volume of trypsin was added to each flask. Cells were centrifuged at 1500 rpm for 3 min and

resuspended in warm acridine orange (Sigma-Aldich, South Africa; working solution made up in PBS in a 1/100 dilution, using a 5 mM final concentration). Green and red fluorescence emission was collected with the 488 nm laser and analysed with a flow cytometer (BD FACSAria I). A minimum of 5000 events were collected.

Red fluorescence of all groups was compared as a percentage of the control to give an indication of the degree of acidity in cells.

3.5 Determination of 2-deoxy-D-³[H] glucose uptake

2DG uptake was measured as previously described (Donthi *et al.*, 2000). Cells were cultured to 60-70% confluency after which they were serum starved overnight in DMEM. Cells were then washed twice with a solution (solution A) which contained in mM: KCl 6, Na₂HPO₄ 1, NaH₂PO₄ 0.2, MgSO₄ 1.4, NaCl 128, HEPES 10, CaCl₂ 1.25 and 2% free fatty acid BSA. Cells were then deprived of all substrates that may be present in the culture medium for 3 hours, by incubation at 37°C in a humidified atmosphere, in solution A. After 3 hours the solution was aspirated. Myocyte glucose uptake was measured in Solution A. Cells were stimulated with or without insulin for 15 min, in duplicate. Thereafter, they were incubated with 1.5 µCi/ml 2DG (PerkinElmer, Boston) in a final concentration of 1.8 µM deoxyglucose for 30 min. 400 µM phloretin was added to stop the carrier-mediated (Glut 1 and Glut 4) glucose uptake. The medium containing the 2DG was then aspirated. Cells were washed twice with a basic buffer that contained in mM: KCl 6,

Na₂HPO₄ 1, MgSO₄ 1.4, NaH₂PO₄ 0.2, NaCl 128 and HEPES 10 . Following this, cells were lysed with 250 µl of 1 M NaOH at 70°C in a waterbath for 15 min. To yield a concentration of 0.5 M NaOH, 250 µl distilled H₂O was added to the lysed cell samples.

To determine the cell-associated radioactivity, 150 µl of the cell lysates was mixed with 2 ml scintillation fluid. All measurements were done in duplicate and were kept overnight in the dark. A liquid scintillation counter (Beckman) was used for counting radioactivity.

The remaining 200 µl of the cell lysates was used for determination of protein content with the use of the Lowry method (Lowry *et al.*, 1951) (see Appendix A, P203).

3.6 Statistical analysis

Values were expressed as mean ± standard error of the mean (SEM). Multiple comparisons of more than 2 variables were made by two-way analysis of variance (ANOVA), followed by the Fisher post-hoc test. Comparisons of 2 variables were made by one-way ANOVA, followed by the Fisher post-hoc test. The statistics software, Graph Pad Prism 5 and Statistica 9, were used to perform statistical tests. Differences were considered significant at values of p<0.05.

CHAPTER 4

Pilot studies

A. Simulated ischaemic conditions

To investigate the role of MKP-1 in cell death during simulated ischaemia/reperfusion, a pilot study was done to determine appropriate simulated ischaemic conditions. Ischaemic conditions were simulated by creating an experimental environment for cells, where oxygen concentrations were lowered to 1% and metabolic parameters were altered with the use of a modified ischaemic buffer (Esumi *et al.*, 1991), with or without 2DG (Fuglestad *et al.*, 2008). In the presence of 2DG, glycolysis is inhibited by trapping phosphate as 2DG-phosphate, which further inhibits glycolysis, and so mimics ischaemic conditions. Cells were exposed to these conditions for 3 or 4 hours.

The mitochondrial viability based on MTT reduction, decreased significantly after 3h Esumi treatment and Esumi/2DG treatment and also after 4 h Esumi treatment and Esumi/2DG treatment, compared to the normoxic control cells. The reduction capacity of the Esumi treatment and the Esumi/2DG treatment for both 3 and 4 hours, differed significantly.

For the remainder of experiments simulated ischaemia was therefore mimicked by treating cells with modified ischaemic buffer supplemented with 2DG, for 3 hours.

B. MKP-1 inhibition

To investigate the role of MKP-1 in autophagic cell death, apoptosis and necrosis during ischaemia/reperfusion injury, it had to be investigated in both inhibited and induced states.

It has been shown that triptolide, a root extract from a Chinese medicinal vine, blocks the transcription of MKP-1 (Wang *et al.*, 2006). Therefore triptolide was investigated as a possible MKP-1 inhibitor for the current study. DMSO was used as a vehicle and did not significantly alter cell viability. However, no significant decrease of MKP-1 induction was found in the presence of triptolide (Fig 8.5).

Sanguinarine was then investigated as a possible MKP-1 inhibitor as it has been shown to selectively inhibit MKP-1 activity (Vogt *et al.*, 2005; Garcia *et al.*, 2006). A MTT assay was done to assess the relative viability of the cells in the presence of different sanguinarine concentrations to ensure the optimal concentration which does not cause damage to the cells under normoxic conditions. Methanol which was used as the vehicle did not significantly influence relative cell viability. 50 μ M sanguinarine treatment resulted in a significant decrease in relative viability based on MTT reduction (Fig 8.6). Furthermore, MKP-1 was significantly inhibited by 10 μ M sanguinarine (Fig 8.7). Sanguinarine at a concentration of 10 μ M was therefore used to inhibit MKP-1 induction.

C. MKP-1 induction

Insulin was investigated as a possible MKP-1 inducer as it is known that insulin induces MKP-1 activation (Jacob *et al.*, 2002; Morisco *et al.*, 2007). Insulin concentrations of 100 nM are suggested by literature for *in vitro* cardiac studies (Morisco *et al.*, 2007). In this study we found that insulin did not result in significant MKP-1 induction after ischaemia (Fig 8.8) or after reperfusion (Fig 8.12).

To determine whether the cells are in actual fact insulin sensitive, glucose uptake was measured in the presence of insulin. It was however not stimulated by insulin (Fig 8.35). H9c2 cells were therefore considered to be insulin resistant.

Attention was then turned to dexamethasone which is also known to result in increased MKP-1 induction (Fan *et al.*, 2009). A western blot was done to investigate dexamethasone induced MKP-1 activity, using three different concentrations (Lasa *et al.*, 2002; Vogt *et al.*, 2008; Fan *et al.*, 2009). MKP-1 induction was higher in cells treated with 10 μ M dexamethasone (Fig 8.37). 10 μ M dexamethasone was therefore used to induce MKP-1 induction.

No significant differences in autophagic activity were observed with MKP-1 inhibition after ischaemia, therefore western blots were done to investigate the role of MKP-1 in autophagy and apoptosis after simulated reperfusion, with the use of dexamethasone and sanguinarine (see sections 4.3 and 4.4).

For a detailed layout of the pilot studies see chapter 8.

Results

4.1 MKP-1 and MAPK signaling after 3 hrs stimulated ischaemia

Phosphorylation and dephosphorylation cascades involving MAPKs and MKP-1 play an important role in the signaling events during ischaemia/reperfusion. MKP-1 induction, p38 MAPK, ERK and JNK phosphorylation after 3 h simulated ischaemia, in the presence or absence of dexamethasone or sanguinarine, were investigated with the use of western blot analysis.

MKP-1 induction was significantly decreased after SI control treatment (64.38 ± 3.63) compared to normoxic control (100 ± 1.19) and normoxic sanguinarine (96.84 ± 3.54) treatments ($p < 0.001$). MKP-1 induction after simulated ischaemia was significantly lower in the SI sanguinarine (45.84 ± 4.36) groups compared to normoxic groups ($p < 0.001$) and SI control ($p < 0.01$). (Fig 4.1)

After simulated ischaemia, p38 MAPK phosphorylation was significantly higher in the presence of sanguinarine (327.4 ± 26.2) compared to the SI control (93.95 ± 6.65) treatments, and also when compared to normoxic control (93.19 ± 7.4) and -sanguinarine (139.5 ± 22.76) treatment groups ($p < 0.001$). (Fig 4.2)

The sum total of p44/p42 MAPK was compared between treatment groups. Significantly increased levels of phosphorylated ERK 1 and ERK 2 were present in normoxic control (77.91 ± 6.83) and -sanguinarine (84.46 ± 6.37)

groups compared to SI control (15.3 ± 1.88) ($p < 0.001$) and SI sanguinarine (56.74 ± 2.96) ($p < 0.05$) treated groups. After simulated ischaemia, ERK 1 and ERK2 were significantly more phosphorylated in the presence of sanguinarine than in control treated groups ($p < 0.001$). It is interesting to note that ERK phosphorylation was decreased after ischaemia in the control groups and that total ERK phosphorylation was lower compared to that of normoxic groups. Another interesting observation was that the total ERK in the SI control groups was lower than that seen in normoxic and SI sanguinarine groups. A possible explanation may be that ERK was not active after 3 hrs ischaemia, resulting in its breakdown (Fig 4.3).

The sum total of both isoforms of JNK was compared between treatment groups. After SI, JNK phosphorylation was significantly higher in normoxic control (280 ± 62.92) groups compared to SI sanguinarine treated groups (141.7 ± 51) ($p < 0.05$). It was observed that both total JNK isoforms were not seen. A possible explanation may be that inactivity of JNK may have resulted in its breakdown (Fig 4.4).

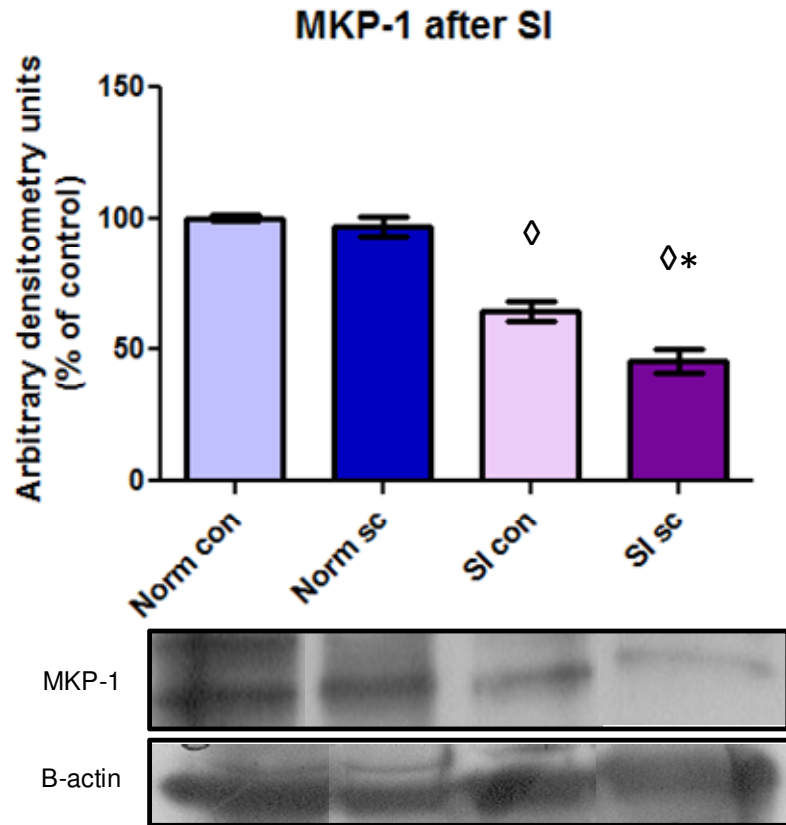


Figure 4.1: MKP-1 induction, showing normoxic control (Norm con), normoxic sanguinarine (Norm sc), simulated ischaemia control (SI con) and simulated ischaemia sanguinarine (SI sc). Data expressed as mean \pm SEM. \diamond p<0.001 vs. norm con and norm sc, *p<0.01 vs. SI con, n>3

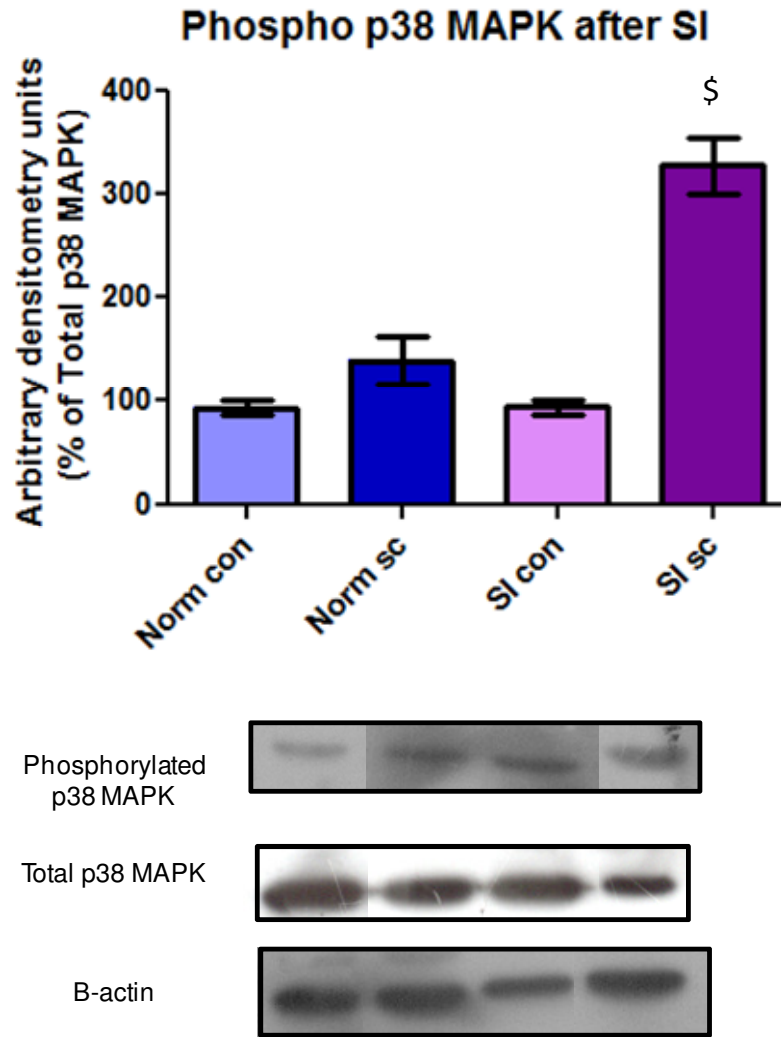


Figure 4.2: p38 MAPK phosphorylation, showing normoxic control (Norm con), normoxic sanguinarine (Norm sc), simulated ischaemia control (SI con) and simulated ischaemia sanguinarine (SI sc). Data expressed as mean \pm SEM. \$p<0.001 vs normoxic groups and SI con. n>3

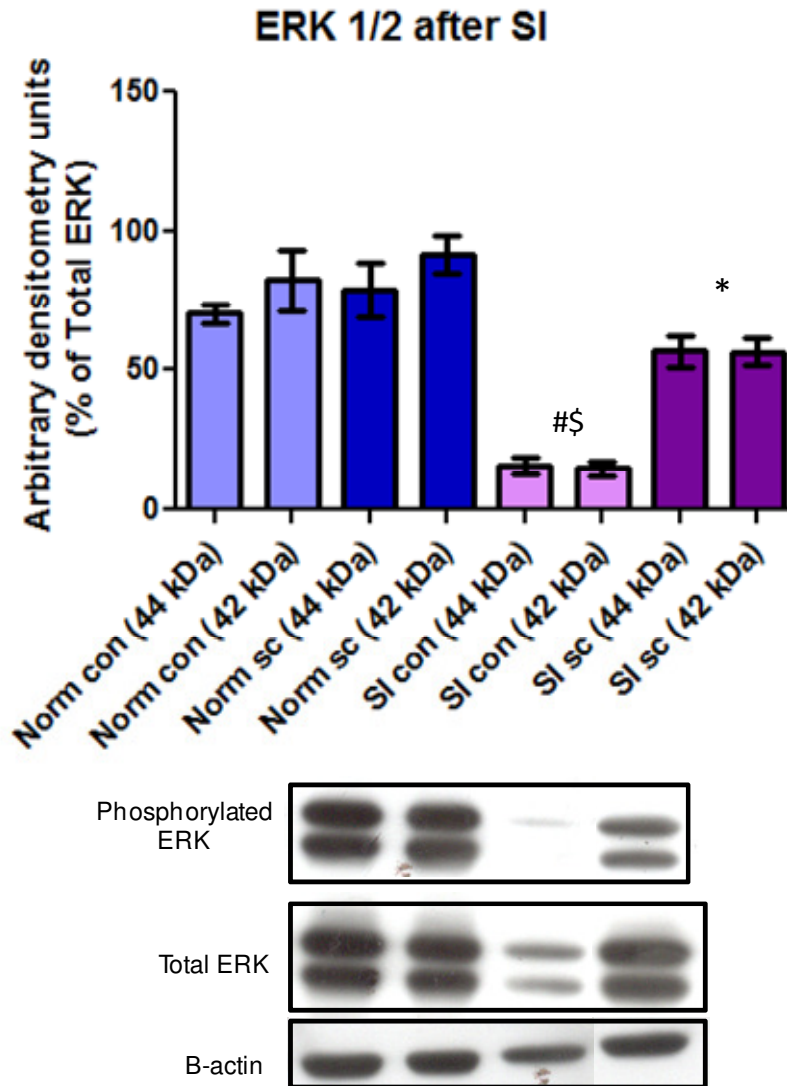


Figure 4.3: ERK 1 and 2 phosphorylation, showing normoxic control (Norm con), normoxic sanguinarine (Norm sc), simulated ischaemia control (SI con) and simulated ischaemia sanguinarine (SI sc). Data expressed as mean \pm SEM. # p <0.001 vs. normoxic groups, * p <0.05 vs. normoxic groups, \$ p <0.001 vs. SI sc. n >3

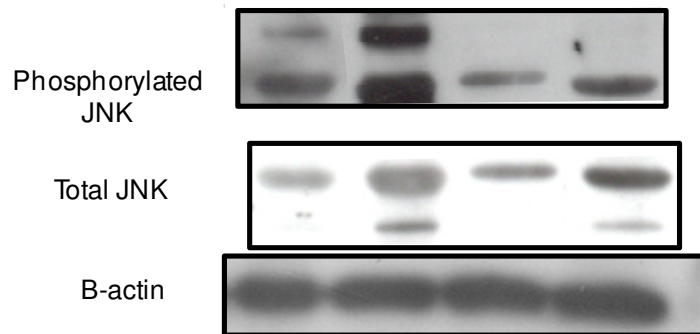
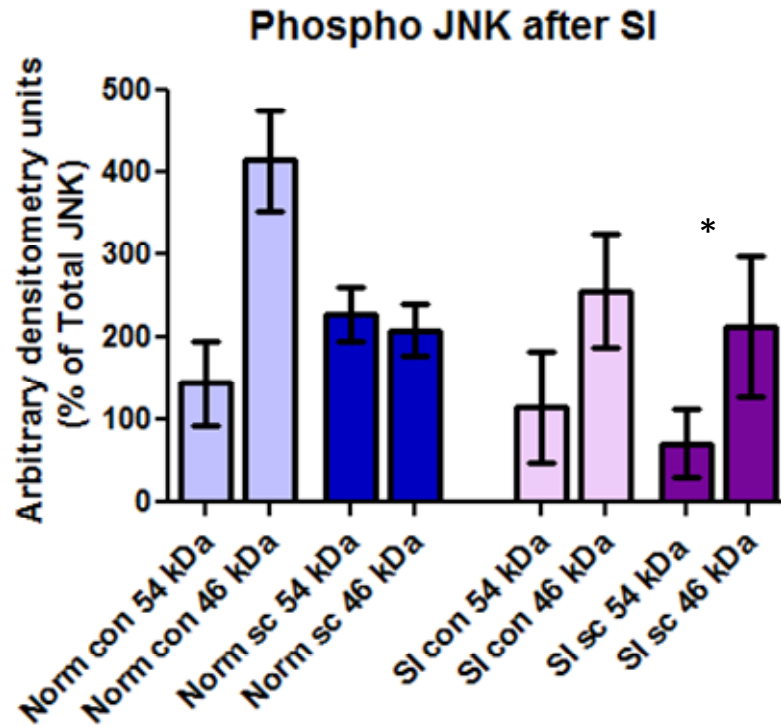


Figure 4.4: JNK phosphorylation, showing normoxic control (Norm con), normoxic sanguinarine (Norm sc), simulated ischaemia control (SI con) and simulated ischaemia sanguinarine (SI sc). Data expressed as mean±SEM. *p<0.05 vs. norm con. n>3

4.2 MKP-1 and MAPK signaling after 3 hrs simulated ischaemia/reperfusion

After SI/R the dexamethasone treated cells (105.2 ± 3.82) had significantly higher MKP-1 induction than normoxic dexamethasone (94.58 ± 1.85) ($p < 0.05$), normoxic sanguinarine (89.51 ± 3.1) ($p < 0.01$), SI/R control (90.64 ± 1.56) ($p < 0.01$), and SI/R sanguinarine (72.04 ± 2.83) ($p < 0.001$). MKP-1 induction was highest in SI/R groups in the presence of dexamethasone and lowest in the presence of sanguinarine. (Fig 4.5)

p38 MAPK phosphorylation was significantly higher after SI/R in the control group (124.2 ± 0.79) when compared to the normoxic control ($p < 0.05$), normoxic dexamethasone ($p < 0.001$) and normoxic sanguinarine ($p < 0.001$) groups, and even more so in the SI/R sanguinarine (157.2 ± 2.6) when compared to normoxic groups ($p < 0.001$). After SI/R, in the presence of dexamethasone (112.9 ± 1.3), p38 MAPK phosphorylation was significantly lower compared to the SI/R sanguinarine group ($p < 0.001$) and the SI/R control group ($p < 0.05$). p38 MAPK was significantly more phosphorylated in the SI/R sanguinarine compared to the SI/R control groups ($p < 0.001$). (Fig 4.6)

ERK phosphorylation was significantly higher in SI/R control cells (88.51 ± 1.9) compared to normoxic control (77.08 ± 6.79) ($p < 0.001$), -dexamethasone (80.52 ± 6.61) ($p < 0.001$) and -sanguinarine (90.62 ± 0.1) ($p < 0.05$) groups. Phosphorylated ERK levels were highest in the SI/R dexamethasone group (99.08 ± 2.27) compared to normoxic groups ($p < 0.001$), SI/R control ($p < 0.01$) and SI/R sanguinarine (63.75 ± 7.6)

($p < 0.001$) treated groups. After SI/R sanguinarine treatment ERK phosphorylation was the lowest compared to all other groups ($p < 0.001$). (Fig 4.7)

After reperfusion, JNK phosphorylation was significantly lower in normoxic sanguinarine groups (89 ± 11.89) compared to SI/R control (132.4 ± 12.56) and significantly higher than SI/R sanguinarine (44.69 ± 12.19) treated groups ($p < 0.05$). JNK phosphorylation was significantly lower in SI/R sanguinarine treated groups compared to normoxic control (119.5 ± 12.91) and SI/R control groups ($p < 0.001$). (Fig 4.8)

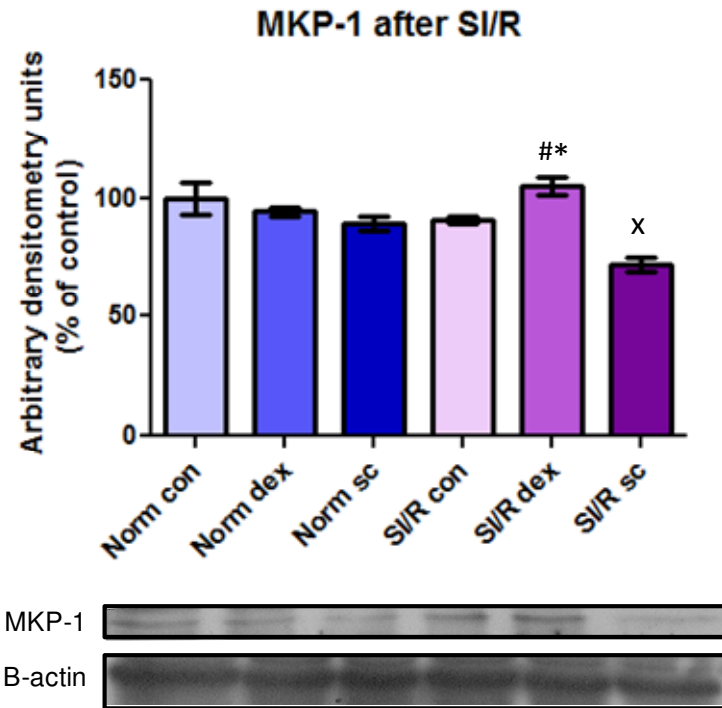


Figure 4.5: MKP-1 induction, showing normoxic control (Norm con), normoxic dexamethasone (Norm dex), normoxic sanguinarine (Norm sc), simulated ischaemia/reperfusion control (SI/R con), simulated ischaemia/reperfusion dexamethasone (SI/R dex) and simulated ischaemia/reperfusion sanguinarine (SI/R sc). Data expressed as mean \pm SEM. * p <0.05 vs. norm dex, # p <0.01 vs. norm sc and SI/R con, x p <0.001 vs. normoxic groups, SI/R con and SI/R dex, n >3.

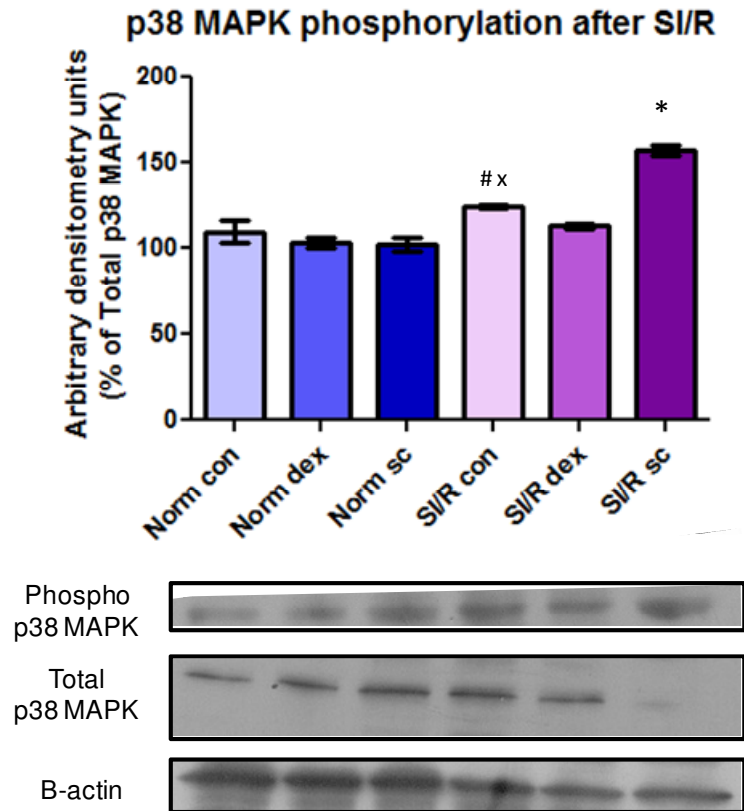


Figure 4.6: p38 MAPK phosphorylation, showing normoxic control (Norm con), normoxic dexamethasone (Norm dex), normoxic sanguinarine (Norm sc), simulated ischaemia/reperfusion control (SI/R con), simulated ischaemia/reperfusion dexamethasone (SI/R dex) and simulated ischaemia/reperfusion sanguinarine (SI/R sc). Data expressed as mean \pm SEM. * p <0.001 vs. normoxic groups, SI/R con and SI/R dex, $^x p$ <0.05 vs. norm con and SI/R dex, # p <0.001 vs. norm dex and norm sc, n >3.

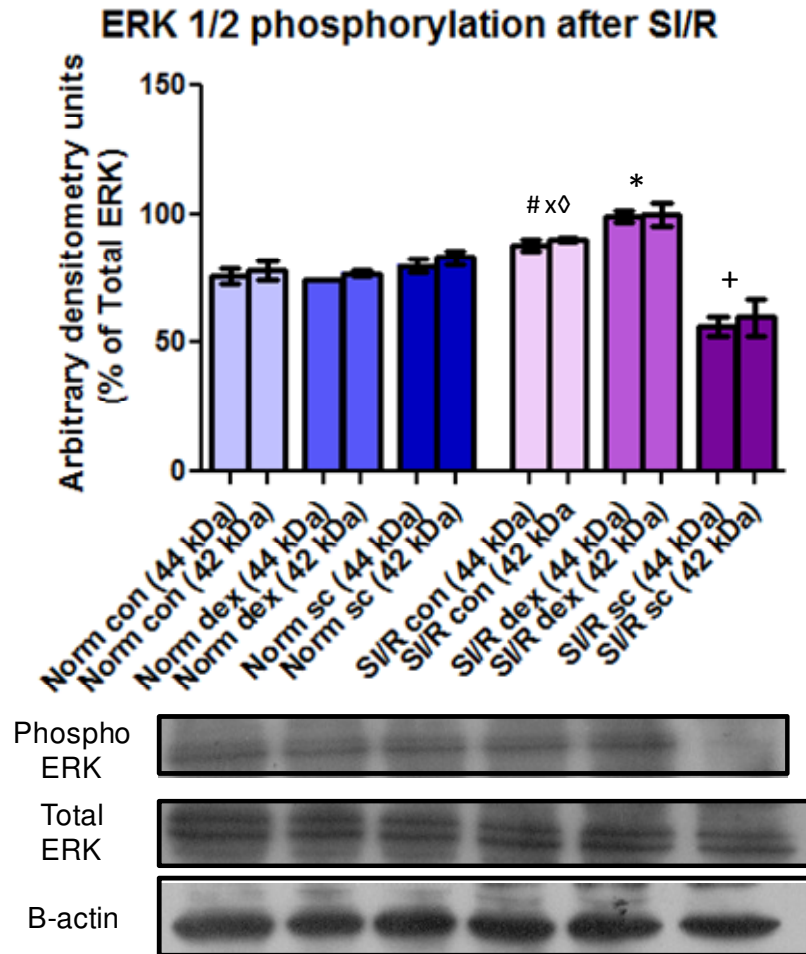


Figure 4.7: ERK 1 and 2 phosphorylation, showing normoxic control (Norm con), normoxic dexamethasone (Norm dex), normoxic sanguinarine (Norm sc), simulated ischaemia/reperfusion control (SI/R con), simulated ischaemia/reperfusion dexamethasone (SI/R dex) and simulated ischaemia/reperfusion sanguinarine (SI/R sc). Data expressed as mean \pm SEM. \diamond p<0.001 vs. norm con, norm dex and SI/R sc, $\#$ p<0.05 vs. norm sc, \times p<0.01 vs. SI/R dex, *p<0.001 vs. normoxic groups and SI/R sc, $^+$ p<0.001 vs. normoxic groups, n>3.

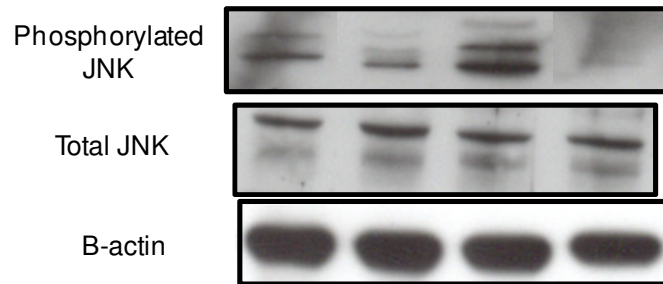
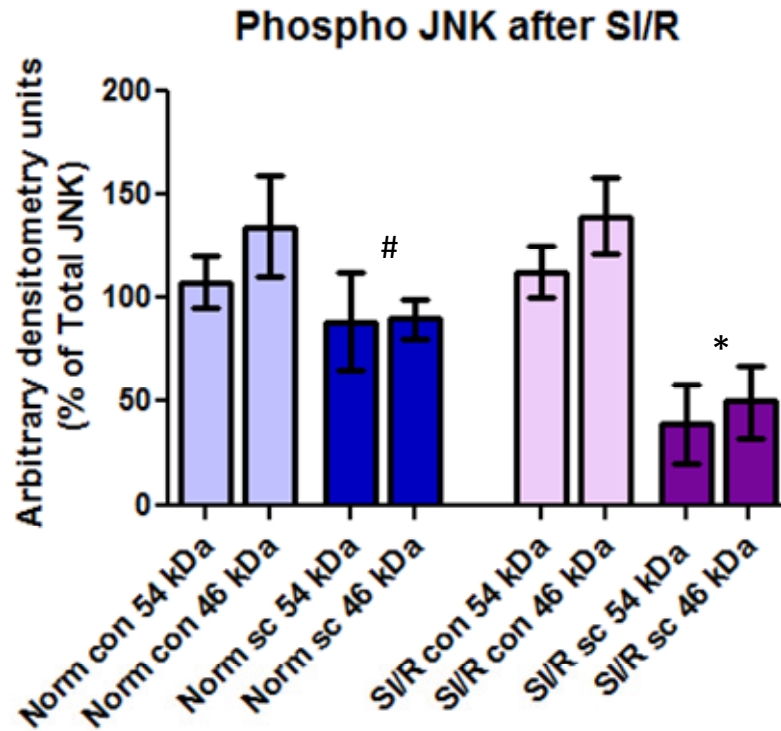


Figure 4.8: JNK phosphorylation, showing normoxic control (Norm con), normoxic sanguinarine (Norm sc), simulated ischaemia/reperfusion control (SI/R con) and simulated ischaemia/reperfusion sanguinarine (SI/R sc). Data expressed as mean±SEM. # $p < 0.05$ vs. SI/R con and SI/R sc, * $p < 0.001$ vs. norm con and SI/R con, $n > 3$.

4.3 Autophagic activity after 3 hrs simulated ischaemia

4.3.1 LysoTracker[®]Red labelling

LysoTracker Red DND-99, a red-fluorescent dye, accumulates in acidic lysosomal compartments in live cells. The amount of dye taken up by the cells can be used as an indicator of lysosome content, and therefore an indicator for the autophagic activity in the cell (Stern *et al.*, 2008).

Micrographs representing cells after 3 h normoxia or simulated ischaemia are depicted below. In normoxic groups red lysosomes seem to be equally scattered throughout the cells. In micrographs representing cells that were exposed to 3 h SI, lysosomes are more concentrated around the cells' nuclei. This morphology is even more pronounced when ischaemic cells were treated with sanguinarine.

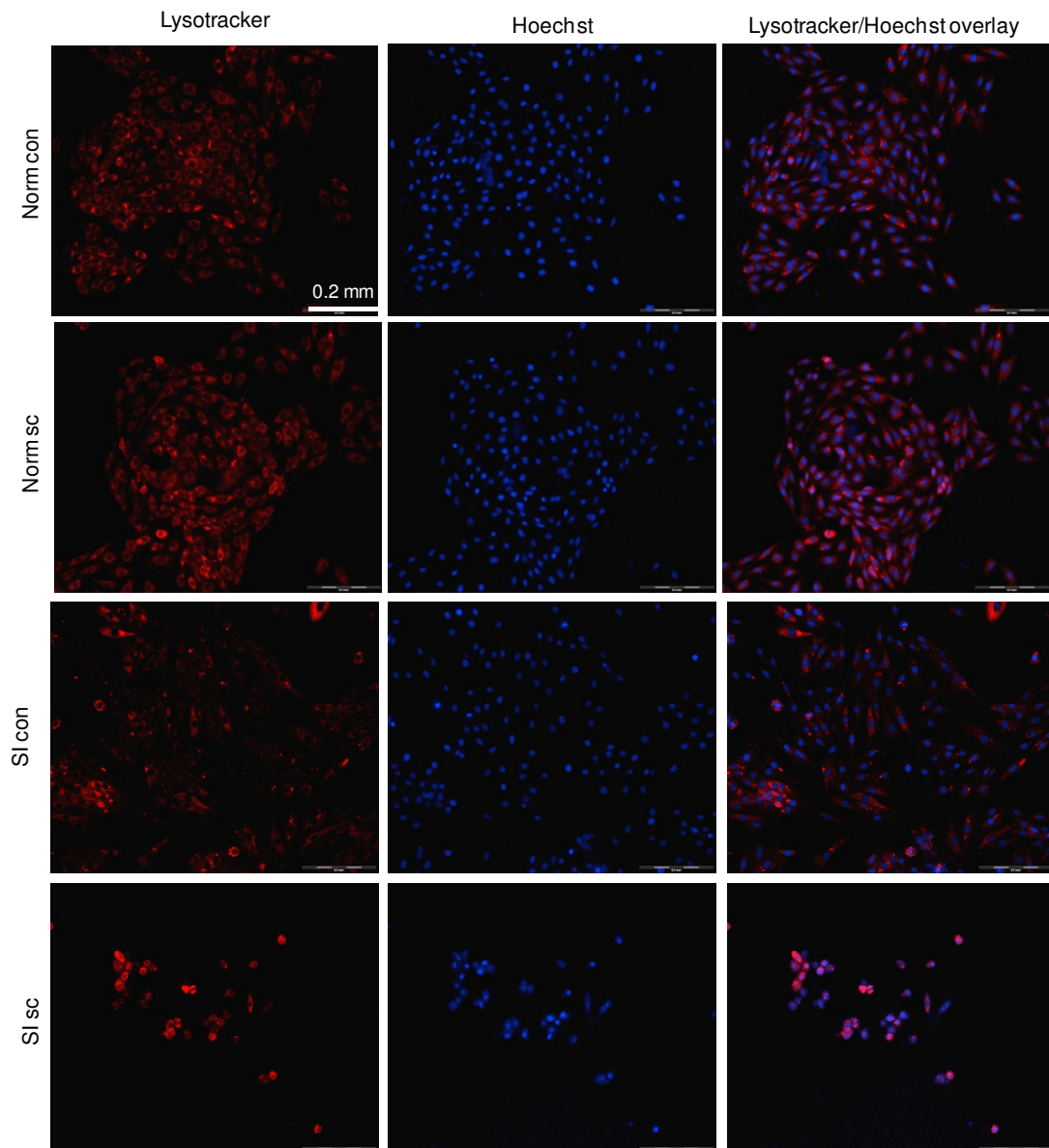


Figure 4.9: After treatment normoxic control (Norm con), normoxic sanguinarine (Norm sc), simulated ischaemia control (SI con) and simulated ischaemia sanguinarine (SI sc) treated groups were stained with Lysotracker Red dye (displayed in red) and Hoechst (displayed in blue), and micrographs were taken.

4.3.2 Flow cytometry

To confirm and quantify the lysotracker/Hoechst micrographs, cells were analysed by flow cytometry.

Acridine orange is a lysosome-tropic agent that freely moves across biological membranes when uncharged. However, when acridine orange is protonated it moves into acidic compartments and forms aggregates. These aggregates are known to fluoresce red (Paglin *et al.*, 2001). It was therefore used for the detection of acidic compartments to signify lysosomal activity during autophagy. Acridine orange is also a DNA intercalating dye, fluorescing green.

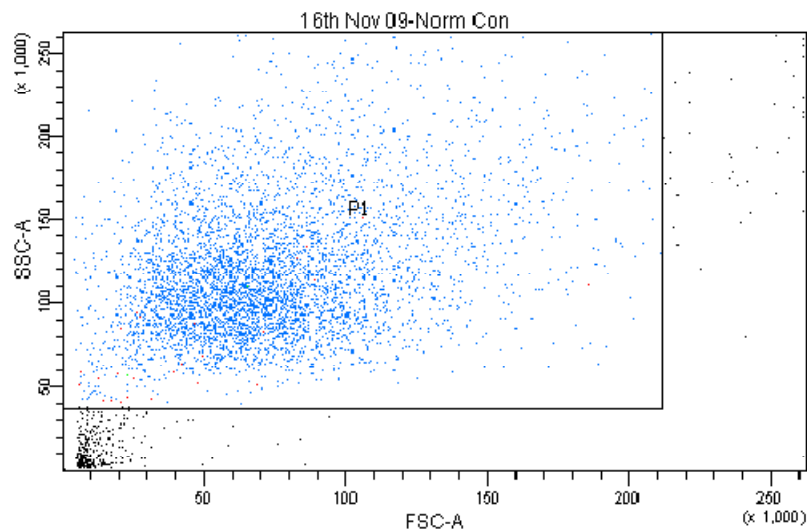


Figure 4.10: Cell sample selected and analysed during flow cytometry (± 5000 cells counted).

The normoxic sanguinarine group (75.64 ± 2.6) had significantly lower red fluorescence intensity than normoxic control (100 ± 5.1) and SI control (106.2 ± 3.8) treated groups ($p < 0.001$). The red fluorescence intensity was also significantly lower in the SI sanguinarine (70.26 ± 1.4) treated group compared to the normoxic control and SI control treated groups ($p < 0.001$). (Fig 4.11)

Low fluorescence intensity signifying decreased autophagy correspond with lysotracker stained lysosomal vacuoles accumulated around nuclei of cells in the SI sanguinarine treated groups with significantly more pyknotic and PI positive cells.

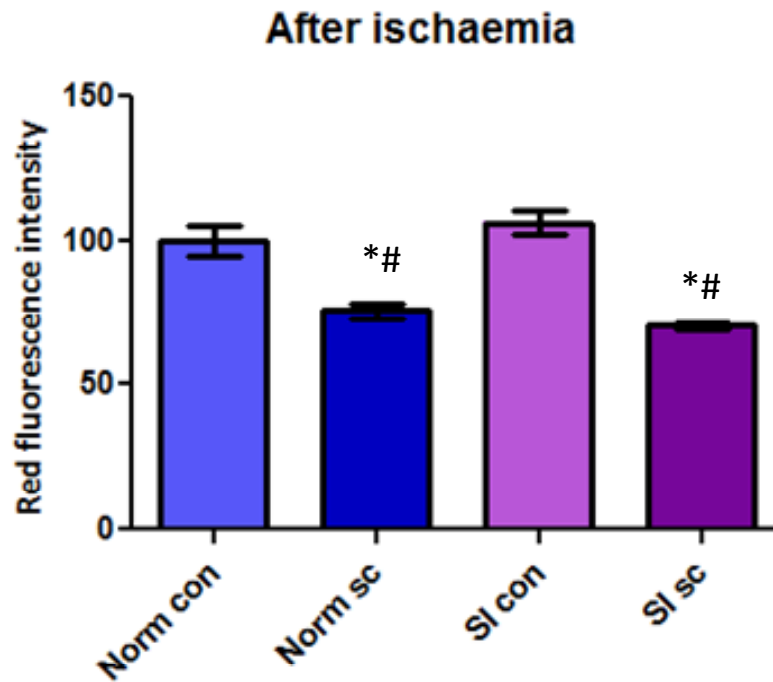


Figure 4.11: Percentage red fluorescence intensity indicating acidic vacuoles, using acridine orange in flow cytometry, showing normoxic control (Norm con), normoxic sanguinarine (Norm sc), simulated ischaemia control (SI con) and simulated ischaemia sanguinarine (SI sc). Data expressed as mean±SEM. #p<0.001 vs. norm con *p<0.001 vs. SI con, n>3

4.3.3 Beclin-1 and LC3-II

To investigate whether the changes in MAPK phosphorylation and MKP-1 induction after SI had an effect on autophagic activity, Beclin-1 and LC3-II induction were investigated.

No significant difference was found when comparing Beclin-1 induction in normoxic control (100 ± 3.34) and -sanguinarine (107.2 ± 2.88) treated groups with SI control (88.77 ± 5.9) or -sanguinarine (105.5 ± 10.81) treated groups. (Fig 4.12)

No significant differences in LC3-II were seen either. (Fig 4.13)

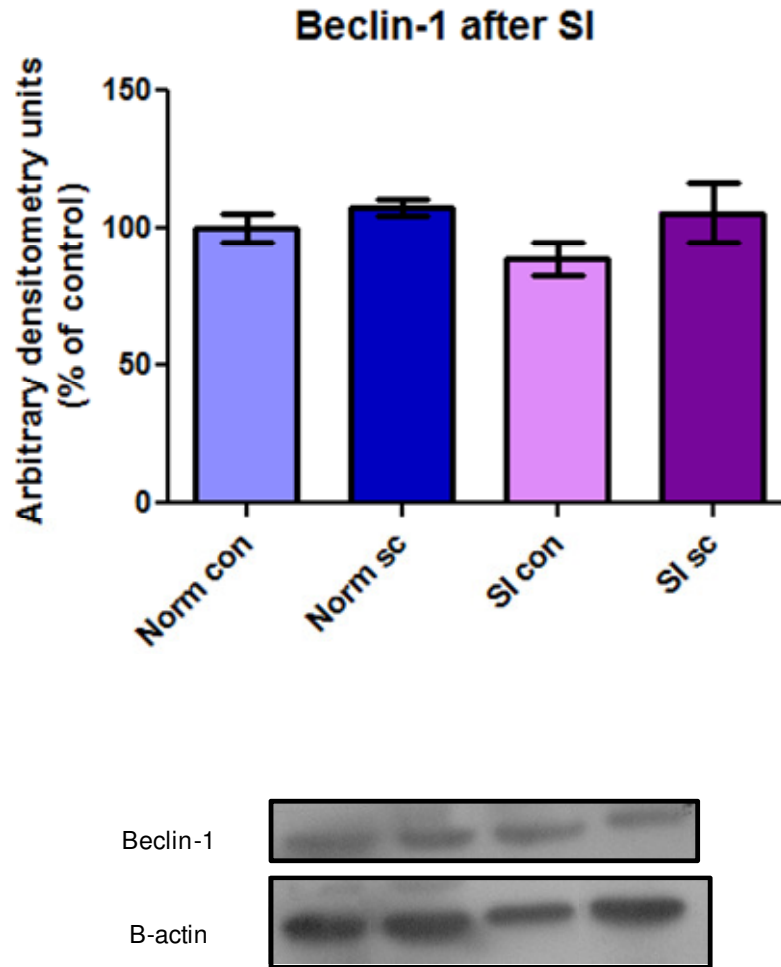


Figure 4.12: Beclin-1 induction, showing normoxic control (Norm con), normoxic sanguinarine (Norm sc), simulated ischaemia control (SI con) and simulated ischaemia sanguinarine (SI sc). Data expressed as mean \pm SEM. $p>0.05$, $n>3$

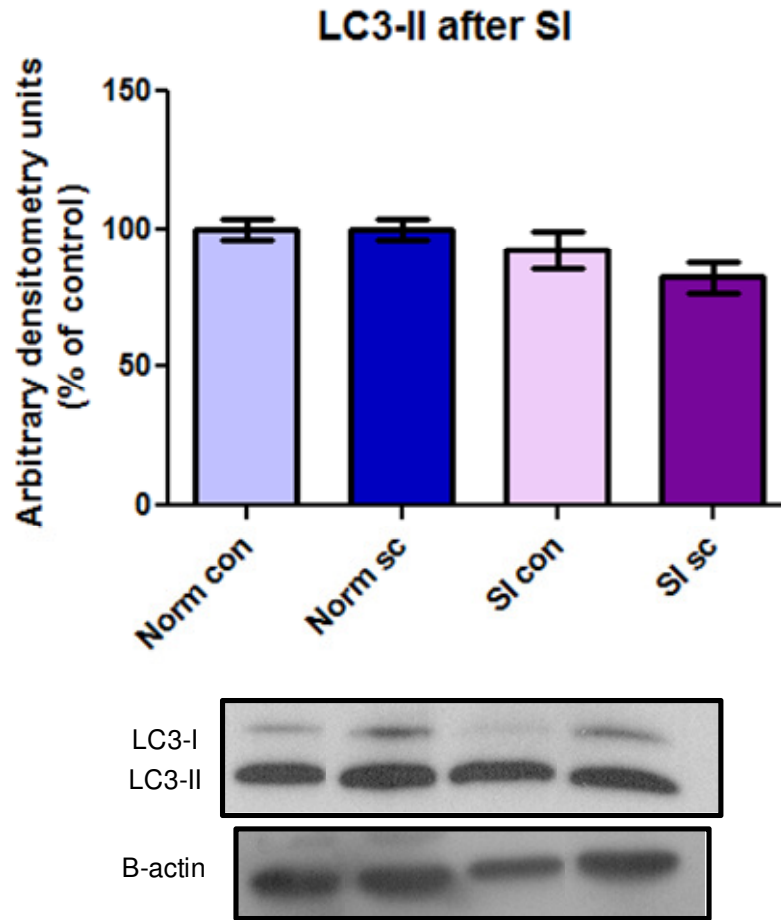


Figure 4.13: LC3-II induction, showing normoxic control (Norm con), normoxic sanguinarine (Norm sc), simulated ischaemia control (SI con) and simulated ischaemia sanguinarine (SI sc). Data expressed as mean \pm SEM. n>3.

4.4 Autophagic activity after simulated ischaemia/reperfusion

4.4.1 LysoTracker[®]Red labelling

Micrographs representing cells that have been exposed to normoxic conditions or SI/R are depicted below. In normoxic groups, red lysosomes are equally scattered throughout the cells. In cells that have been exposed to SI/R, lysosomes are more concentrated around the cells' nuclei and even more so in sanguinarine treated cells.

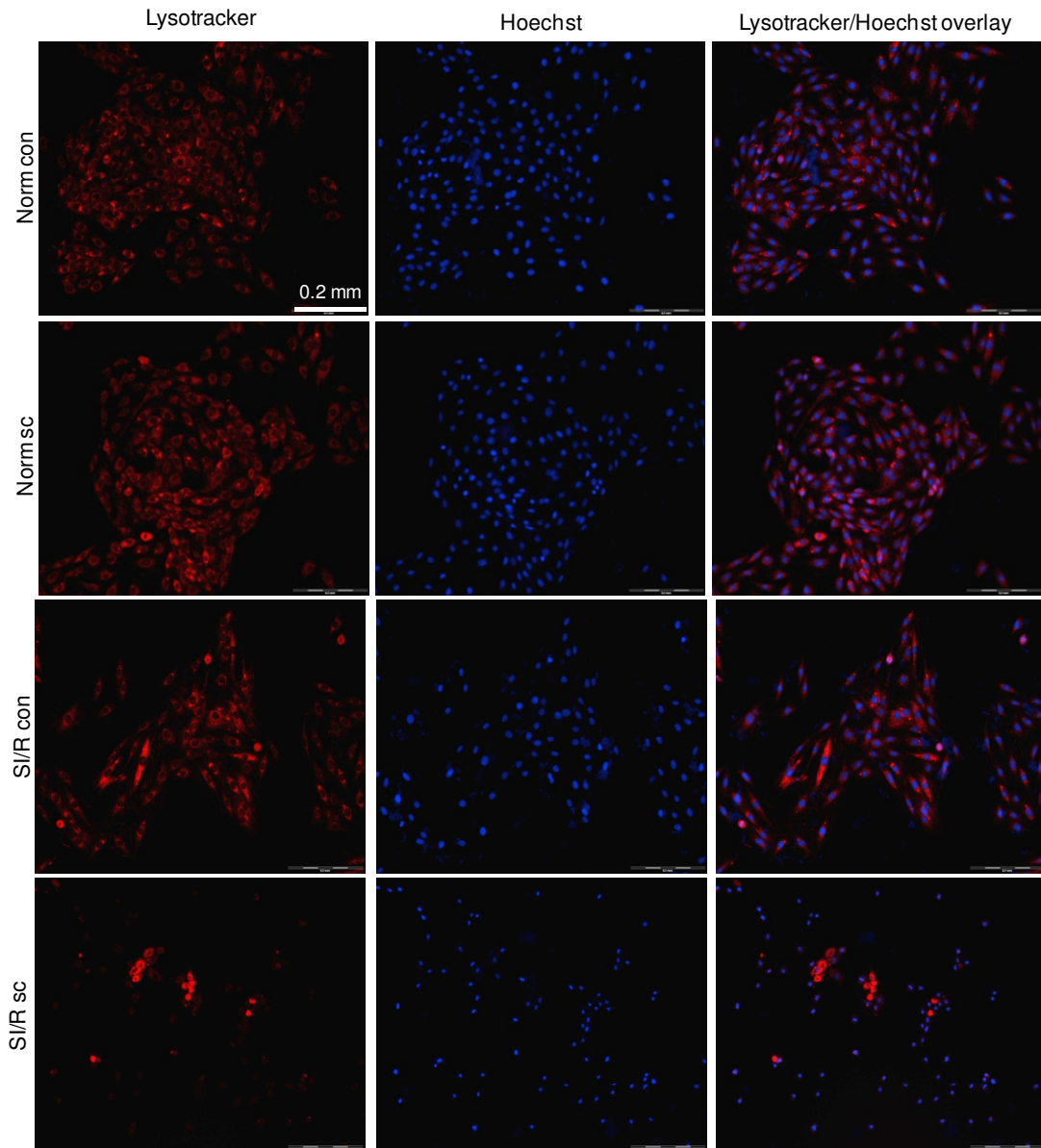


Figure 4.14: After treatment normoxic control (Norm con), normoxic sanguinarine (Norm sc), simulated ischaemia/reperfusion control (SI/R con) and simulated ischaemia/reperfusion sanguinarine (SI/R sc) treated groups were stained with Lysotracker Red dye (displayed in red) and Hoechst (displayed in blue), and micrographs were taken.

4.4.2 Flow cytometry

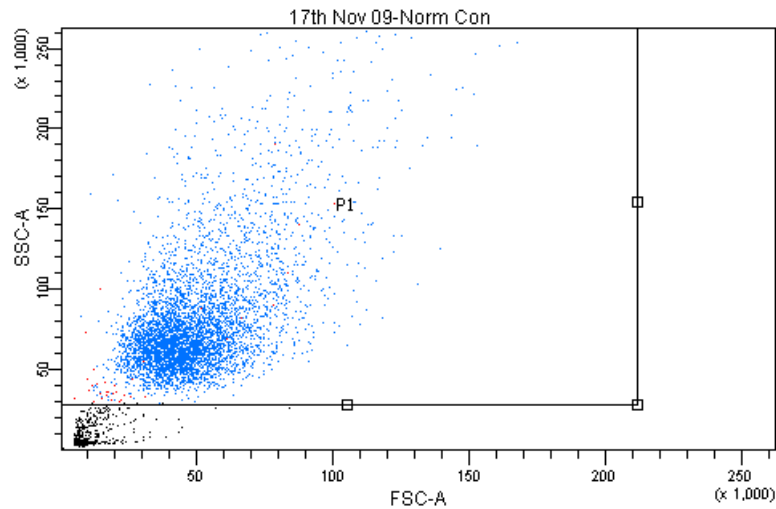


Figure 4.15: Cell sample selected and analysed during flow cytometry (± 5000 cells counted).

The red fluorescent intensity was significantly lower in the normoxic sanguinarine (75.64 ± 2.6) treated group than the SI/R control (94.52 ± 0.6) ($p < 0.05$) treated groups, after reperfusion. The red fluorescent intensity was significantly higher in the normoxic sanguinarine treated group when compared to the SI/R sanguinarine (37.15 ± 3.5) treated group ($p < 0.001$). SI/R sanguinarine treatment also resulted in significantly lower red fluorescence intensity than normoxic control (100 ± 9.7) and SI/R control groups ($p < 0.001$). (Fig 4.16)

As was seen after SI, low fluorescence intensity, signifying decreased autophagy, correspond with lysotracker stained lysosomal vacuoles accumulated around nuclei of cells in the SI sanguinarine treated groups with significantly more pyknotic and PI positive cells.

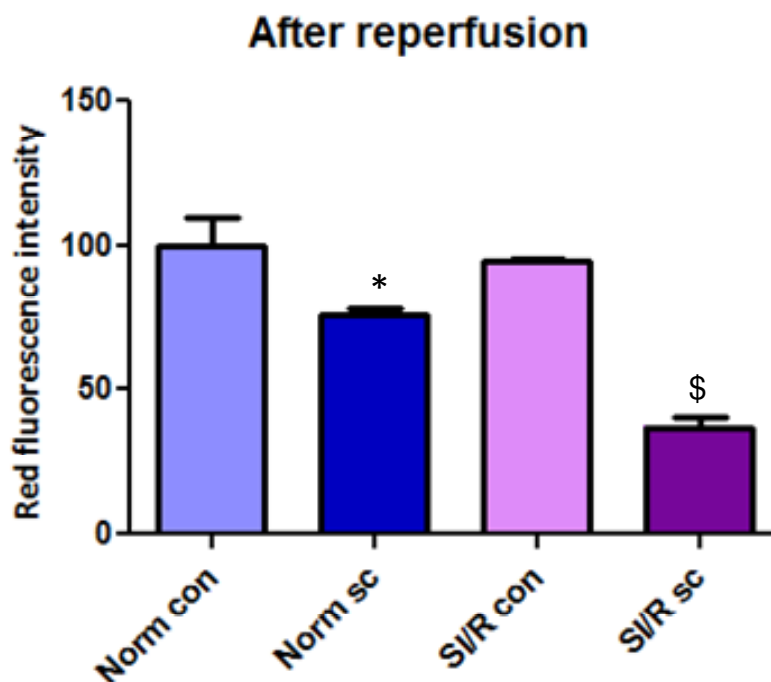


Figure 4.16: Percentage red fluorescence intensity indicating acidic vacuoles, showing normoxic control (Norm con), normoxic sanguinarine (Norm sc), simulated ischaemia/reperfusion control (SI/R con) and simulated ischaemia/reperfusion sanguinarine (SI/R sc). Data expressed as mean±SEM. *p<0.05 vs. SI/R con, \$p<0.001 vs. normoxic groups and SI/R con. n>3

4.4.3 Beclin-1 and LC3-II

As can be seen in figure 4.17 Beclin-1 induction was significantly increased after SI/R when treated with dexamethasone (110 ± 6.85) compared to control (94.2 ± 4.76) ($p<0.05$) and sanguinarine treated (85.2 ± 2.71) ($p<0.01$) groups. SI/R sanguinarine treated groups had lower Beclin-1 induction compared to normoxic control ($p<0.05$), normoxic dexamethasone ($p<0.05$) and normoxic sanguinarine ($p<0.05$) groups.

LC3-II induction was significantly lower after SI/R control (83.61 ± 1.59) treatment compared to normoxic control ($p<0.01$), -dexamethasone ($p<0.001$) and -sanguinarine ($p<0.05$) treatment. LC3-II was increased after SI/R dexamethasone (99.94 ± 1.48) treatment compared to both SI/R control ($p<0.01$) and SI/R sanguinarine (64.88 ± 1.1) ($p<0.001$) treatment. SI/R sanguinarine had even lower LC3-II expression than SI/R control ($p<0.01$). (Fig 4.18)

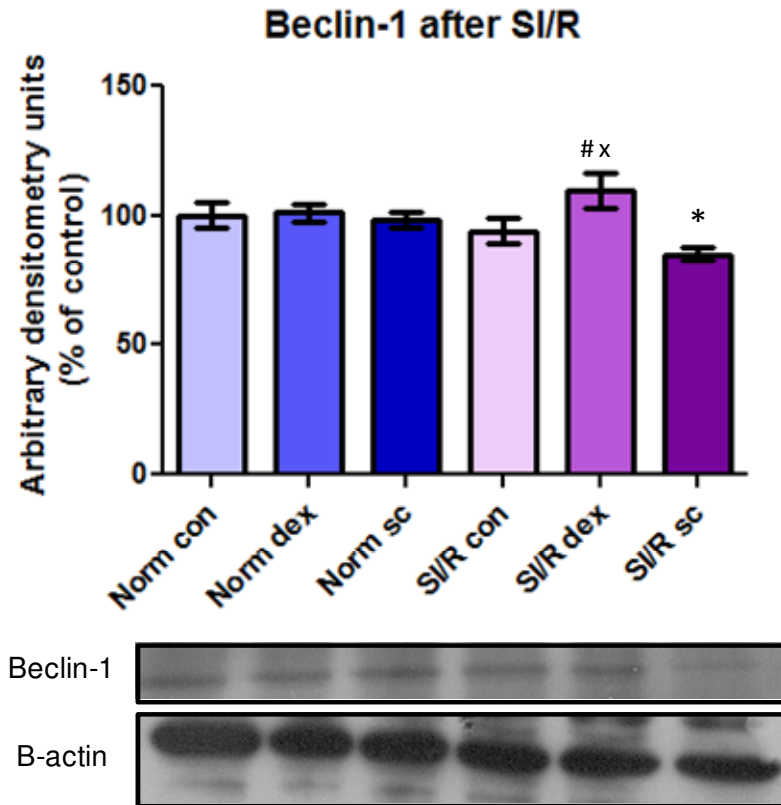


Figure 4.17: Beclin-1 induction, showing normoxic control (Norm con), normoxic dexamethasone (Norm dex), normoxic sanguinarine (Norm sc), simulated ischaemia/reperfusion control (SI/R con), simulated ischaemia/reperfusion dexamethasone (SI/R dex) and simulated ischaemia/reperfusion sanguinarine (SI/R sc). Data expressed as mean±SEM. [#]p<0.05 vs. SI/R con, ^xp<0.01 vs. SI/R sc, ^{*}p<0.05 vs. normoxic groups, n>3.

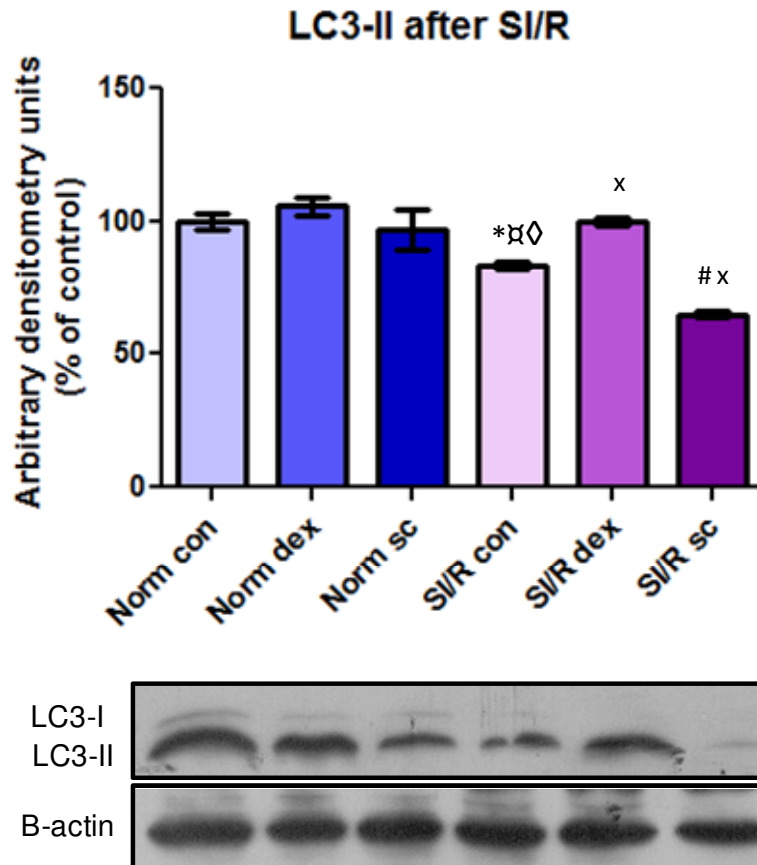


Figure 4.18: LC3-II induction, showing normoxic control (Norm con), normoxic dexamethasone (Norm dex), normoxic sanguinarine (Norm sc), simulated ischaemia/reperfusion control (SI/R con), simulated ischaemia/reperfusion dexamethasone (SI/R dex) and simulated ischaemia/reperfusion sanguinarine (SI/R sc). Data expressed as mean \pm SEM. # p <0.001 vs. normoxic groups and SI/R dex, $^x p$ <0.01 vs. SI/R con, $^* p$ <0.01 vs. norm con, $^{\#} p$ <0.001 vs. norm dex, $^{\diamond} p$ <0.05 vs. norm sc, n >3.

4.5 Cell viability after 3 hrs simulated ischaemia

4.5.1 MTT

A MTT assay was done to assess the cells' metabolic state after 3 hours simulated ischaemia, in the presence of sanguinarine (Gomez *et al.*, 1997). The MTT assay is based on the ability of the cell to reduce MTT into formazan pigments as an indicator of the cell's reductive capacity. This reductive capacity can be used to indicate the cell's relative viability.

Normoxic control ($100\pm 2.4\%$) and sanguinarine ($101.9\pm 15\%$) treated cells had significantly higher relative viability based on MTT reduction, when compared to SI control ($35.47\pm 0.7\%$) and -sanguinarine ($5.85\pm 1.3\%$) treated cells ($p < 0.001$). MTT reduction was even lower in SI sanguinarine treated cells when compared to SI control cells ($p < 0.001$). (Fig 4.19)

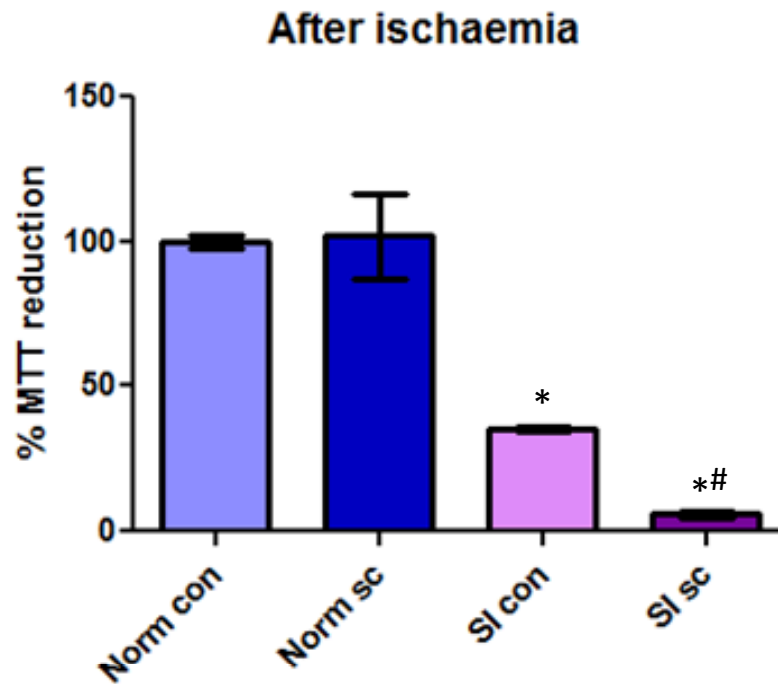


Figure 4.19: Relative viability based of MTT reduction, showing normoxic control (Norm con), normoxic sanguinarine (Norm sc), simulated ischaemia control (SI con) and simulated ischaemia sanguinarine (SI sc). Data expressed as mean±SEM.

*p<0.001 vs. normoxic groups, #p<0.001 vs. SI con, n=6

4.5.2 PI/Hoechst

Morphological changes which signify apoptosis and necrosis have been characterized as cells showing signs of nuclear condensation (pyknosis) and fragmentation (karyorhexis), respectively (Kajstura *et al.*, 1996). Apoptosis and necrosis, occurring after both 3 h normoxia or simulated ischaemia, were quantified using PI, to assess necrosis, and Hoechst, to assess apoptosis (Asoh *et al.*, 2005).

Under normoxic conditions loose chromatin arrangement was observed upon staining cells with Hoechst 33342, where pyknosis was significantly low for normoxic control ($2.16 \pm 0.78\%$) and -sanguinarine ($3.31 \pm 0.81\%$) treated groups compared to SI sanguinarine groups. After 3 h SI, pyknosis in sanguinarine treated cells ($7.81 \pm 1.64\%$) was significantly higher than in normoxic groups and SI control ($3.22 \pm 0.83\%$) treated groups ($p < 0.001$). (Fig 4.21)

Late pyknotic cells were characterised as showing signs of chromatin condensation and PI positive nuclear staining, as loss of membrane integrity results in PI being integrated into the nuclear region. Late pyknotic cells were not significant in normoxic groups (control: $1.6 \pm 0.6\%$ and sanguinarine: $2.09 \pm 0.8\%$) or SI control ($1 \pm 0.46\%$) treated groups. However in the presence of sanguinarine during SI ($26.06 \pm 5.0\%$), significantly more late pyknotic cells were observed ($p < 0.001$). (Fig 4.22)

After 3 h simulated ischaemia $54.07 \pm 4.48\%$ of sanguinarine treated cells were PI positive. This was significantly more than in normoxic control

($1.04 \pm 0.68\%$), -sanguinarine ($2 \pm 0.54\%$) and SI control ($2.97 \pm 2.15\%$) treated groups ($p < 0.001$). (Fig 4.23)

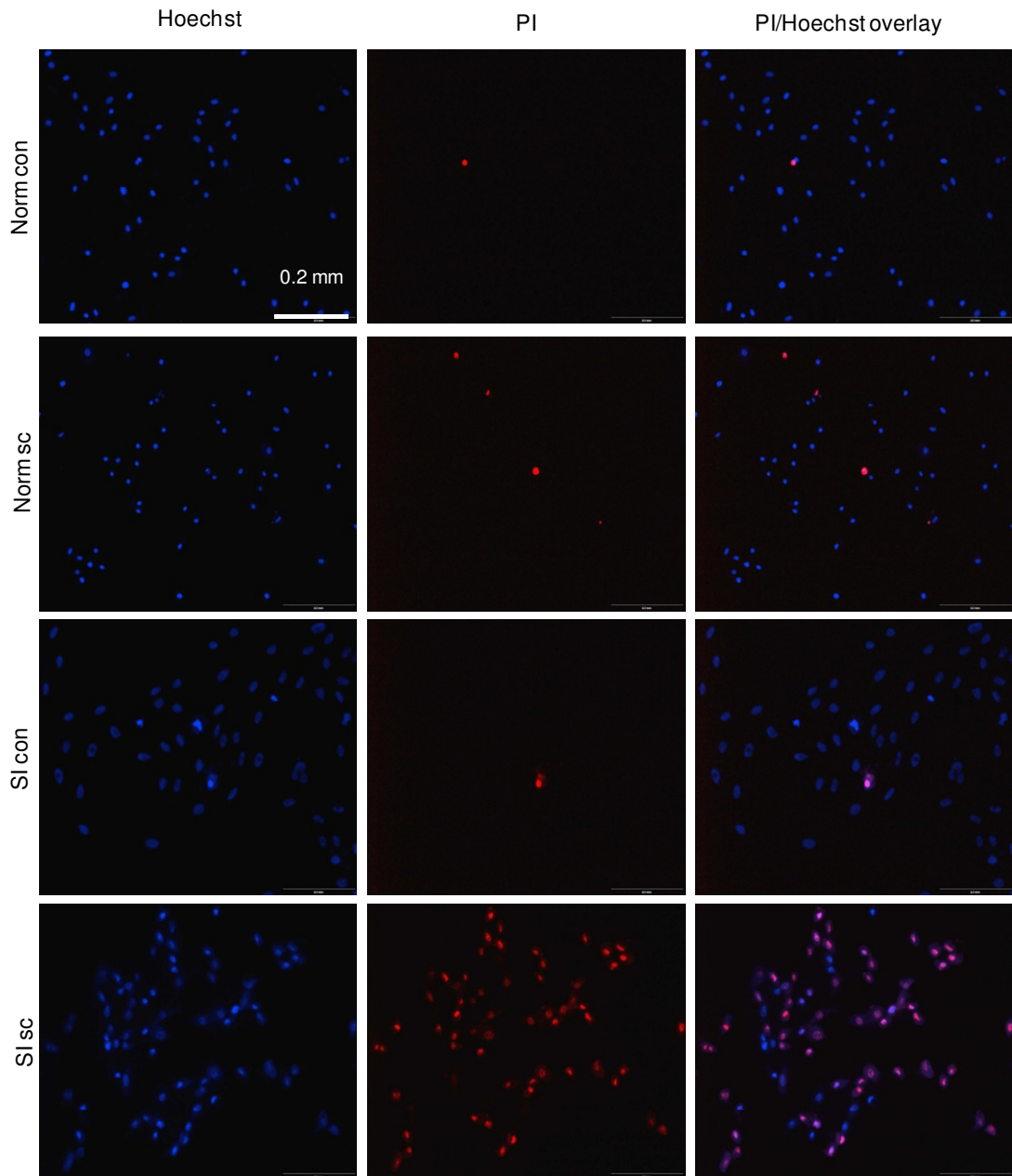


Figure 4.20: Fluorescent micrographs showing nuclear DNA using Hoechst 33342 (blue) and karyorhexis using PI (red). Comparing normoxic control (Norm con), normoxic sanguinarine (Norm sc), simulated ischaemia control (SI con) and simulated ischaemia sanguinarine (SI sc).

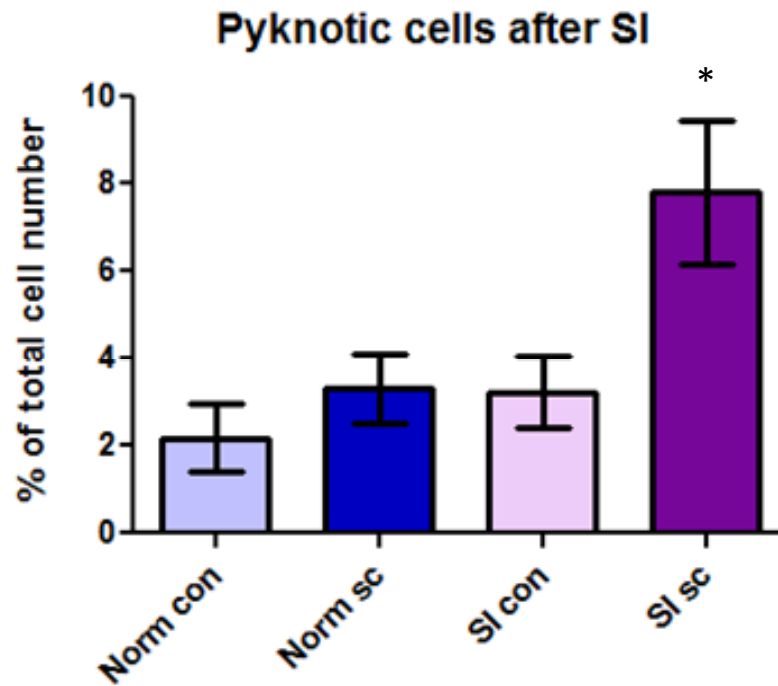


Figure 4.21: Percentage pyknosis, showing normoxic control (Norm con), normoxic sanguinarine (Norm sc), simulated ischaemia control (SI con) and simulated ischaemia sanguinarine (SI sc). Data expressed as mean \pm SEM. * $p < 0.001$ vs. norm groups and SI con, $n = 6$.

Late pyknotic cells after SI

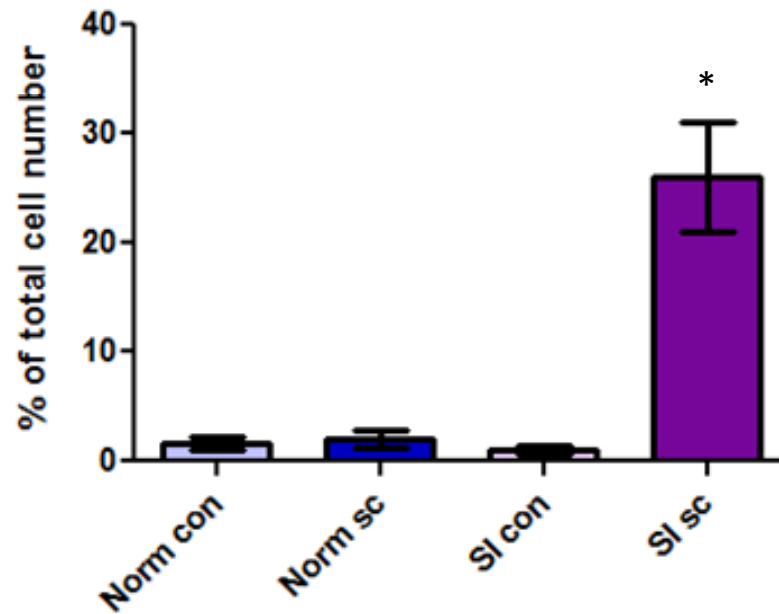


Figure 4.22: Percentage late pyknosis, showing normoxic control (Norm con), normoxic sanguinarine (Norm sc), simulated ischaemia control (SI con) and simulated ischaemia sanguinarine (SI sc). Data expressed as mean \pm SEM. * p <0.001 vs. norm groups and SI con, n =6.

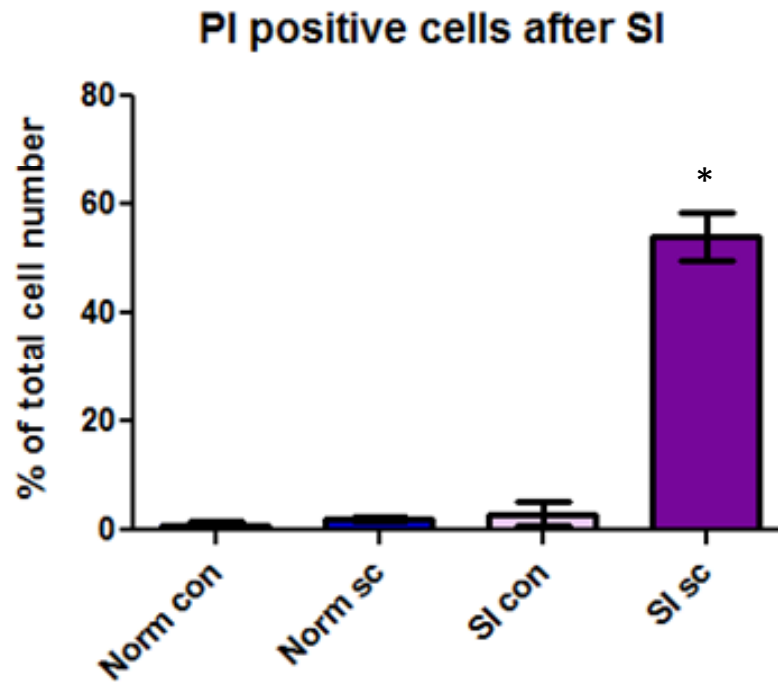


Figure 4.23: Percentage PI positive cells, showing normoxic control (Norm con), normoxic sanguinarine (Norm sc), simulated ischaemia control (SI con) and simulated ischaemia sanguinarine (SI sc). Data expressed as mean \pm SEM. * p <0.001 vs. norm groups and SI con, n =6.

4.5.3 Cleaved caspase-3 and cleaved PARP

Apoptotic activity after 3 hours simulated ischaemia was investigated with western blot analysis probing for cleaved PARP and cleaved caspase-3.

Caspase-3 cleavage was significantly increased after SI in the presence of sanguinarine (1.8 ± 0.13) compared to normoxic control (1.02 ± 0.17), – sanguinarine (1.12 ± 0.18) and SI control (1.01 ± 0.16) treated groups ($p < 0.01$). (Fig 4.24)

PARP cleavage was significantly increased after SI, in the presence of sanguinarine (1.72 ± 0.2) ($p < 0.001$). (Fig 4.25)

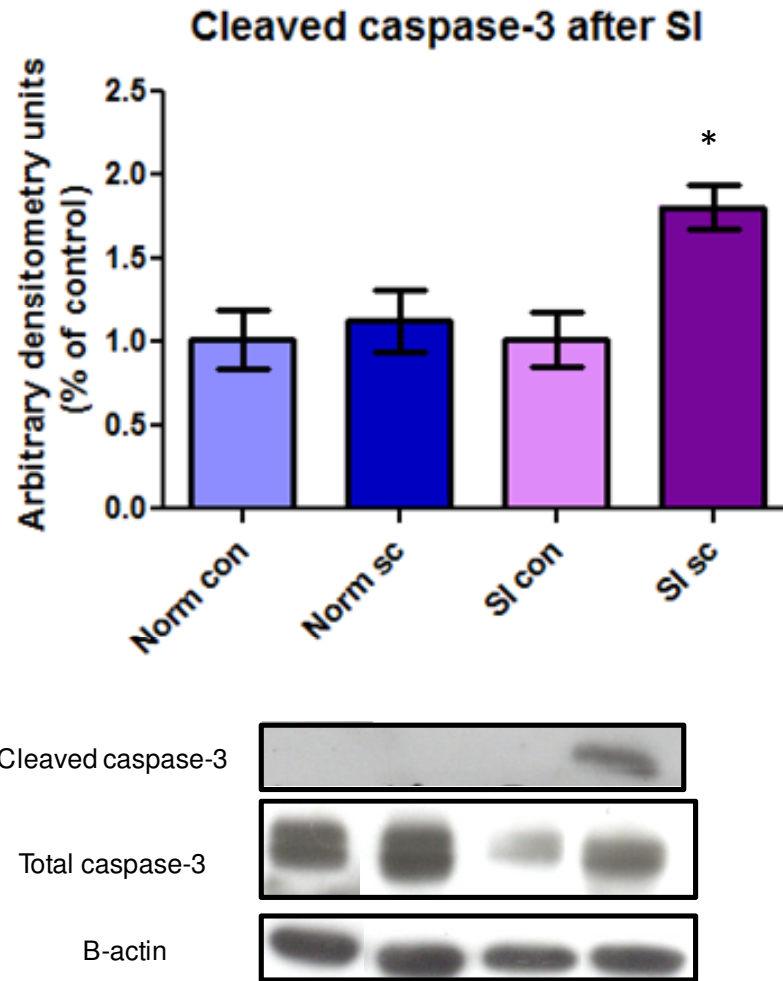


Figure 4.24: Caspase-3 cleavage, showing normoxic control (Norm con), normoxic sanguinarine (Norm sc), simulated ischaemia control (SI con) and simulated ischaemia sanguinarine (SI sc). Data expressed as mean \pm SEM. * p <0.01 vs. normoxic groups and SI con, n >3.

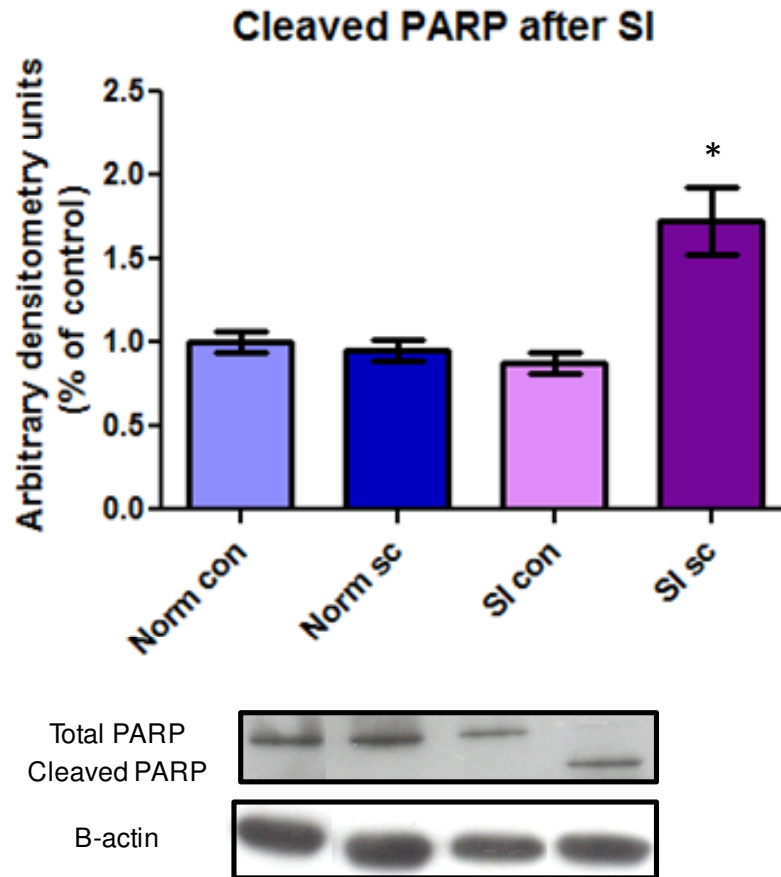


Figure 4.25: PARP cleavage, showing normoxic control (Norm con), normoxic sanguinarine (Norm sc), simulated ischaemia control (SI con) and simulated ischaemia sanguinarine (SI sc). Data expressed as mean±SEM. *p<0.001 vs. normoxic groups, SI con and SI ins. n>3

4.6 Cell viability after simulated ischaemia/reperfusion

4.6.1 MTT

Normoxic control ($100\pm 6.5\%$) and sanguinarine ($101.9\pm 14.7\%$) treated cells had a significantly higher relative viability based on MTT reduction, when compared to SI control ($71.42\pm 7.8\%$) treated cells ($p < 0.01$). MTT reduction was significantly lower in SI sanguinarine ($9.83\pm 4.7\%$) treated cells when compared to normoxic groups and when compared to SI/R control ($p < 0.001$).

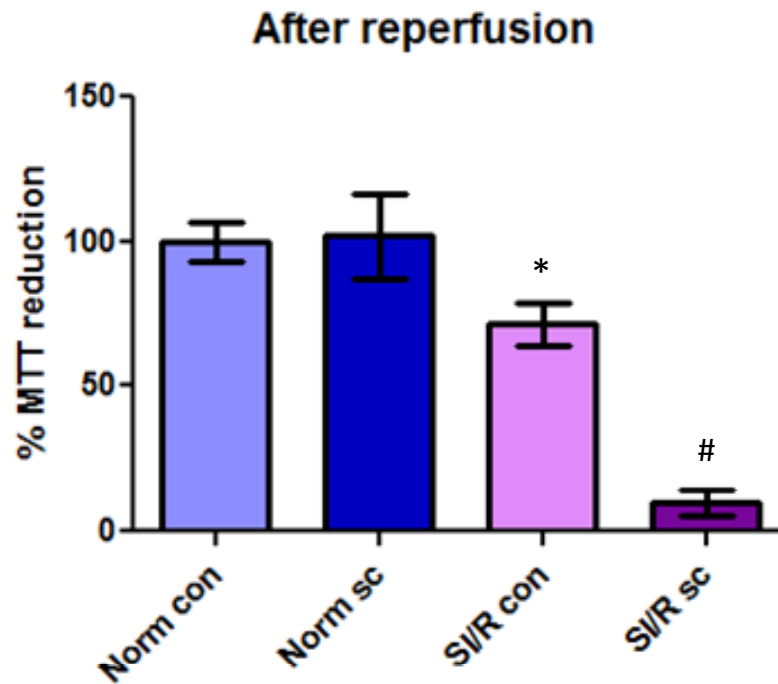


Figure 4.26: Relative viability based of MTT reduction, showing normoxic control (Norm con), normoxic sanguinarine (Norm sc), simulated ischaemia/reperfusion control (SI/R con) and simulated ischaemia/reperfusion sanguinarine (SI/R sc). Data expressed as mean \pm SEM. * p <0.01 vs. normoxic groups, # p <0.001 vs. normoxic groups and SI/R con. n >3

4.6.2 PI/Hoechst

After SI/R the sanguinarine ($0.46\pm 0.46\%$) treated group had significantly less pyknotic cells than the normoxic sanguinarine ($2.47\pm 0.5\%$) ($p < 0.05$) treated groups.

Late pyknosis was significantly increased in SI/R control ($8.79\pm 1.38\%$) compared to normoxic control ($1.6\pm 0.7\%$) ($p < 0.01$) and normoxic sanguinarine ($2.39\pm 0.86\%$) ($p < 0.01$) treated groups. After SI/R late pyknosis was significantly higher in sanguinarine treated groups ($24.49\pm 2.86\%$) than normoxic groups (control: $1.6\pm 0.7\%$, sanguinarine: $2.39\pm 0.86\%$) and SI/R control ($8.79\pm 1.38\%$) groups ($p < 0.001$).

Significantly increased numbers of PI positive cells were present in SI/R control ($24.49\pm 5.66\%$) and SI/R sanguinarine ($68.96\pm 4.1\%$) compared to normoxic groups ($p < 0.001$). When comparing SI/R groups, more PI positive cells were found in the sanguinarine treated groups than the control treated groups ($p < 0.001$).

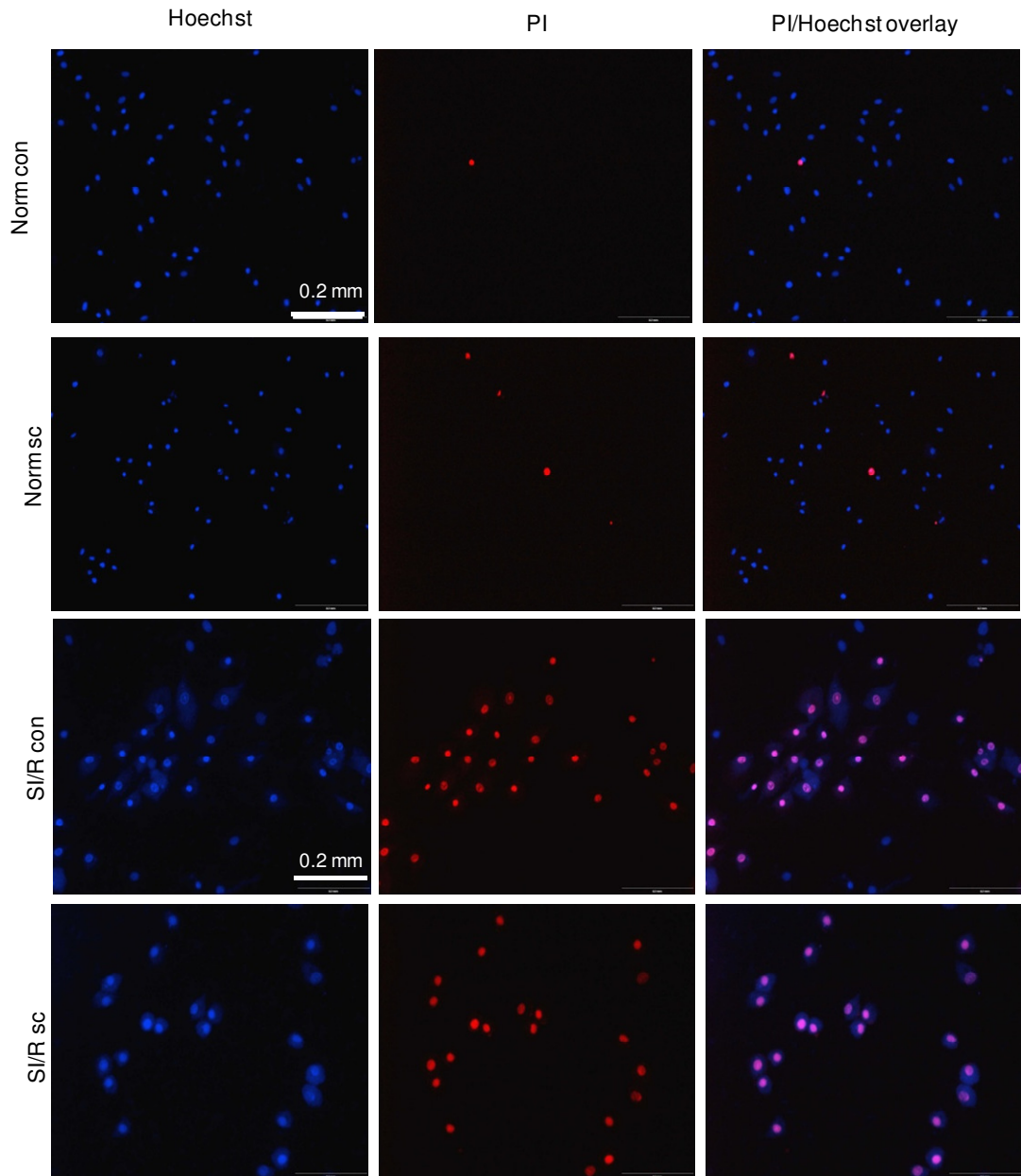


Figure 4.27: Fluorescent micrographs showing nuclear DNA using Hoechst 33342 (blue) and karyorhexis using PI (red). Comparing normoxic control (Norm con), normoxic sanguinarine (Norm sc), simulated ischaemia/reperfusion control (SI/R con) and simulated ischaemia/reperfusion sanguinarine (SI/R sc).

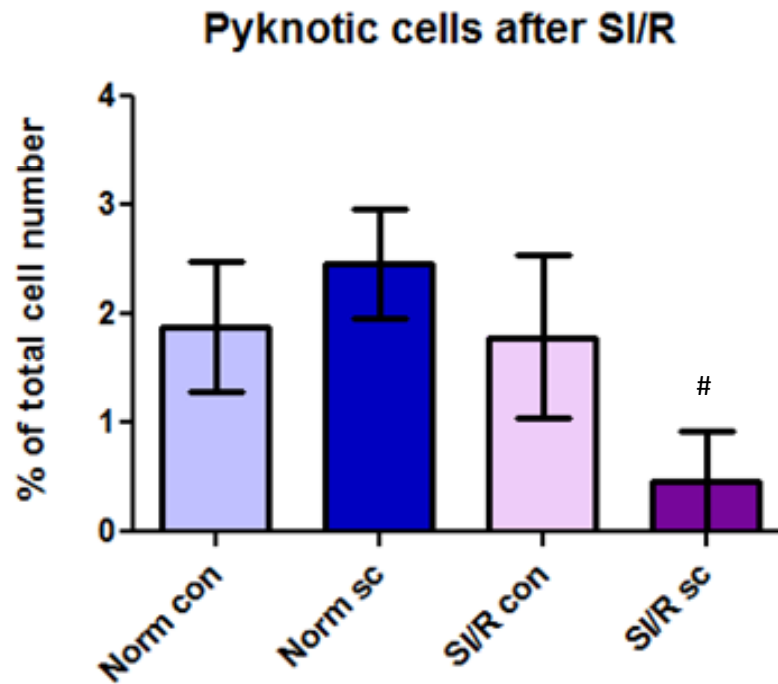


Figure 4.28: Percentage pyknosis, showing normoxic control (Norm con), normoxic sanguinarine (Norm sc), simulated ischaemia/reperfusion control (SI/R con) and simulated ischaemia/reperfusion sanguinarine (SI/R sc). Data expressed as mean±SEM. #p<0.05 vs. norm sc, n=6.

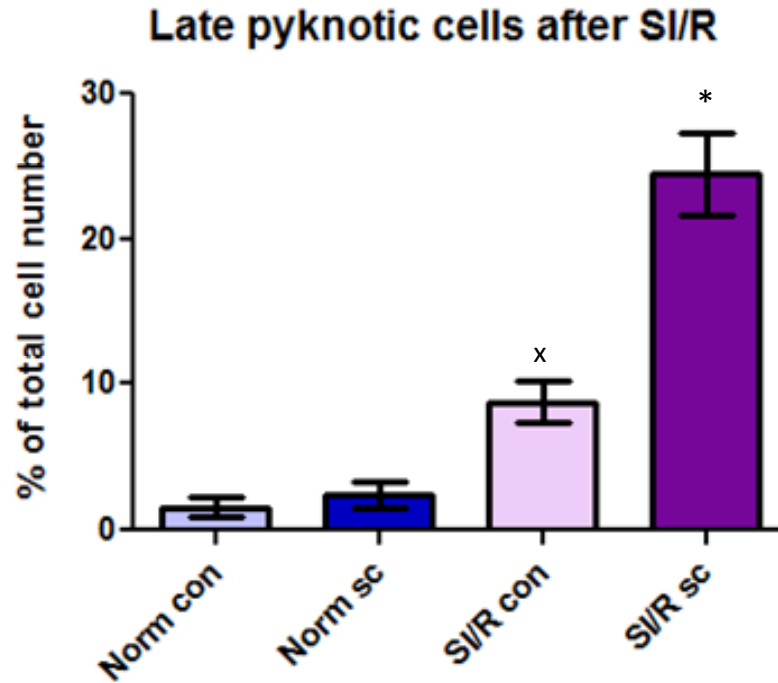


Figure 4.29: Percentage late pyknosis, showing normoxic control (Norm con), normoxic sanguinarine (Norm sc), simulated ischaemia/reperfusion control (SI/R con) and simulated ischaemia/reperfusion sanguinarine (SI/R sc). Data expressed as mean±SEM. *p<0.001 vs. normoxic groups and SI/R con, ^xp<0.01 vs. norm con and norm sc, n=6.

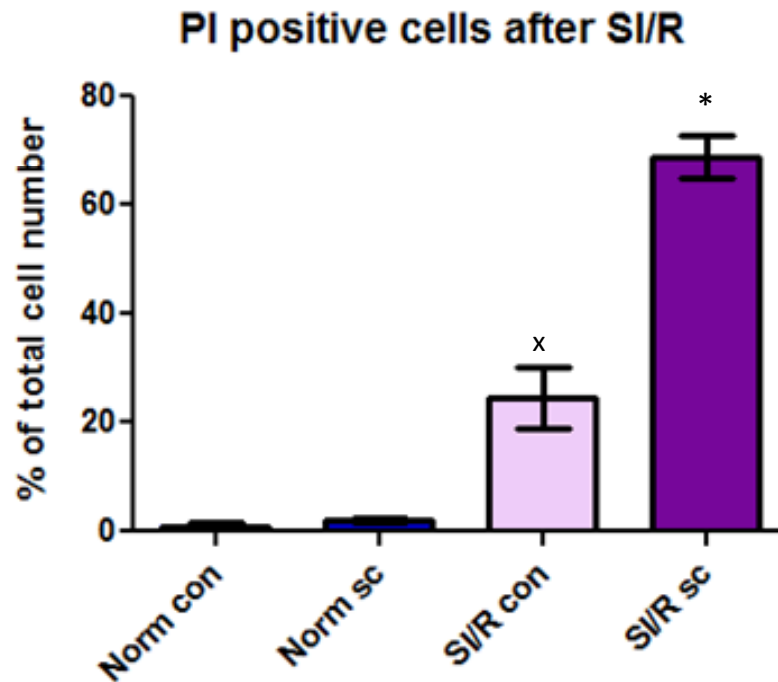


Figure 4.30: Percentage PI positive cells, showing normoxic control (Norm con), normoxic sanguinarine (Norm sc), simulated ischaemia/reperfusion control (SI/R con) and simulated ischaemia/reperfusion sanguinarine (SI/R sc). Data expressed as mean \pm SEM. ^xp<0.001 vs. normoxic groups, *p<0.001 vs. normoxic groups and SI/R con, n=6.

4.6.3 LDH assay

A LDH assay was done to determine the LDH release which occurred during reperfusion. The percentage LDH release is an index of irreversible injury or necrosis.

After SI/R LDH release was found to be significantly higher in the presence of sanguinarine (197.9 ± 69.59) compared to normoxic control (100 ± 12.65) ($p < 0.01$), normoxic sanguinarine (65.65 ± 14.71) ($p < 0.001$) and SI/R control (73.06 ± 10.22) ($p < 0.01$) groups.

The significant LDH release in the SI/R sc groups corresponds with the significantly high amount of PI positive cells found SI/R sanguinarine treatment.

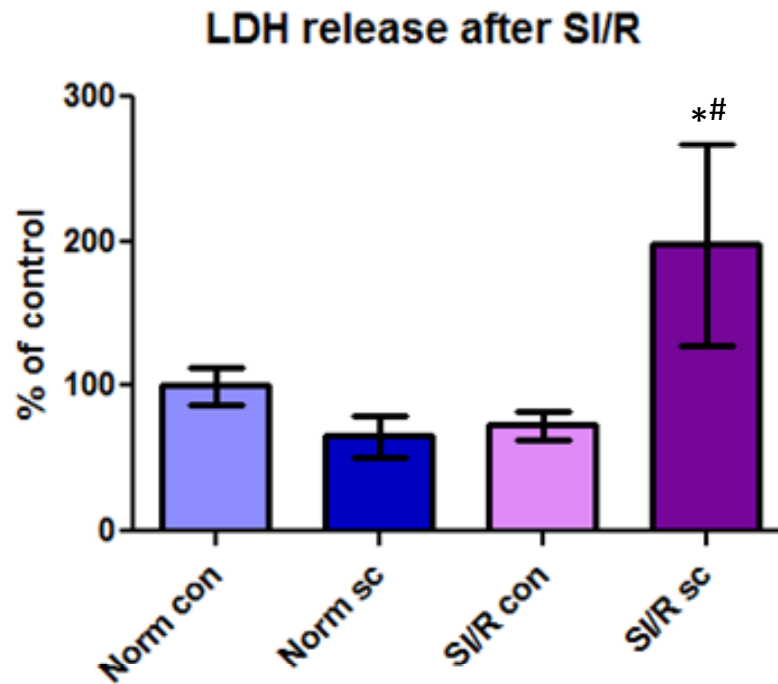


Figure 4.31: Relative viability based on LDH release, showing normoxic control (Norm con), normoxic sanguinarine (Norm sc), simulated ischaemia/reperfusion control (SI/R con) and simulated ischaemia/reperfusion sanguinarine (SI/R sc). Data expressed as mean \pm SEM. * $p < 0.01$ vs. norm con and SI/R con, # $p < 0.001$ vs. norm sc. $n > 3$

4.6.4 Cleaved caspase-3 and cleaved PARP

Caspase-3 cleavage was also significantly higher in the SI/R sanguinarine treated group (1.3 ± 0.12) compared to normoxic groups ($p < 0.01$) and SI/R control and –dexamethasone ($p < 0.01$) groups.

Significant PARP cleavage occurred in the sanguinarine treated group (1.6 ± 0.64), after SI/R ($p < 0.001$).

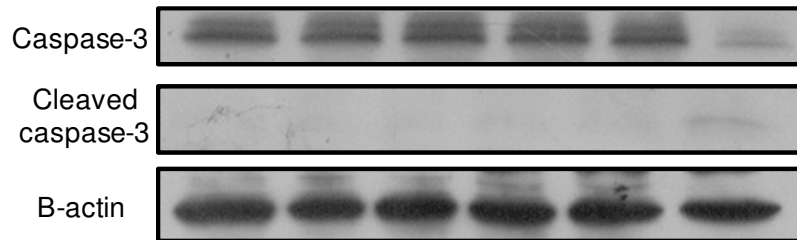
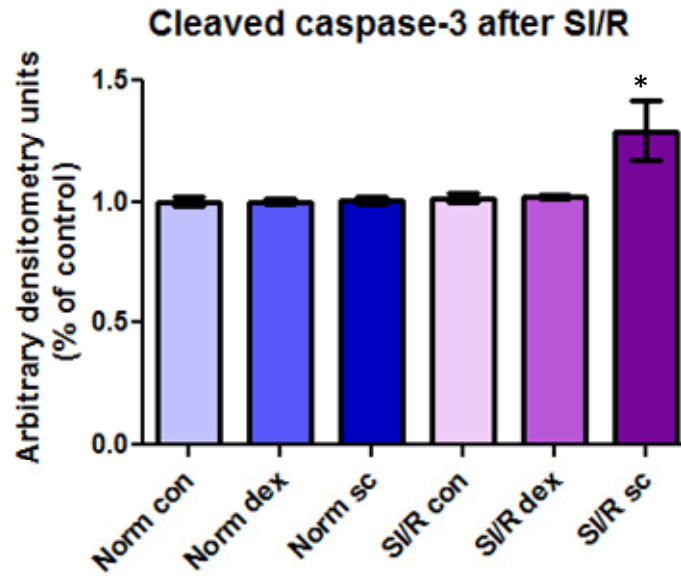


Figure 4.32: Caspase-3 cleavage, showing normoxic control (Norm con), normoxic dexamethasone (Norm dex), normoxic sanguinarine (Norm sc), simulated ischaemia/reperfusion control (SI/R con), simulated ischaemia/reperfusion dexamethasone (SI/R dex) and simulated ischaemia/reperfusion sanguinarine (SI/R sc). Data expressed as mean \pm SEM. * p <0.01 vs. norm groups, SI/R con and SI/R dex, n >3

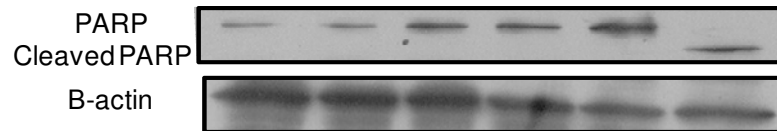
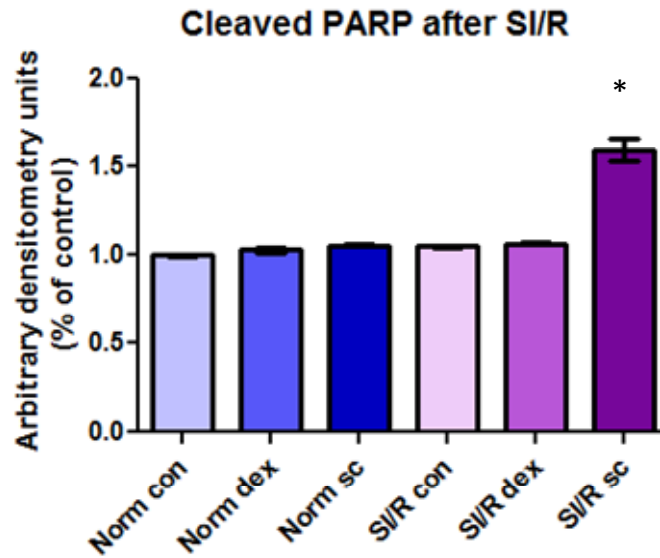


Figure 4.33: PARP cleavage, showing normoxic control (Norm con), normoxic dexamethasone (Norm dex), normoxic sanguinarine (Norm sc), simulated ischaemia/reperfusion control (SI/R con), simulated ischaemia/reperfusion dexamethasone (SI/R dex) and simulated ischaemia/reperfusion sanguinarine (SI/R sc). Data expressed as mean±SEM. *p<0.001 vs. normoxic groups, SI/R con and SI/R dex, n>3.

CHAPTER 5

Discussion

It has become evident that the MAPK signaling pathway is a major regulator of cell death during ischaemia/reperfusion, in the heart. MKP-1 is known to be involved in these signaling pathways as it dephosphorylates MAPKs. MKP-1 has been shown to attenuate ischaemia/reperfusion injury in the heart. However, little is known about the mechanism involved and its effect on cell death modes. Therefore, the aim of the study was to investigate the role of MKP-1 induction/inhibition on cell death modes during ischaemia/reperfusion. In addition phosphorylation patterns of p38 MAPK, JNK and ERK MAPKs, known to be involved in both signal transduction during ischaemia/reperfusion and cell death modes, were investigated.

5.1 Experimental model

To investigate the role of MKP-1 in cell death modes during simulated ischaemia/reperfusion conditions in cardiomyocytes, without interference from other cell types, we made use of an *in vitro* cardiomyocyte model. The H9c2 cell line was established by Kimes and Brandt in 1976 through selective serial passaging of cardiac cells obtained from embryonic BDIX rat heart ventricle tissue (Kimes & Brandt, 1976). H9c2 cells have become a well established model as they share most of the molecular and functional

features of isolated adult cardiomyocytes (Hescheler *et al.*, 1991). Recently it has also been shown that the H9c2 cell line is a valuable *in vitro* model to study metabolic activity of the heart (Zordoky & El-Kadi, 2007). H9c2 cells have however, been found to dedifferentiate if the passage number is increased too much and therefore great care has to be taken to not over passage the cell line. H9c2 cells do not express gap junctions, caveolae, myofibrils with organised sarcomeres, or T-tubules. Similar to isolated cardiomyocytes, H9c2 cells are rich in rough endoplasmic reticulum (Hescheler *et al.*, 1991).

Simulated ischaemic conditions were created in our model by exposing cells to glycolytic inhibition, induced by 2DG supplementation. This prevents ATP production and reduces the availability of NADH. It should be kept in mind that the process of 2DG trapping phosphate as 2DG-phosphate to prevent ATP production is irreversible and may have an impact on recovery during reperfusion. The ischaemic buffer used in this study had a significant reduction in pH which also simulates myocardial ischaemia. In addition, a hypoxic environment was created by reducing the O₂ tension to 1%. Although the use of an *in vitro* model of ischaemia has its advantages, it is important to keep in mind that H9c2 cardiomyocytes may have undergone various morphological changes and biochemical differentiation and that the responses elicited may differ from those occurring in an *in vivo* setting.

It is important to consider that MAPK phosphorylation states during ischaemia/reperfusion may vary depending on the degree and duration of the ischaemic insult. Therefore, when interpreting MAPK phosphorylation states,

it should be kept in mind that the results obtained may be dependent on the specific ischaemic and reperfusion conditions that were simulated.

It is also important to consider heterogeneity of tissue culture models when investigating cell viability during ischaemia/reperfusion injury. Apoptotic markers can for instance show an increase as a result of a few cells presenting with high levels of apoptosis or as a result of many cells having low levels of apoptosis.

5.2 MKP-1 induction and MAPK phosphorylation, during ischaemia/reperfusion

To investigate the role of MKP-1 induction on the phosphorylation patterns of three major MAPKs; ERK, JNK and p38, during ischaemia/reperfusion injury, MKP-1 was induced by dexamethasone and inhibited by sanguinarine. MKP-1 is a dual specificity phosphatase that has been shown to dephosphorylate MAPKs during ischaemia/reperfusion thereby attenuating ischaemia/reperfusion injury (Engelbrecht *et al.*, 2005).

After 3 hrs simulated ischaemia, MKP-1 induction was significantly inhibited by sanguinarine which was associated with significantly increased p38 MAPK and ERK phosphorylation. No differences were however observed in JNK phosphorylation.

Interestingly, no significant increases in MKP-1 were observed after ischaemia or reperfusion. This is in accordance with results observed by Fan

et al. (2009) in perfused hearts and Engelbrecht *et al.* (2005) in neonatal cardiomyocytes were MKP-1 induction was not significantly increased after ischaemia/reperfusion injury (Engelbrecht *et al.*, 2005; Fan *et al.*, 2009). However, in the present study after reperfusion significant MKP-1 induction by dexamethasone and inhibition by sanguinarine could be elicited (Fig 4.5). These findings correlate with those obtained by Fan *et al.* (2009) who have shown that MKP-1 induction is achieved by dexamethasone during reperfusion (Fan *et al.*, 2009). It has also been shown that MKP-1 inhibition is achieved in the presence of sanguinarine (Vogt *et al.*, 2005).

As expected, p38 MAPK phosphorylation was significantly reduced during MKP-1 induction and significantly increased during MKP-1 inhibition after reperfusion (Fig 4.6). Contrary to expectations, ERK phosphorylation decreased during MKP-1 inhibition and increased during MKP-1 induction in simulated ischaemia followed by reperfusion (Fig.4.7). JNK phosphorylation was similarly decreased during MKP-1 inhibition (Fig 4.8). Lasa *et al.* (2002) showed p38 MAPK dephosphorylation to decrease in the presence of dexamethasone-induced MKP-1 expression in HeLa cells (Lasa *et al.*, 2002). In contrast to our findings phospho-ERK and phospho-JNK have been found to increase in the presence of sanguinarine induced MKP-1 inhibition in pancreatic cancer cells (Vogt *et al.*, 2005). These discrepancies may be due to either the cell type or the experimental conditions for example the ischaemia/reperfusion injury duration and severity that was induced in this study in the presence of sanguinarine. Discrepancies between p38, ERK and JNK phosphorylation seen after reperfusion may be due to activation times of the MAPKs as p38 MAPK is known to be activated during both ischaemia

and reperfusion, whereas ERK and JNK are activated during reperfusion only (Bogoyevitch *et al.*, 1996). It may also be due to the fact that MKP-1 has a higher affinity to dephosphorylate p38 MAPK than ERK and JNK (Chu *et al.*, 1996; Franklin & Kraft, 1997; Franklin *et al.*, 1998; Li *et al.*, 1999; Boutros *et al.*, 2008a). As sanguinarine is a selective MKP-1 inhibitor other MKPs, such as MKP-3 which is specific for ERK dephosphorylation (Cowan & Storey, 2003) are free to dephosphorylate JNK and ERK.

5.3 Role of MKP-1 in autophagy during simulated ischaemia/reperfusion

It is well known that autophagy plays an important role in the heart at three levels; firstly during basal conditions, secondly during ischaemia, when it is stimulated largely by the glucose and oxygen deprivation and thirdly during reperfusion, most probably to clear up damaged organelles (Codogno & Meijer, 2005; Matsui *et al.*, 2007; Nishida *et al.*, 2009). However, no evidence exists for a role for MKP-1 in autophagy during ischaemia and reperfusion.

After ischaemia autophagic activity indicated by acridine orange was significantly decreased in the presence of MKP-1 inhibition (Fig 4.11). However, no significant differences were found in beclin-1 (Fig 4.12) and LC3-II (Fig 4.13) activity. This discrepancy may be viewed in the light of acridine orange being an indicator of lysosomal compartments per se and not a direct indicator of autophagic activity.

As was seen in ischaemia a significant decrease in autophagic activity, indicated by acridine orange, was seen during MKP-1 inhibition during reperfusion (Fig 4.16). Correspondingly beclin-1 (Fig 4.17) and LC3-II (Fig 4.18) induction were decreased during MKP-1 inhibition and increased during dexamethasone-induced MKP-1 induction (Fig 4.5). Furthermore, increased p38 MAPK phosphorylation (Fig 4.6) correlated with attenuation of autophagy and vice versa. These findings coincide with very recent literature where autophagy induction was shown to be mediated by MKP-1 activation, in oral cancer cells (Lu *et al.*, 2010). It was also previously shown that the p38 phosphorylation state is involved in the negative control of autophagy in the human liver, in response to cellular hydration (vom Dahl *et al.*, 2001). Furthermore, while autophagy was decreased during MKP-1 inhibition, JNK phosphorylation was decreased as well. This is in agreement with Ogata *et al.* who have shown that JNK activation is needed for ER stress induced autophagy (Ogata *et al.*, 2006). In our study, decreased ERK phosphorylation coincided with decreased autophagy during MKP-1 inhibition while MKP-1 induction resulted in increased autophagy accompanied by increased phospho-ERK levels. It has also been shown in human colon cancer cells that ERK activation stimulates autophagy (Ogier-Denis *et al.*, 2000; Pattingre *et al.*, 2003).

During reperfusion, inhibition of MKP-1, subsequent increased p38 MAPK phosphorylation and decreased ERK and JNK phosphorylation, may lead to decreased autophagic activity. Furthermore, induction of MKP-1, decreased p38 MAPK phosphorylation and increased ERK phosphorylation leads to increased autophagic activity. This may suggest that MKP-1 has a more

significant role in autophagic activity during reperfusion than during ischaemia. This may be viewed in the light of MAPK activation which leads to MKP-1 activation. Only p38 MAPK is activated during ischaemia whereas ERK, JNK and p38 are activated during reperfusion. This may result in increased MKP-1 activation, by all three MAPKs, and therefore have an increased effect on autophagic activity during reperfusion.

The data suggest an association between MAPK activation, MKP-1 and autophagy. We propose that autophagy is either indirectly regulated via MAPKs by MKP-1 or that an unknown pathway exists whereby MKP-1 induction directly regulates autophagy induction.

5.4 Role of MKP-1 in apoptosis and necrosis during simulated ischaemia/reperfusion

Apoptotic cell death is markedly increased during myocardial ischaemia/reperfusion (Freude *et al.*, 2000; Elmore, 2007). It is also known that p38 MAPK and JNK are activated and play an important role in regulation of apoptosis during ischaemia/reperfusion (Tobiume *et al.*, 2001; Li *et al.*, 2003b).

After 3 hrs ischaemia the relative viability based on MTT reduction was decreased and even more while MKP-1 was inhibited (Fig 4.19). Pyknosis (Fig 4.21), late pyknosis (Fig 4.22), caspase-3 cleavage (Fig 4.24) and PARP cleavage (Fig 4.25) were increased during MKP-1 inhibition. This coincides

with increased p38 MAPK phosphorylation after SI (Fig 4.2). PI positive cells were increased after 3 hrs ischaemia in the presence of the MKP-1 inhibition (Fig 4.23).

After reperfusion the percentage MTT reduction in control groups had increased from before reperfusion, even though it remained significantly lower than during basal conditions. During MKP-1 inhibition, MTT reduction did however not improve and was significantly lower than that of normoxic conditions and SI/R control groups (Fig 4.26). Pyknosis was significantly decreased after SI/R during MKP-1 inhibition (Fig 4.28), however, late pyknosis increased after reperfusion, and even more during MKP-1 inhibition (Fig 4.29). Caspase-3 cleavage (Fig 4.32) and PARP cleavage (Fig 4.33) were increased while MKP-1 induction was inhibited during reperfusion. These results indicate that apoptosis was significantly increased during MKP-1 inhibition after reperfusion. It has been shown that MKP-1 induction exerts a cardioprotective effect through the inhibition of caspases-3 cleavage and protects the heart from p38 MAPK induced injury (Morisco *et al.*, 2007). It has also been shown that p38 MAPK is required in apoptosis induction in cellular models (Tobiume *et al.*, 2001; Tanaka *et al.*, 2002; Li *et al.*, 2003b; Junttila *et al.*, 2008).

Furthermore, ERK phosphorylation was significantly lower after reperfusion during MKP-1 inhibition which resulted in apoptosis being most prominent. We also showed that JNK phosphorylation was significantly decreased during MKP-1 inhibition which was associated with increased apoptosis. JNK, has however been shown to promote apoptosis. ERK has been shown

to be involved in survival signaling in response to ischaemia/reperfusion (Yue *et al.*, 2000). ERK inhibition has been shown to result in increased apoptosis in cardiomyocytes following daunomycin treatment (Zhu *et al.*, 1999). Khan *et al.* (2004) showed that ERK activation during reperfusion leads to increased cardiac functional recovery, while p38 MAPK activation has been related to myocardial dysfunction during reperfusion (Khan *et al.*, 2004). Contradictory to our findings it has been shown that JNK is proapoptotic as it phosphorylates p53, known to induce apoptosis (Khan *et al.*, 2004). An explanation for these discrepancies may be the time point at which reperfusion was investigated. It was previously shown that JNK is activated early in reperfusion, therefore after 30 minutes it could have returned to baseline levels (Engelbrecht *et al.*, 2004). In this case we can assume that the involvement of MAPKs in the apoptotic insult was not mediated by JNK during MKP-1 inhibition, but rather via the increased p38 MAPK phosphorylation and decreased ERK phosphorylation.

Necrosis was most severe after reperfusion during MKP-1 inhibition. After reperfusion PI positive cells were increased in control reperfusion conditions and even more so during MKP-1 inhibition (Fig 4.30). Furthermore, significant LDH release occurred during MKP-1 inhibition (Fig 4.31). The relationship between MKP-1 and necrosis is not well defined. From our results we can see that necrosis resulted during ischaemia/reperfusion when MKP-1 was inhibited. Secondary necrosis is usually observed *in vitro* in cultured cells where phagocytic cells are absent; resulting in failure to remove apoptotic cells (Majno & Joris, 1995; Zong & Thompson, 2006). As

high levels of apoptosis and late apoptosis were seen at the same time, it could be an indication that secondary necrosis occurred.

CHAPTER 6

Summary

The aim of the study was to investigate the role of MKP-1 in autophagy and apoptotic and necrotic cell death during ischaemia/reperfusion in the heart. This was done by experimental manipulation of MKP-1 induction by dexamethasone and MKP-1 inhibition by sanguinarine during simulated ischaemia/reperfusion. Our results suggest that MKP-1 induction does indeed play a role in cell death modes during ischaemia/reperfusion in the heart.

During ischaemia MKP-1 inhibition resulted in increased ERK and p38 MAPK phosphorylation, which subsequent increased apoptotic and necrotic cell death. Autophagy was however not significantly influenced by MKP-1 inhibition during ischaemia. However, after reperfusion alterations in MKP-1 induction did cause fluctuations in autophagy induction. During increased MKP-1 induction, accompanied by decreased p38 MAPK phosphorylation and increased ERK phosphorylation, autophagy was significantly increased. In contrast, MKP-1 inhibition, accompanied by increased p38 MAPK phosphorylation and decreased ERK phosphorylation, led to decreased autophagic activity. Apoptotic and necrotic cell death were significantly increased during this time. It can thus be concluded that MKP-1 and autophagy are intricately involved in reperfusion as autophagic protection was abolished in the absence of MKP-1, where cells died from apoptosis or

necrosis, and autophagic protection was permitted in the presence of dexamethasone induced MKP-1 expression, where apoptotic and necrotic cells were significantly decreased. MKP-1 induced cardioprotection may thus be mediated via autophagy induction during reperfusion.

Upregulation of MKP-1 is known to attenuate cardiomyocyte injury during ischaemia/reperfusion injury. From the results obtained in this study we can conclude that MKP-1 induced attenuation of ischaemic injury is however not conveyed via autophagic regulation by MKP-1. However, reperfusion injury is indeed attenuated via induction of autophagy by MKP-1.

According to our knowledge, this is the first demonstration of the induction of autophagy by MKP-1 during reperfusion in the heart.

CHAPTER 7

Future directions

It would be of great importance to confirm our findings in an *in vivo* setting where physiological conditions of the entire organ can be better reflected and to accurately reproduce the scenario in the ischaemic myocardium. Directed by our findings we speculate that autophagic regulation by MKP-1 could either occur indirectly via MAPK phosphorylation patterns being altered by MKP-1 or that there may exist an alternative, direct link by which MKP-1 regulates autophagy during ischaemia/reperfusion. It would be of great benefit to investigate and identify the exact mechanism whereby MKP-1 results in autophagic induction during reperfusion. If there is indeed a direct link it could be manipulated to further increase MKP-1 induction during ischaemia/reperfusion injury in the clinical setting. It would also be wise to investigate the induction states of MKP-1 at different time points during the ischaemia/reperfusion insult to gain insight into the most appropriate time at which MKP-1 induction can be manipulated to better attenuate ischaemia/reperfusion injury. Furthermore, the role of p38 MAPK in this setting could for instance be evaluated by using a blocker.

CHAPTER 8

Pilot studies

8.1 Determination of simulated ischaemia conditions

To investigate the role of MKP-1 in cell death during simulated ischaemia/reperfusion, a pilot study was done to determine appropriate simulated ischaemic conditions. Ischaemia which results from low blood flow was mimicked by creating an experimental environment for cells, where oxygen concentrations were lowered to 1% and metabolic parameters were also altered. This is known as simulated ischaemia.

Thus, simulated ischaemic environments were created by exposing cells to a hypoxic environment, in the presence of a modified ischaemic buffer (Esumi *et al.*, 1991), with or without 2DG (Fuglestad *et al.*, 2008). In the presence of 2DG, glycolysis is inhibited by trapping phosphate as 2DG-phosphate, which further inhibits glycolysis, and so mimics ischaemic conditions.

Cells were exposed to these conditions for 3 or 4 hours.

The relative cell viability based on MTT, decreased significantly after 3h Esumi treated ($55.25 \pm 1.7\%$) and Esumi/2DG ($42.17 \pm 1.8\%$) treated groups and also after 4 h Esumi treated ($59.35 \pm 2.1\%$) and Esumi/2DG ($43.88 \pm 1.1\%$) treated groups, compared to the normoxic control cells ($p < 0.001$). When comparing the reduction capacity between Esumi treated and Esumi/2DG

treated groups treated for both 3 and 4 hours, a significant difference was found ($p < 0.001$).

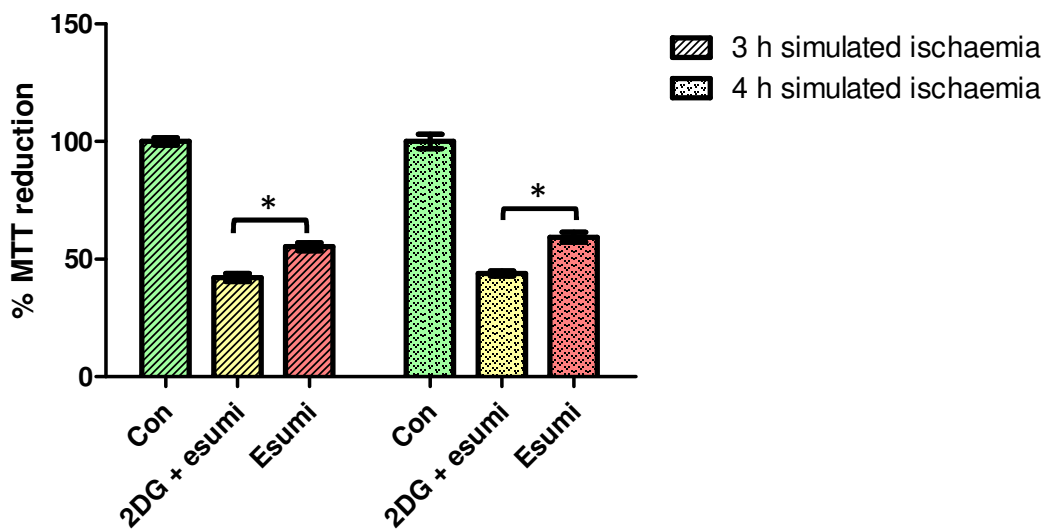


Figure 8.1: Esumi and Esumi supplemented with 2DG groups treated for 3 h and 4 h. Data expressed as mean \pm SEM. * $p < 0.001$, n=6

For the remainder of experiments simulated ischaemia was therefore mimicked by treating cells with modified ischaemic buffer supplemented with 2DG, for 3 hours.

8.2 MKP-1 inhibition

In order to investigate the role of MKP-1 in autophagic cell death, apoptosis and necrosis during ischaemia/reperfusion injury, it had to be investigated in both inhibited and induced states. It is well known that insulin significantly induces MKP-1 activation (Jacob *et al.*, 2002; Morisco *et al.*, 2007). Insulin concentrations of 100 nM are suggested by literature for *in vitro* cardiac studies (Morisco *et al.*, 2007). It has been shown that triptolide, a root extract from a Chinese medicinal vine, blocks the transcription of MKP-1 (Wang *et al.*, 2006).

A MTT assay was done to investigate the myocyte survival rate in the presence of both insulin and triptolide, to determine concentrations during which these treatments, alone, would not cause damage to the cells under normoxic conditions.

8.2.1 Triptolide

No significant difference was found between the percentage MTT reduction capacity when cells were treated with different concentrations of triptolide.

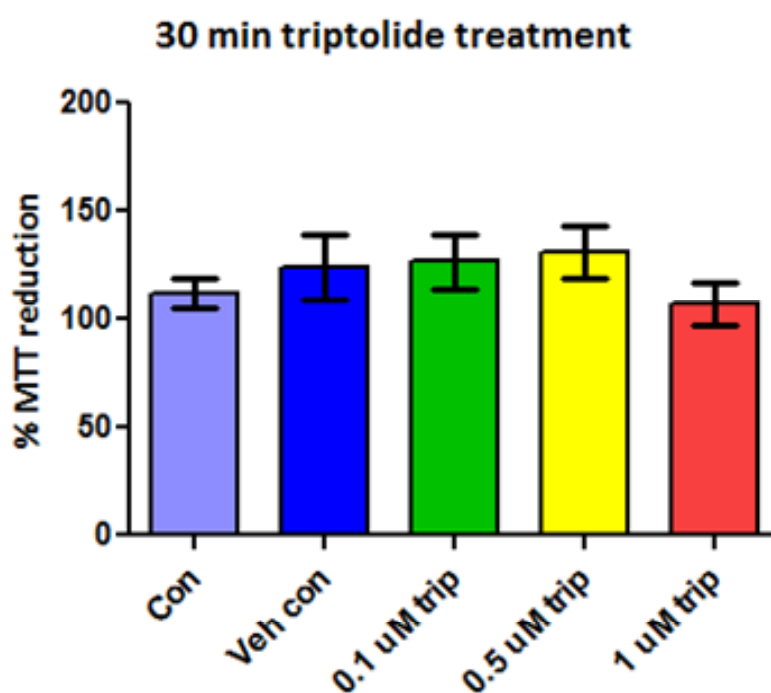


Fig 8.2: Relative viability based of MTT reduction, triptolide concentration curve showing control (Con), vehicle control (Veh con) and triptolide (trip). Data expressed as mean \pm SEM. n=6

Cells were then exposed to simulated ischaemic conditions using 100 nM insulin or 1 μ M triptolide. Hoechst 33342 was used to stain cells to determine nuclear condensation.

Significantly more pyknotic cells were present in the SI/R control (11.1 ± 0.9) and even more so in the SI/R triptolide (15.93 ± 2.2) treatment groups compared to the normoxic treated groups ($p < 0.001$). Pyknosis in the SI/R control groups was significantly higher than that of SI/R insulin (6.37 ± 1.49) treated groups ($p < 0.05$). Insulin significantly decreased pyknosis compared to SI/R triptolide treated groups ($p < 0.05$).

Pyknotic cells after reperfusion

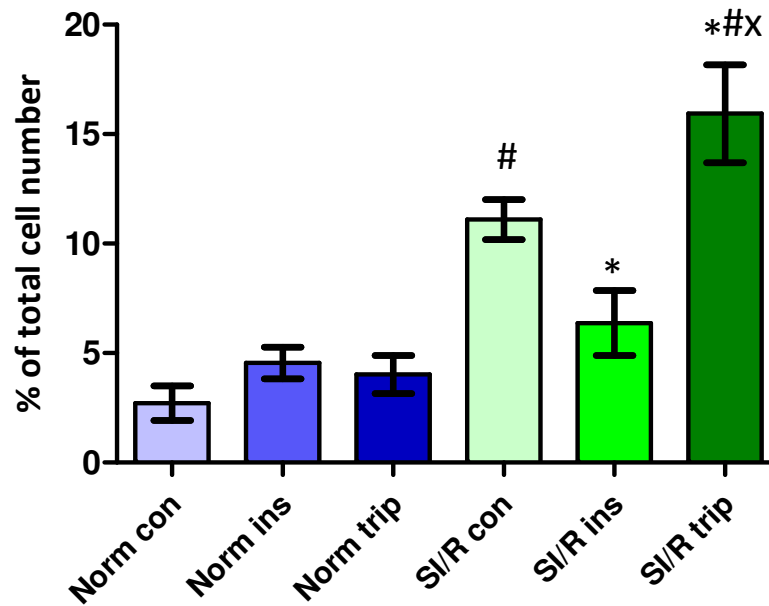


Fig 8.3: Percentage pyknosis after SI/R, showing normoxic control (Norm con), normoxic insulin (Norm ins), normoxic triptolide (Norm trip), simulated ischaemia/reperfusion control (SI/R con), simulated ischaemia/reperfusion insulin (SI/R ins) and simulated ischaemia/reperfusion triptolide (SI/R trip). Data expressed as mean \pm SEM. # p <0.001 vs. normoxic groups, * p <0.05 vs. SI/R con, x p <0.001 vs SI/R ins. $n=9$.

Lysotracker Red was then used to investigate autophagic events during SI/R, in the presence of insulin and triptolide.

No visual difference in red fluorescence was detected, when comparing control, insulin and triptolide treatments. Acidic vacuoles do however seem to accumulate around the nuclear regions after SI/R compared to normoxic cells where they are more evenly dispersed across the entire cell.

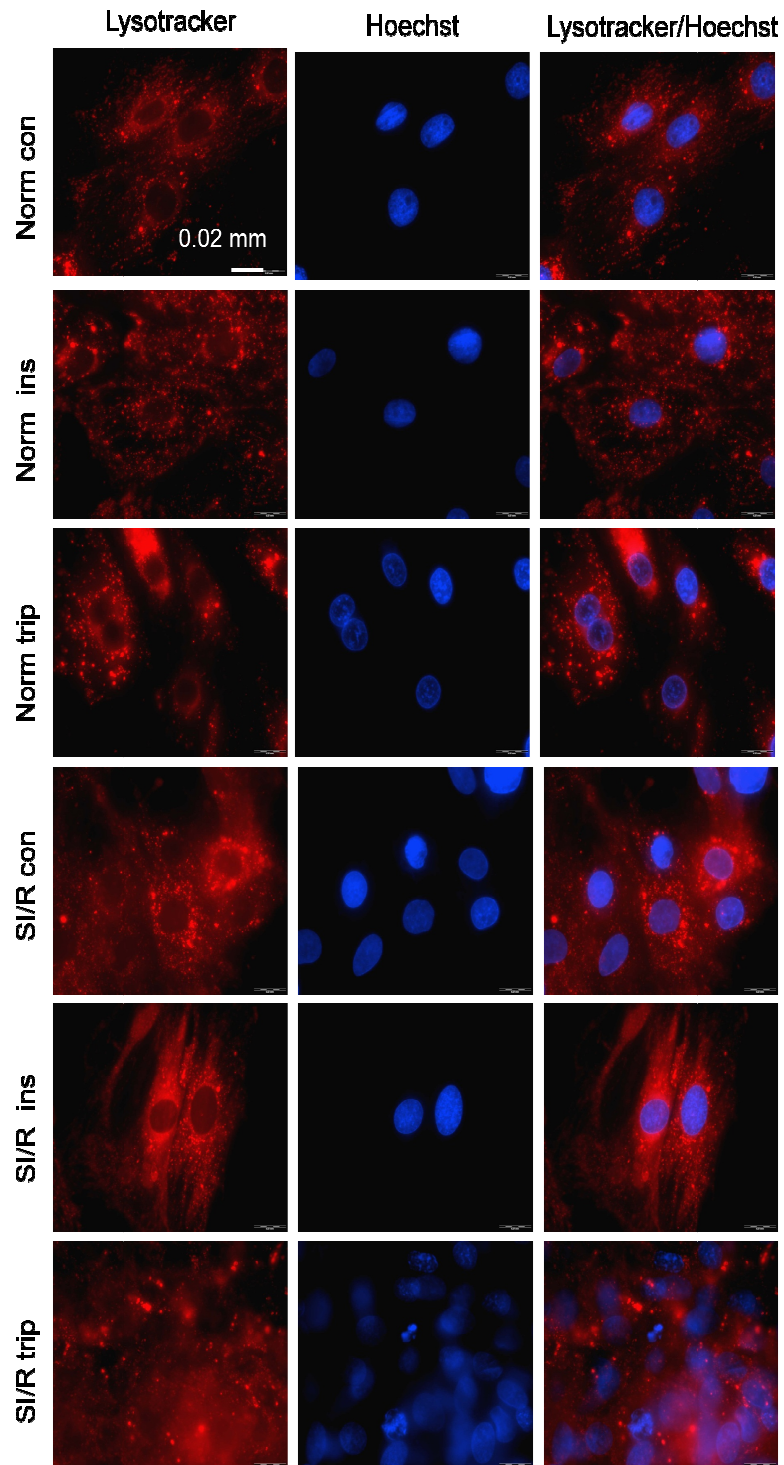


Figure 8.4: Fluorescent micrographs showing cells with acidic vacuoles (red) and nuclei (blue) after normoxia or SI/R, showing normoxic control (Norm con), normoxic insulin (Norm ins), normoxic triptolide (Nom trip), simulated ischaemia/reperfusion control (SI/R con), simulated ischaemia/reperfusion insulin (SI/R ins and simulated ischaemia/reperfusion triptolide (SI/R trip).

Western blots were done to assess MKP-1 induction in the presence of 0.5 μ M triptolide or 1 μ M triptolide, after 30 min.

In the 0.5 μ M triptolide (121 ± 10) treatment group MKP-1 induction was significantly more than that of the 1 μ M triptolide (89.5 ± 5.5) treatment group ($p<0.05$).

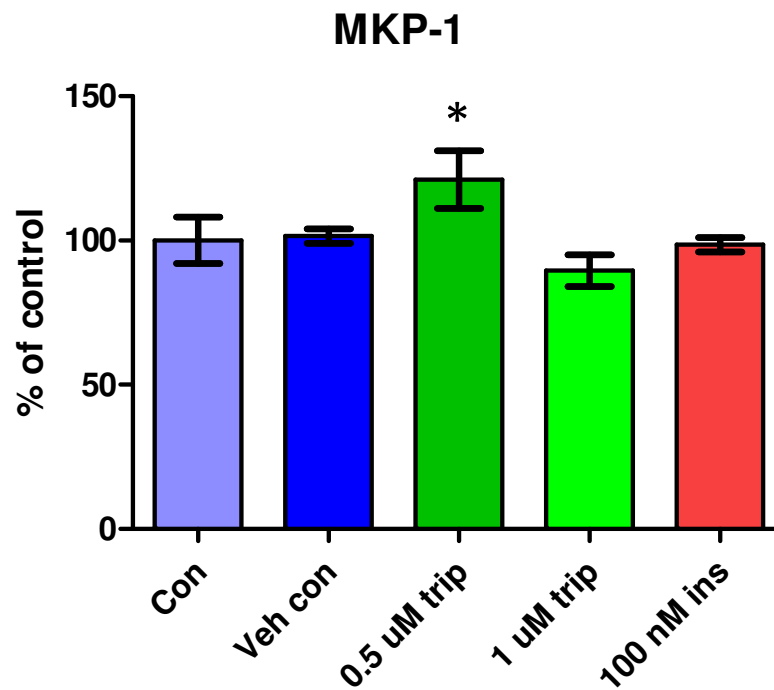


Fig 8.5: MKP-1 induction after triptolide or insulin treatment, showing control (Con), vehicle control (Veh con), triptolide (trip) and insulin (ins). Data expressed as mean \pm SEM, * $p<0.05$ vs. 1 μ M trip, $n>3$.

As MKP-1 inhibition was not achieved in the presence of triptolide, attention was turned to sanguinarine, also known to selectively inhibit MKP-1 (Vogt *et al.*, 2005).

8.2.2 Sanguinarine

Sanguinarine, an alkaloid from the toxic plant *Chelidonium majus*, has been shown to selectively inhibit MKP-1 activity (Vogt *et al.*, 2005; Garcia *et al.*, 2006).

A MTT assay was done to assess the relative viability of the cells in the presence of different sanguinarine concentrations, to ensure the optimal concentration which does not cause damage to the cells under normoxic conditions.

50 μ M sanguinarine ($38.4\pm 1\%$) treatment resulted in a significant decrease in relative viability based on MTT reduction ($p < 0.001$). Therefore sanguinarine was used at a 10 μ M concentration for further experimentation.

30 min sanguinarine chloride treatment

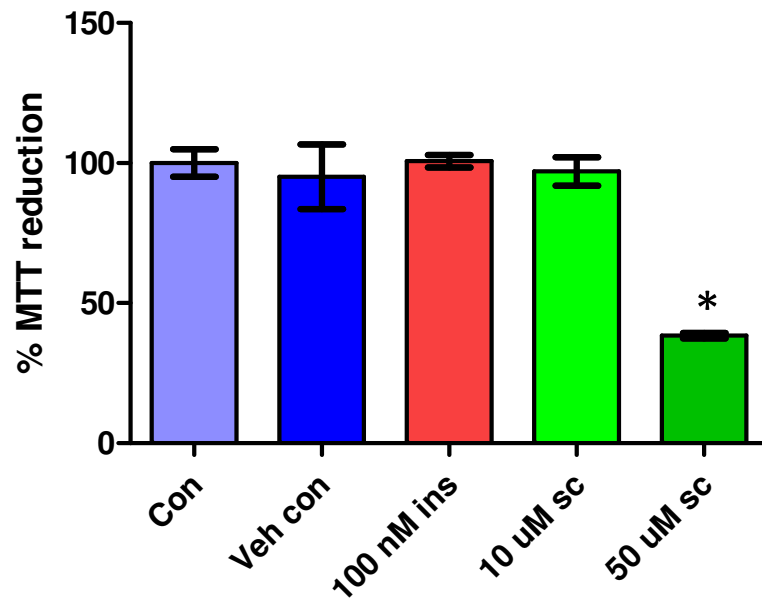


Fig 8.6: Relative viability based of MTT reduction, sanguinarine concentration determination curve, showing control (Con), vehicle control (Veh con), insulin (ins) and sanguinarine (sc). Data expressed as mean±SEM. *p<0.001, n=6.

A western blot was done to assess the inhibitory effects of on MKP-1 activity.

The sanguinarine (66.05±4.01) treated group had significantly decreased MKP-1 induction compared to the control (100±3.31) and insulin (93±5.76) treated group (p<0.01).

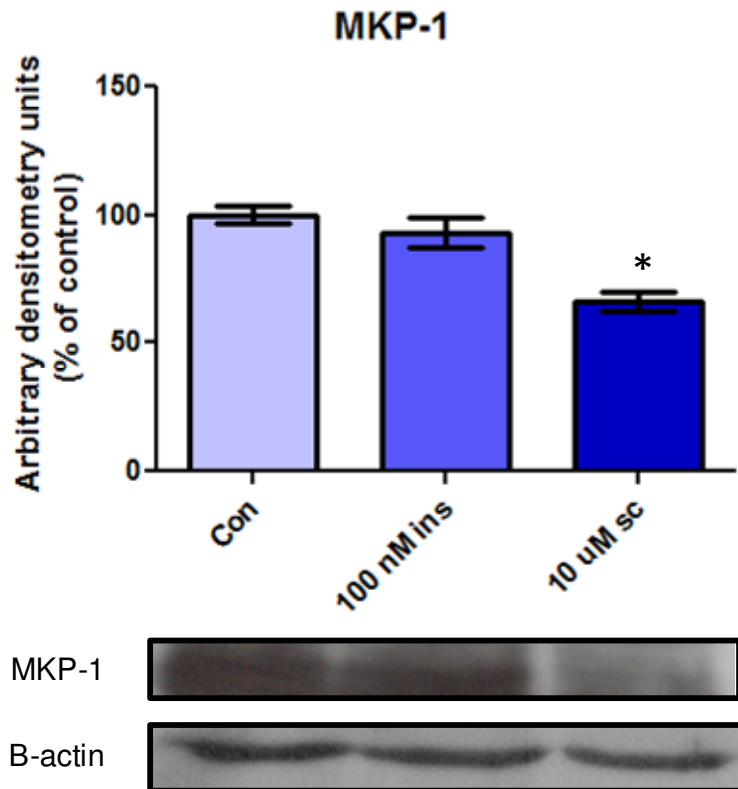


Figure 8.7: MKP-1 induction after insulin or sanguinarine treatment, showing control (Con), insulin (ins) and sanguinarine (sc). Data expressed as mean \pm SEM. * p <0.01, n >3.

Sanguinarine at a concentration of 10 μ M was decided upon for further use, to inhibit MKP-1 induction.

8.3 Results: after insulin treatment

8.3.1 MKP-1 and MAPK signaling after 3 hrs stimulated ischaemia

No significant differences were found in MKP-1 induction or p38, ERK and JNK phosphorylation states when comparing control and insulin treatment groups after simulated ischaemia.

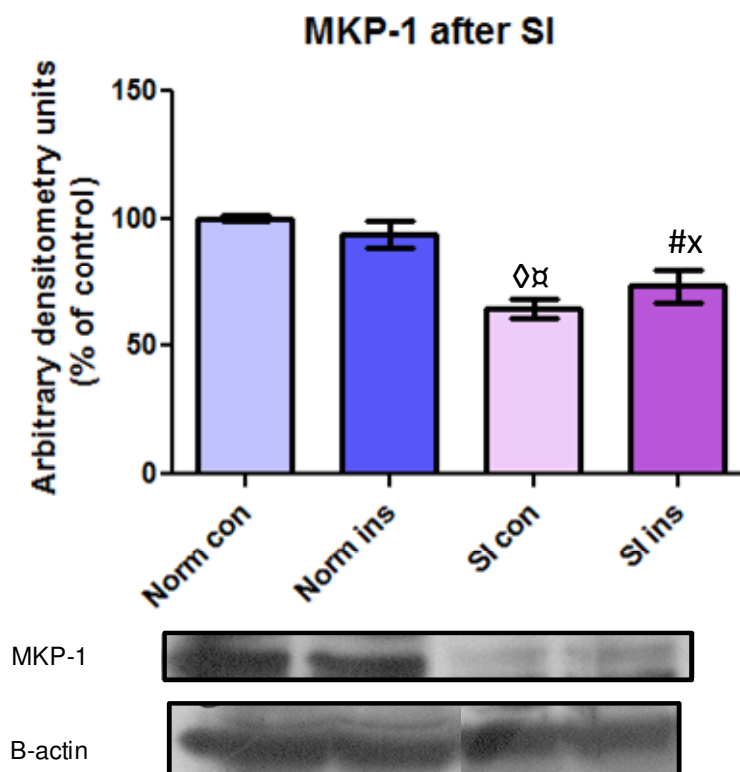


Figure 8.8: MKP-1 induction after SI, showing normoxic control (Norm con), normoxic insulin (Norm ins), simulated ischaemia control (SI con) and simulated ischaemia insulin (Ins). Data expressed as mean \pm SEM. \diamond p<0.001 vs. norm con, $\#$ p<0.01 vs. norm ins, $\#$ p<0.01 vs. norm con, x p<0.05 vs. norm ins, n>3.

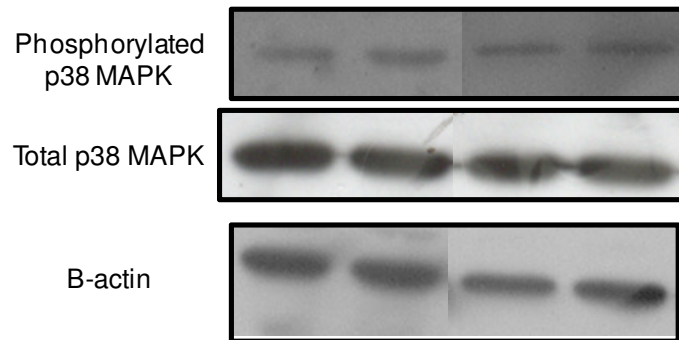
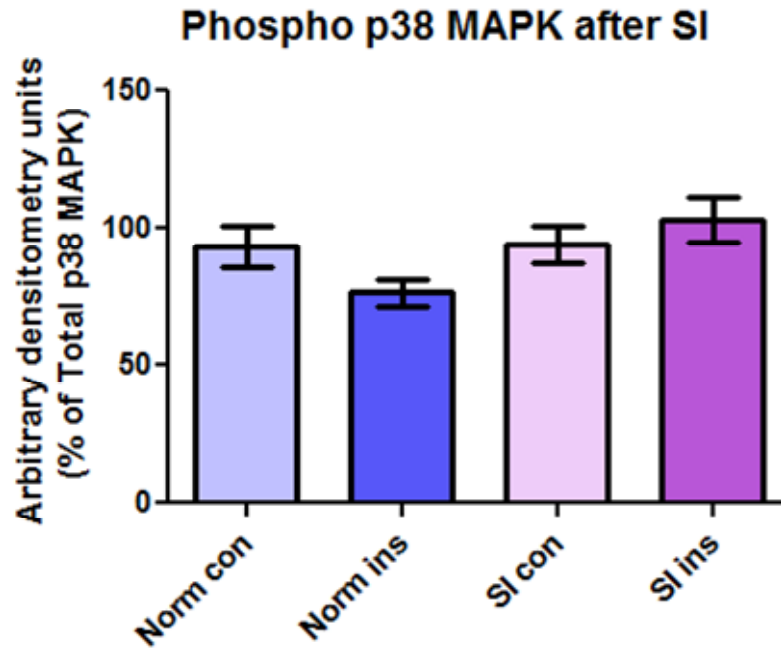


Figure 8.9: Phosphorylated p38 MAPK after SI, showing normoxic control (Norm con), normoxic insulin (Norm ins), simulated ischaemia control (SI con) and simulated ischaemia insulin (Ins). Data expressed as mean \pm SEM. n>3.

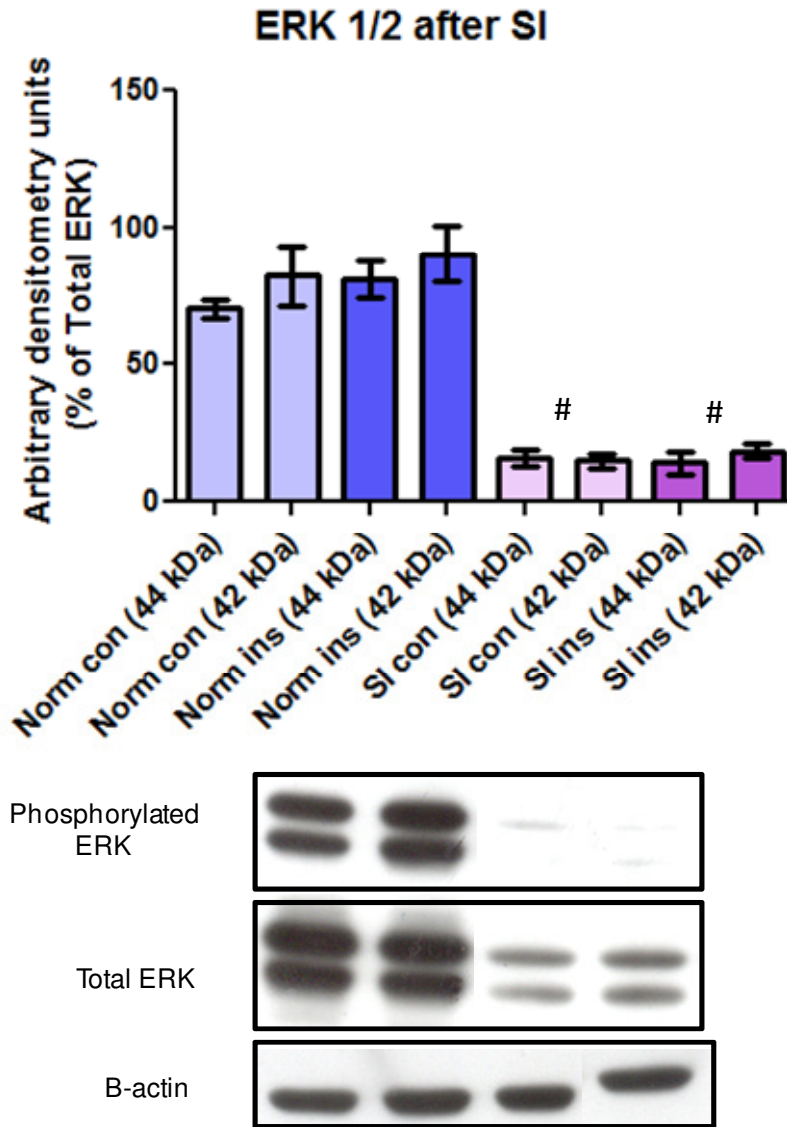


Figure 8.10: Phosphorylated ERK after SI, showing normoxic control (Norm con), normoxic insulin (Norm ins), simulated ischaemia control (SI con) and simulated ischaemia insulin (Ins). Data expressed as mean \pm SEM. # p <0.001 vs. normoxic groups, n >3.

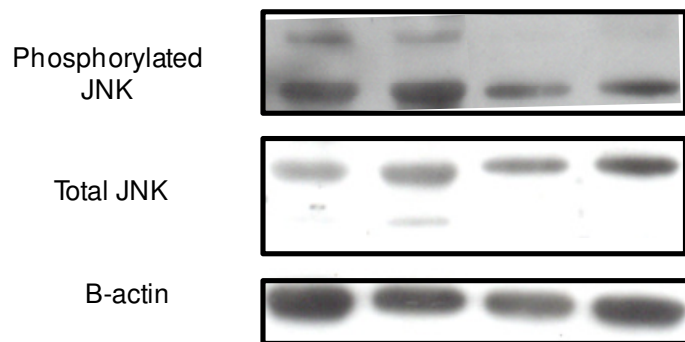
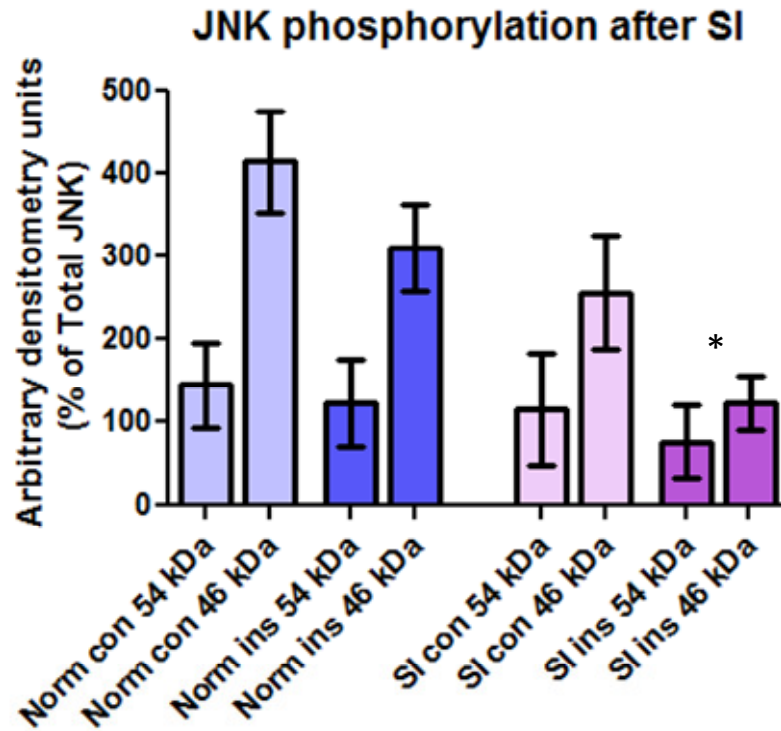


Figure 8.11: Phosphorylated JNK after SI, showing normoxic control (Norm con), normoxic insulin (Norm ins), simulated ischaemia control (SI con) and simulated ischaemia insulin (Ins). Data expressed as mean \pm SEM. $p < 0.05$ vs. norm con, $n > 3$.

8.3.2 MKP-1 and MAPK signaling after 3 hrs stimulated ischaemia/reperfusion

No significant differences were found in MKP-1 induction or p38, ERK and JNK phosphorylation states when comparing control and insulin treatment groups after reperfusion.

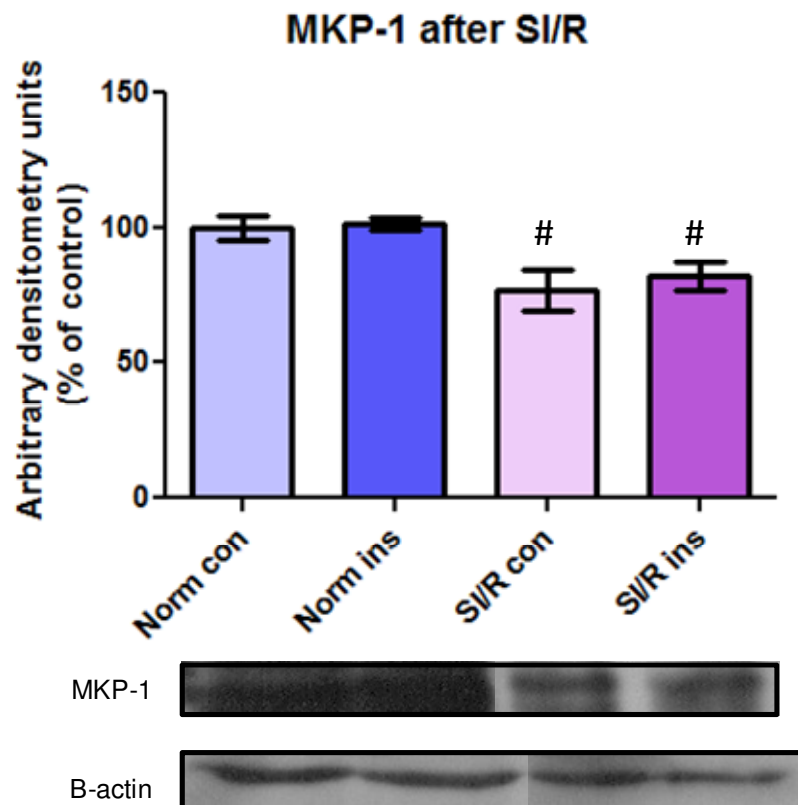


Figure 8.12: MKP-1 induction after SI/R, showing normoxic control (Norm con), normoxic insulin (Norm ins), simulated ischaemia/reperfusion control (SI/R con) and simulated ischaemia/reperfusion insulin (SI/R Ins). Data expressed as mean \pm SEM. [#]p<0.01 vs. normoxic groups, n>3.

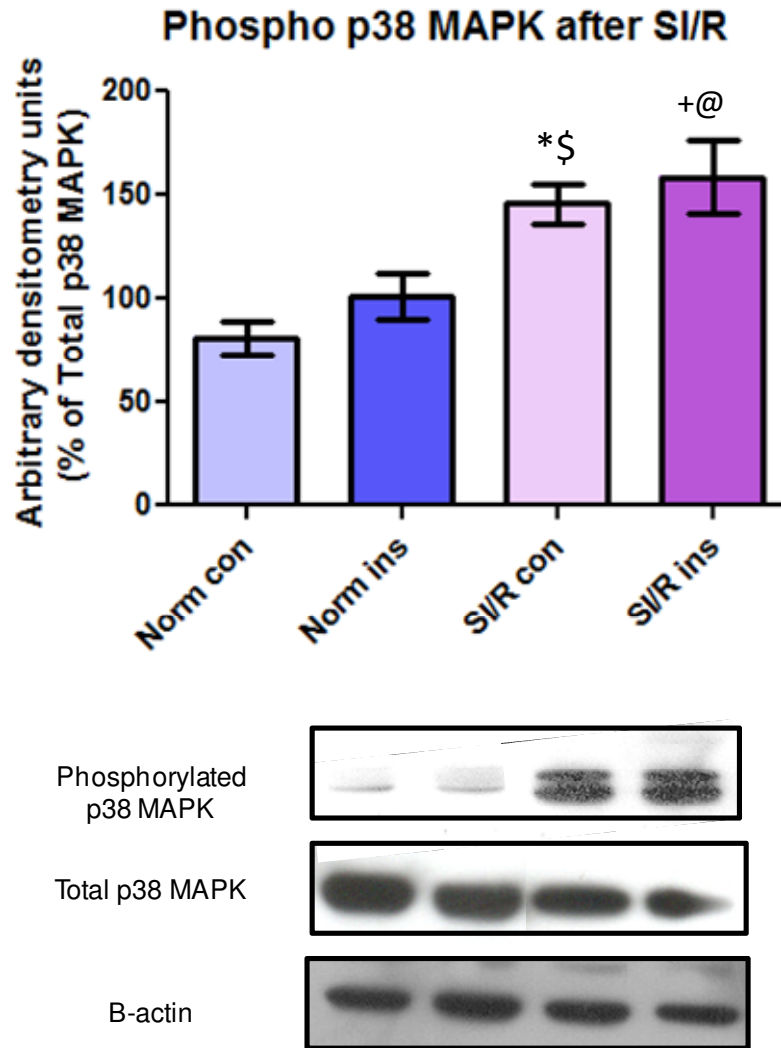


Figure 8.13: Phosphorylated p38 MAPK after SI/R, showing normoxic control (Norm con), normoxic insulin (Norm ins), simulated ischaemia/reperfusion control (SI/R con) and simulated ischaemia/reperfusion insulin (SI/R Ins). Data expressed as mean±SEM. *p<0.01 vs. norm con, +p<0.001 vs. norm con, \$p<0.05 vs. norm ins, @p<0.01 vs. norm ins,n>3.

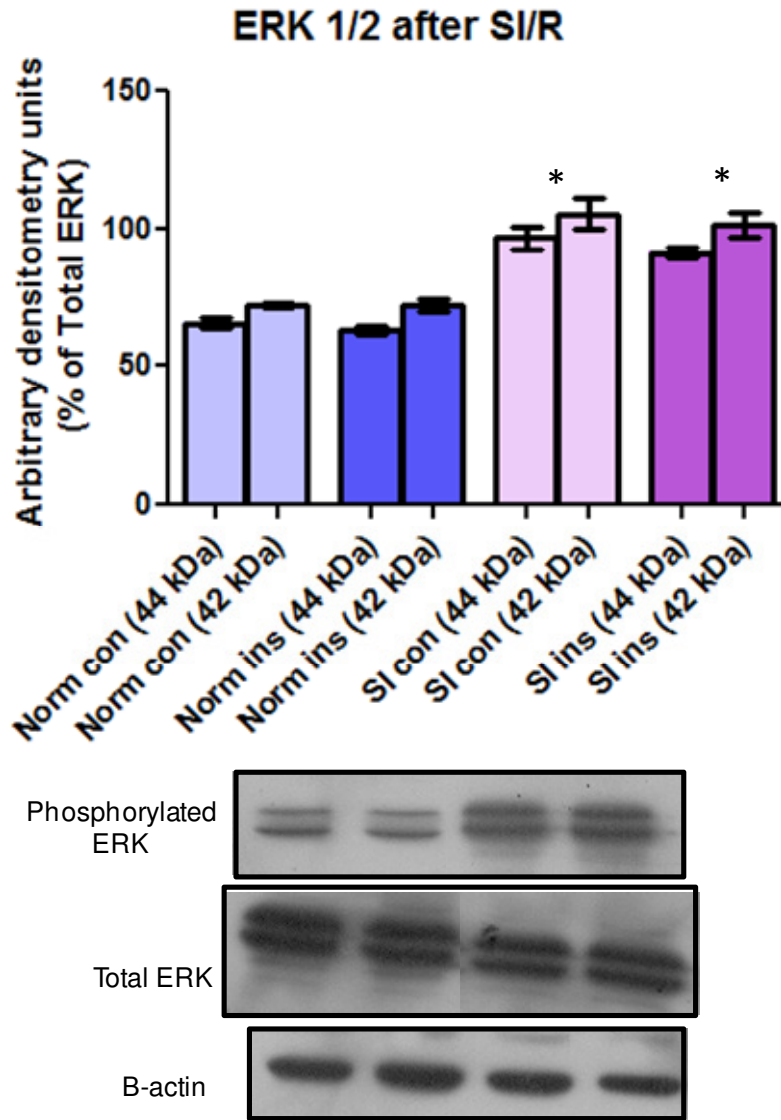


Figure 8.14: Phosphorylated ERK after SI/R, showing normoxic control (Norm con), normoxic insulin (Norm ins), simulated ischaemia/reperfusion control (SI/R con) and simulated ischaemia/reperfusion insulin (SI/R Ins). Data expressed as mean±SEM. *p<0.001 vs. normoxic groups, n>3.

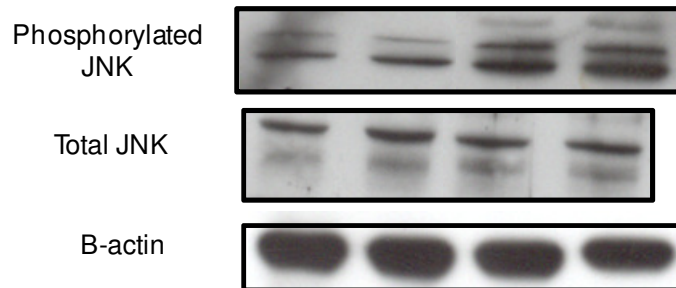
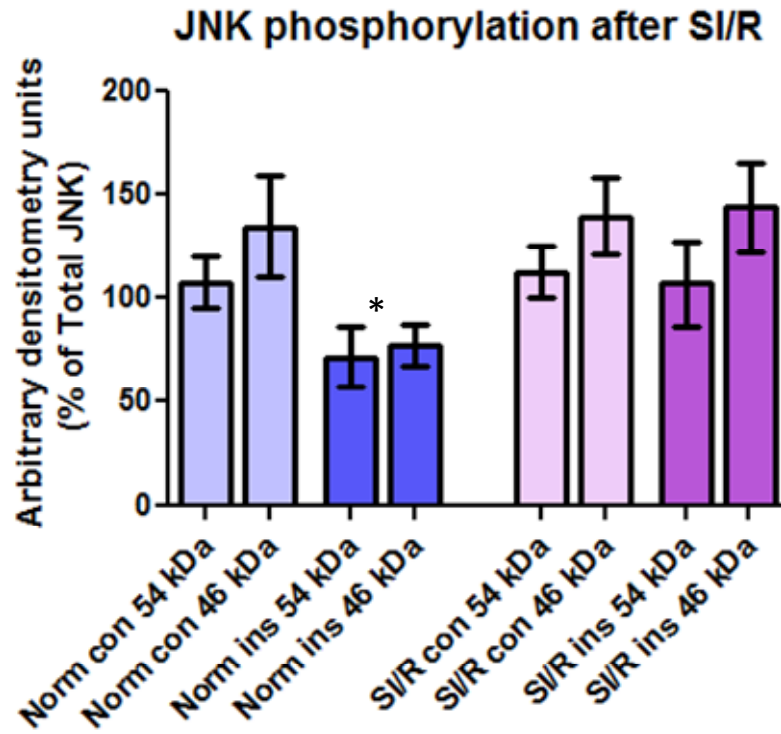


Figure 8.15: Phosphorylated JNK after SI/R, showing normoxic control (Norm con), normoxic insulin (Norm ins), simulated ischaemia/reperfusion control (SI/R con) and simulated ischaemia/reperfusion insulin (SI/R Ins). Data expressed as mean±SEM. $p < 0.01$ vs. norm con, SI/R con and SI/R ins, $n > 3$.

8.3.3 Autophagic activity after 3 hrs simulated ischaemia

Autophagic activity was not significantly different between simulated ischaemic groups after control or insulin treatment.

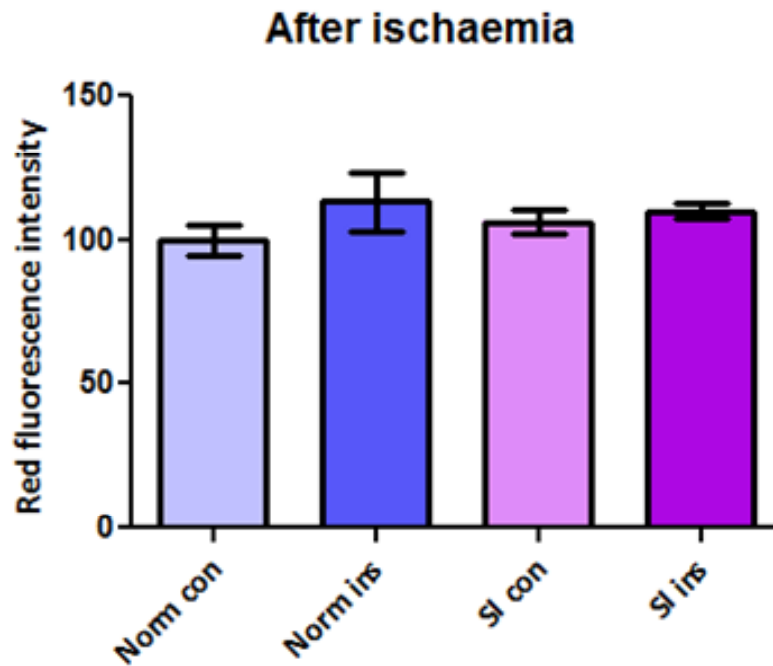


Figure 8.16: Percentage red fluorescence intensity indicating acidic vacuoles, showing normoxic control (Norm con), normoxic insulin (Norm ins), simulated ischaemia control (SI con) and simulated ischaemia insulin (Ins). Data expressed as mean ± SEM. n > 3.

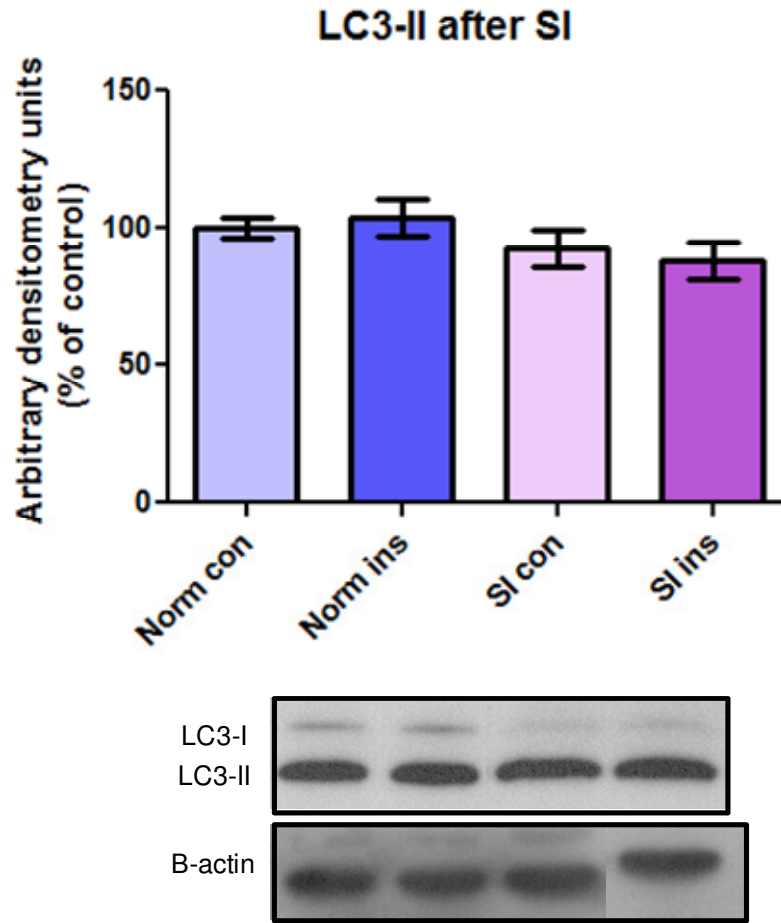


Figure 8.17: LC3-II induction after SI, showing normoxic control (Norm con), normoxic insulin (Norm ins), simulated ischaemia control (SI con) and simulated ischaemia insulin (Ins). Data expressed as mean±SEM. n>3.

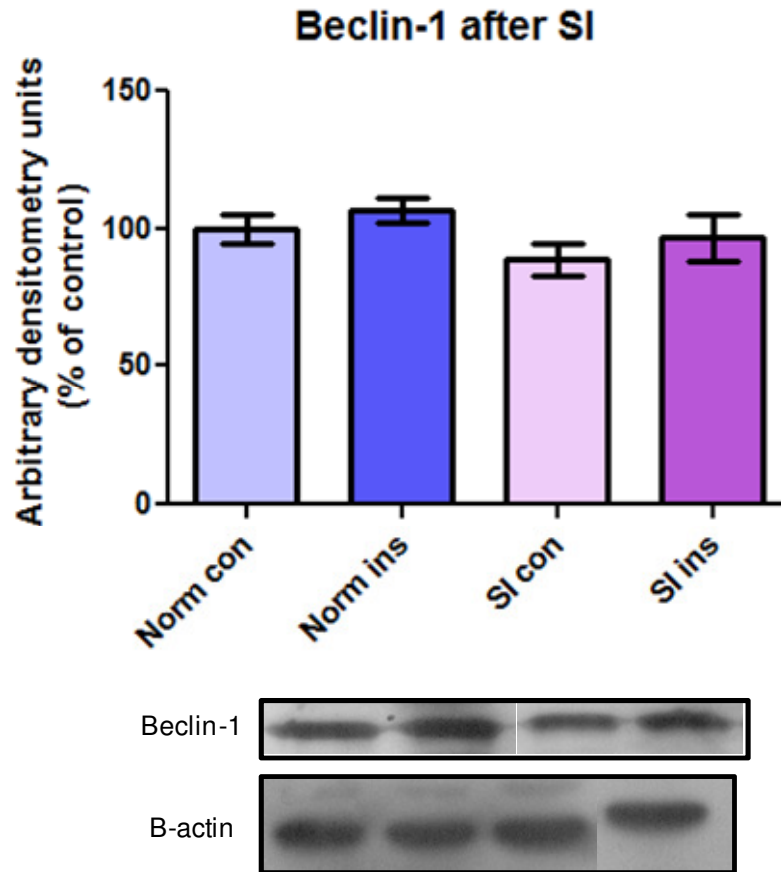


Figure 8.18: Beclin-1 induction after SI, showing normoxic control (Norm con), normoxic insulin (Norm ins), simulated ischaemia control (SI con) and simulated ischaemia insulin (Ins). Data expressed as mean \pm SEM. n>3.

8.3.4 Autophagic activity after 3 hrs simulated ischaemia/reperfusion

Autophagic activity was not significantly different between control and insulin treated groups after reperfusion.

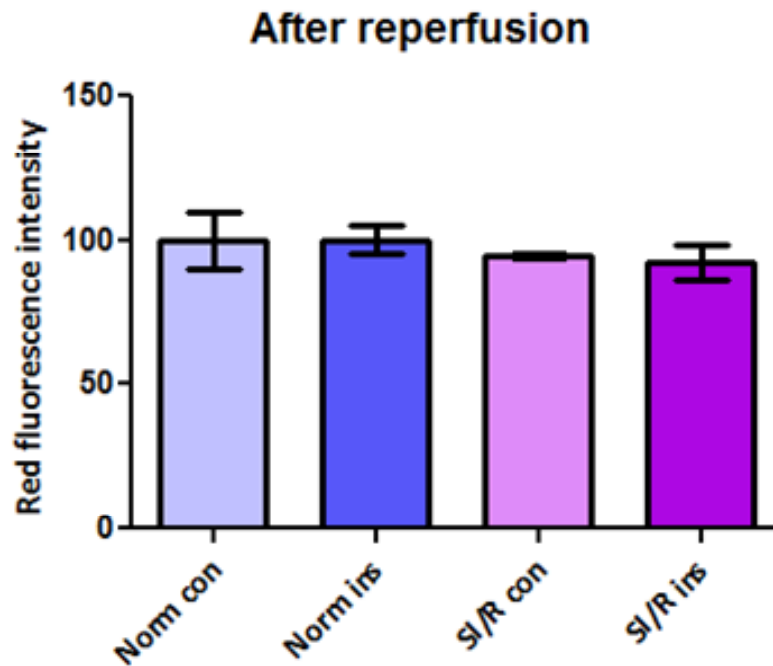


Figure 8.19: Percentage red fluorescence intensity indicating acidic vacuoles normoxic control (Norm con), normoxic insulin (Norm ins), simulated ischaemia/reperfusion control (SI/R con) and simulated ischaemia/reperfusion insulin (SI/R Ins). Data expressed as mean±SEM. n>3.

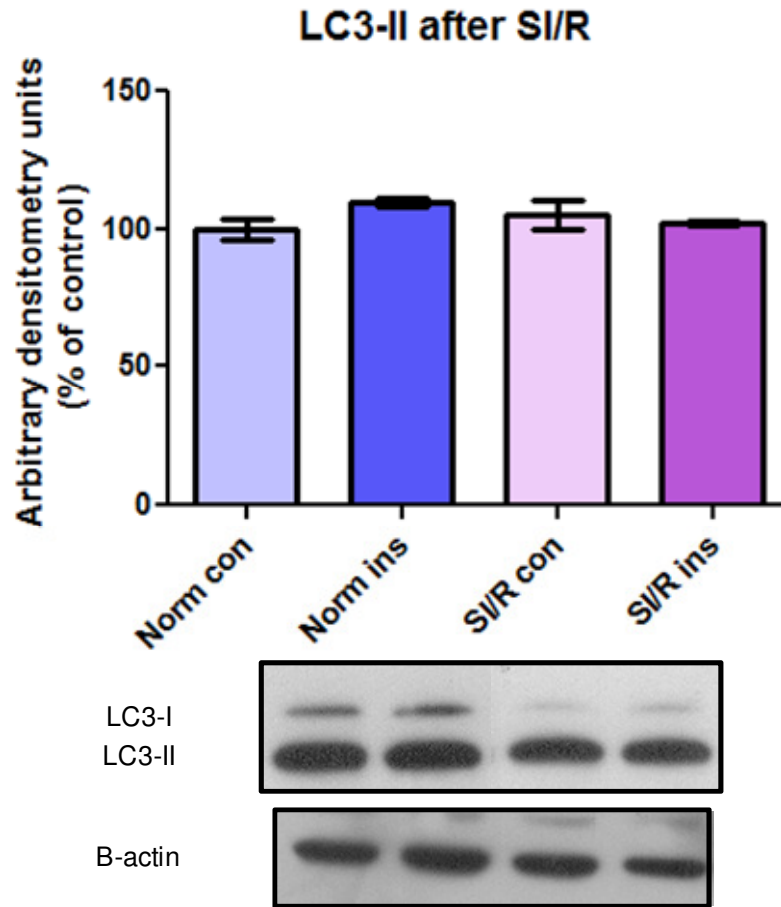


Figure 8.20: LC3-II induction after SI/R, showing normoxic control (Norm con), normoxic insulin (Norm ins), simulated ischaemia/reperfusion control (SI/R con) and simulated ischaemia/reperfusion insulin (SI/R Ins). Data expressed as mean \pm SEM. n>3.

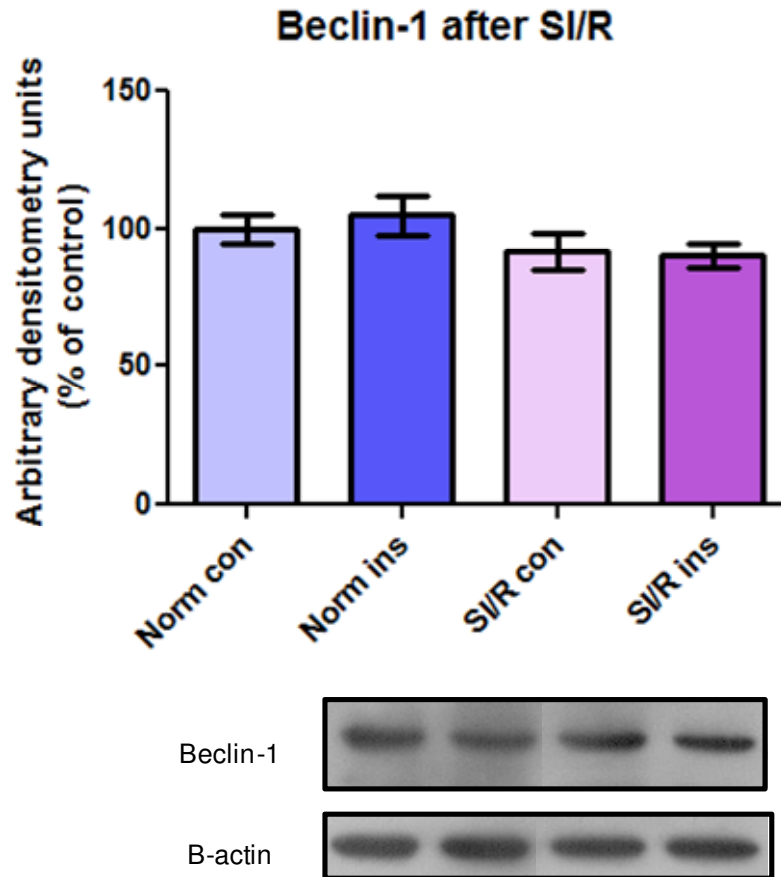


Figure 8.21: Beclin-1 induction after SI/R, showing normoxic control (Norm con), normoxic insulin (Norm ins), simulated ischaemia/reperfusion control (SI/R con) and simulated ischaemia/reperfusion insulin (SI/R Ins). Data expressed as mean \pm SEM. n>3.

8.3.5 Cell viability after 3 hrs simulated ischaemia

No significant differences in cell viability were found between insulin and control treated groups after ischaemia.

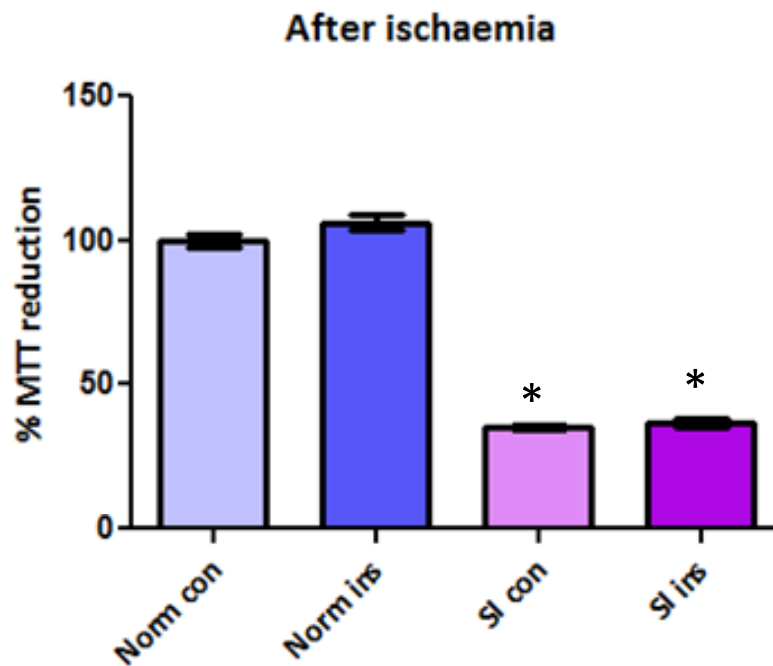


Figure 8.22: Relative viability based of MTT reduction, showing normoxic control (Norm con), normoxic insulin (Norm ins), simulated ischaemia control (SI con) and simulated ischaemia insulin (Ins). Data expressed as mean±SEM. *p<0.001 vs. normoxic groups, n>3.

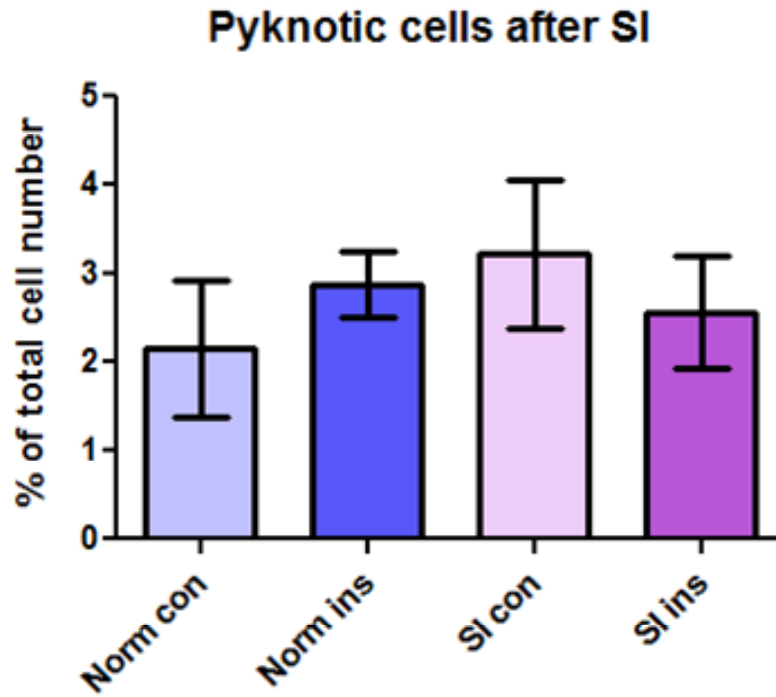


Figure 8.23: Percentage pyknosis, showing normoxic control (Norm con), normoxic insulin (Norm ins), simulated ischaemia control (SI con) and simulated ischaemia insulin (Ins). Data expressed as mean \pm SEM. n>3.

Late pyknotic cells after SI

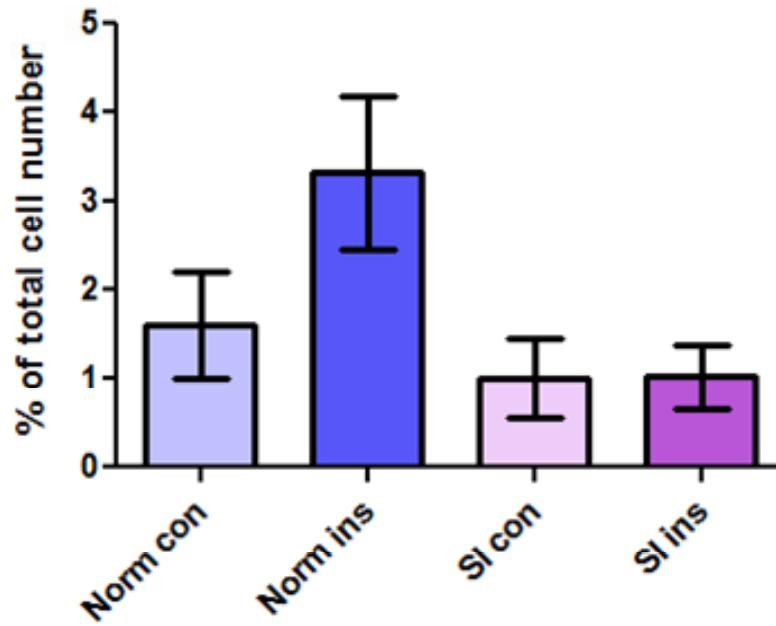


Figure 8.24: Percentage late pyknosis, showing normoxic control (Norm con), normoxic insulin (Norm ins), simulated ischaemia control (SI con) and simulated ischaemia insulin (Ins). Data expressed as mean \pm SEM. n>3.

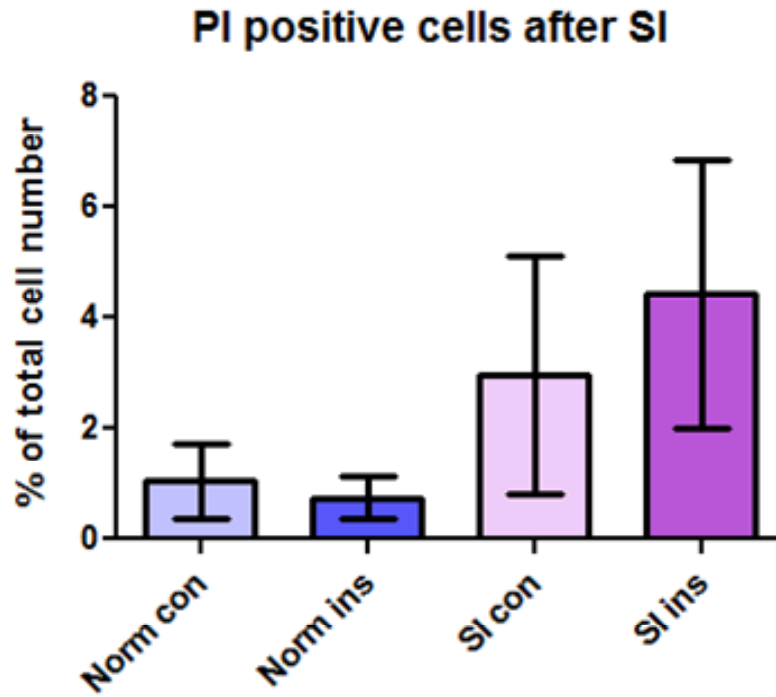


Figure 8.25: Percentage PI positive cells, showing normoxic control (Norm con), normoxic insulin (Norm ins), simulated ischaemia control (SI con) and simulated ischaemia insulin (Ins). Data expressed as mean \pm SEM. n>3.

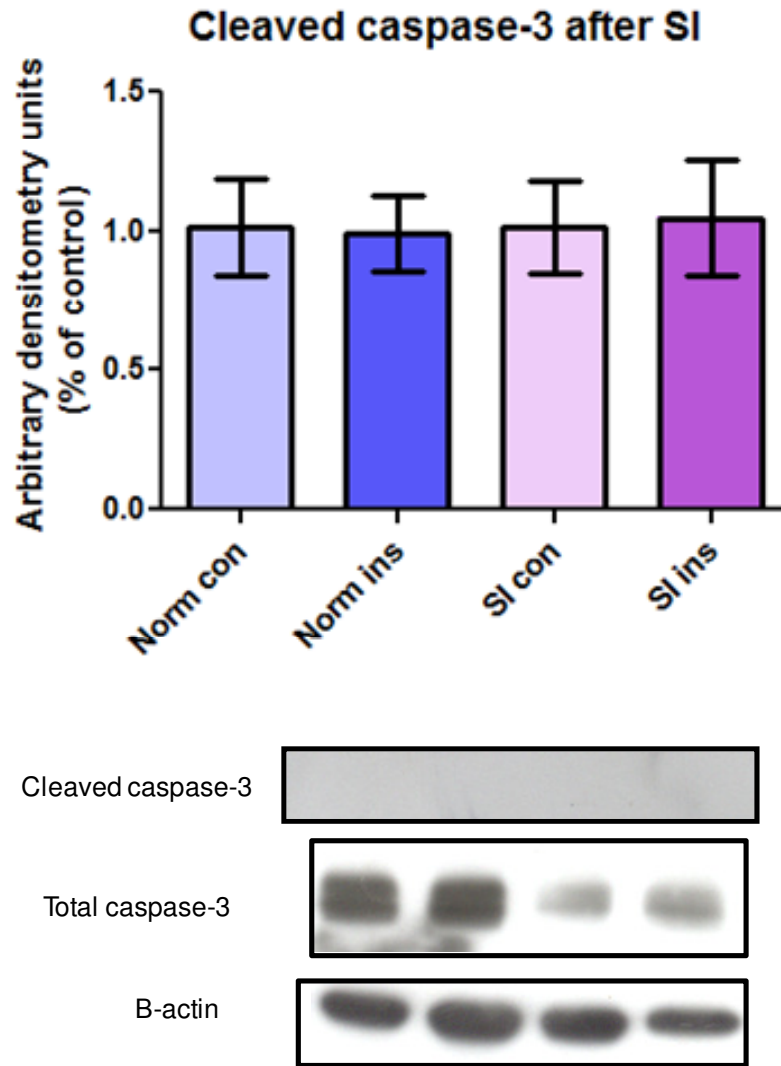


Figure 8.26: Caspase-3 cleavage after SI, showing normoxic control (Norm con), normoxic insulin (Norm ins), simulated ischaemia control (SI con) and simulated ischaemia insulin (Ins). Data expressed as mean \pm SEM. n>3.

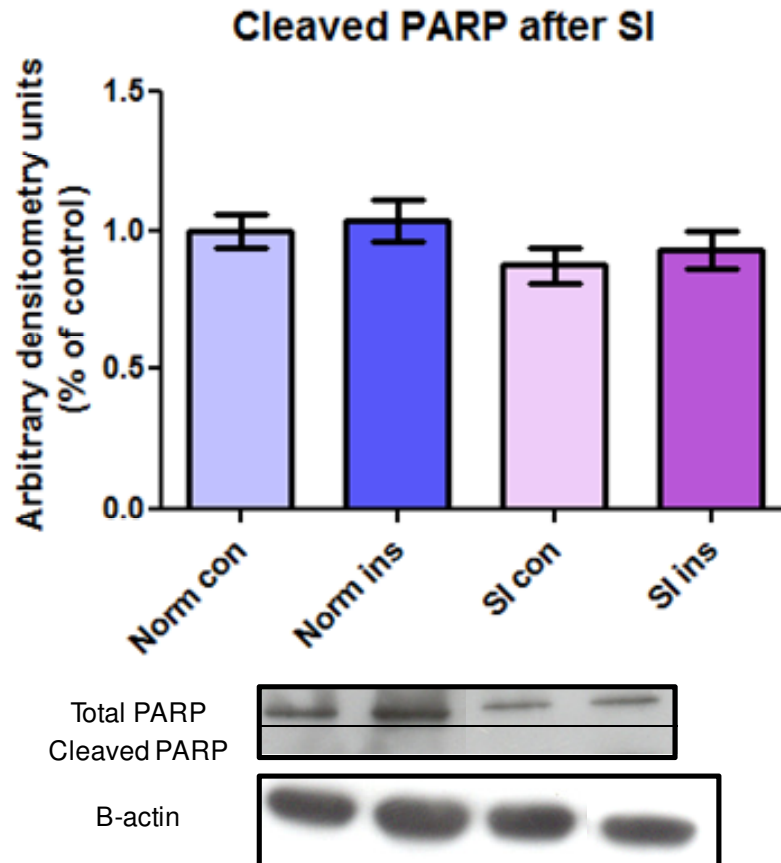


Figure 8.27: PARP cleavage after SI, showing normoxic control (Norm con), normoxic insulin (Norm ins), simulated ischaemia control (SI con) and simulated ischaemia insulin (Ins). Data expressed as mean \pm SEM. n>3.

8.3.6 Cell viability after 3 hrs simulated ischaemia/reperfusion

No significant differences in cell viability were found between insulin and control treated groups after reperfusion.

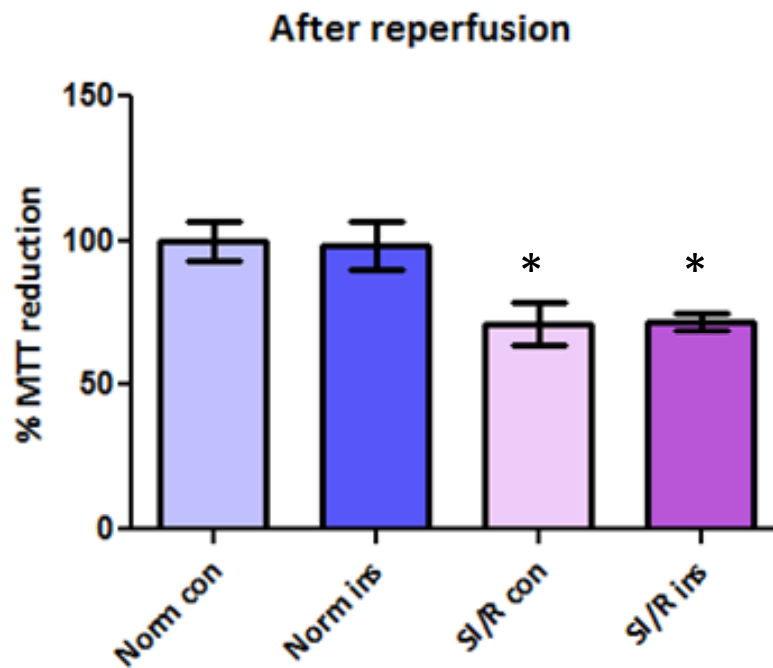


Figure 8.28: Relative viability based of MTT reduction, showing normoxic control (Norm con), normoxic insulin (Norm ins), simulated ischaemia/reperfusion control (SI/R con) and simulated ischaemia/reperfusion insulin (SI/R Ins). Data expressed as mean±SEM. *p<0.01 vs. normoxic groups, n>3.

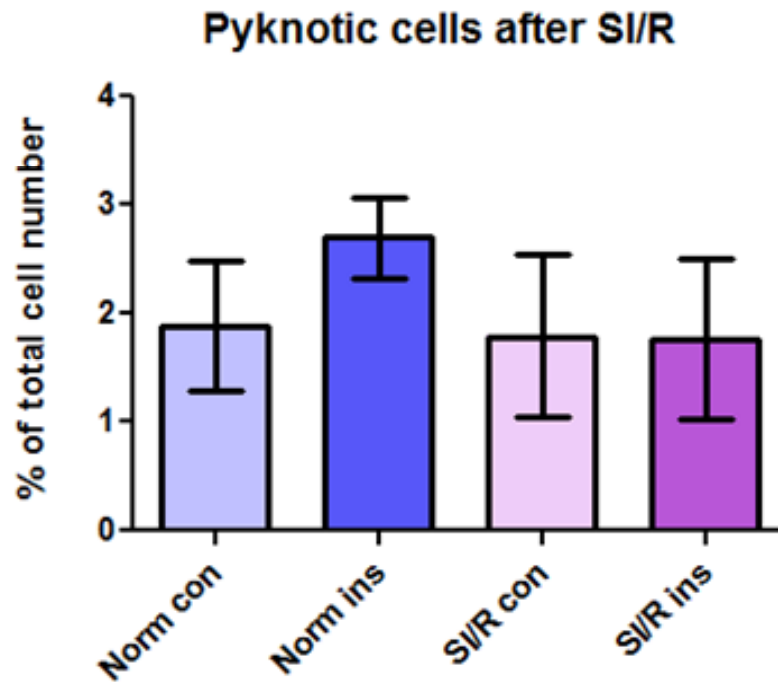


Figure 8.29: Percentage pyknosis, showing normoxic control (Norm con), normoxic insulin (Norm ins), simulated ischaemia/reperfusion control (SI/R con) and simulated ischaemia/reperfusion insulin (SI/R Ins). Data expressed as mean \pm SEM. n>3.

Late pyknotic cells after SI/R

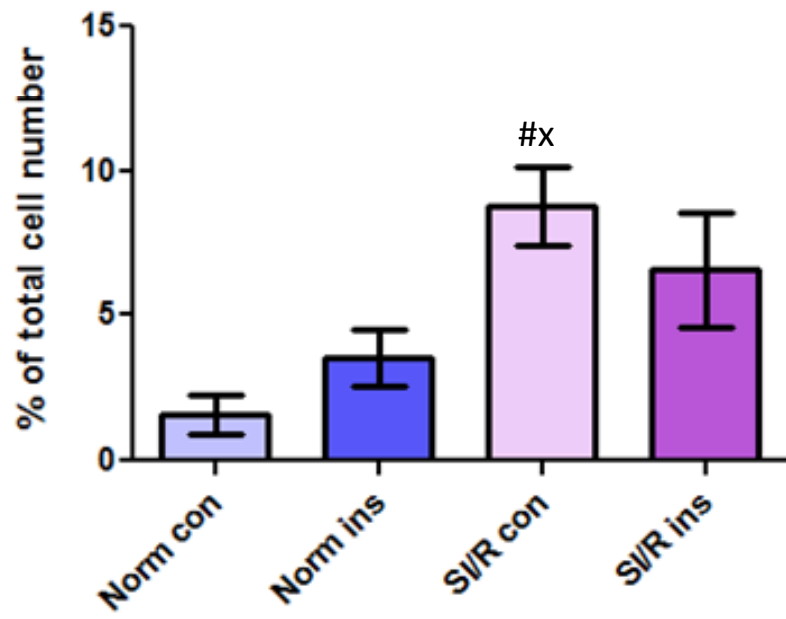


Figure 8.30: Percentage late pyknotic cells, showing normoxic control (Norm con), normoxic insulin (Norm ins), simulated ischaemia/reperfusion control (SI/R con) and simulated ischaemia/reperfusion insulin (SI/R Ins). Data expressed as mean±SEM. #p<0.05 vs. norm ins, x p<0.01 vs. norm con, n>3.

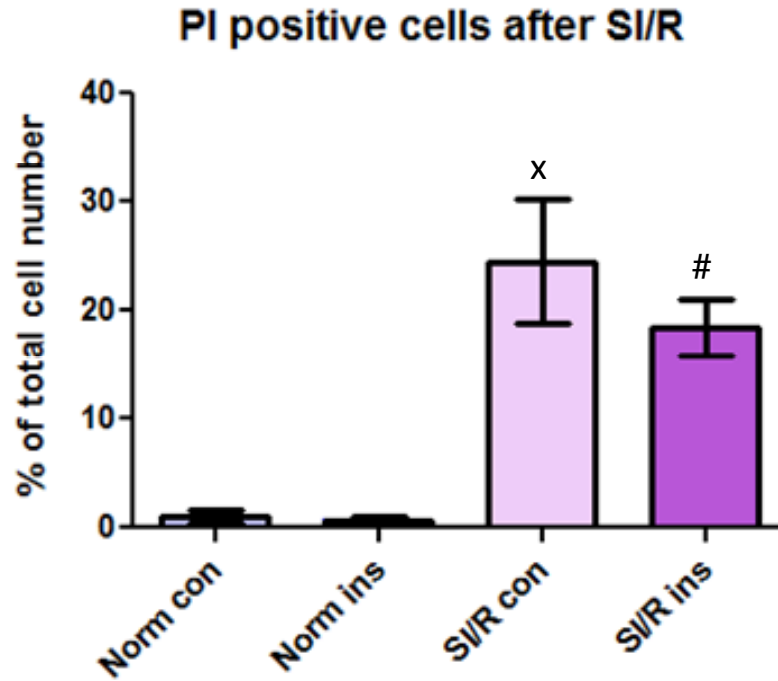


Figure 8.31: Percentage PI positive cells, showing normoxic control (Norm con), normoxic insulin (Norm ins), simulated ischaemia/reperfusion control (SI/R con) and simulated ischaemia/reperfusion insulin (SI/R Ins). Data expressed as mean±SEM. ^xp<0.001 vs. normoxic groups, [#]p<0.01 vs. normoxic groups, n>3.

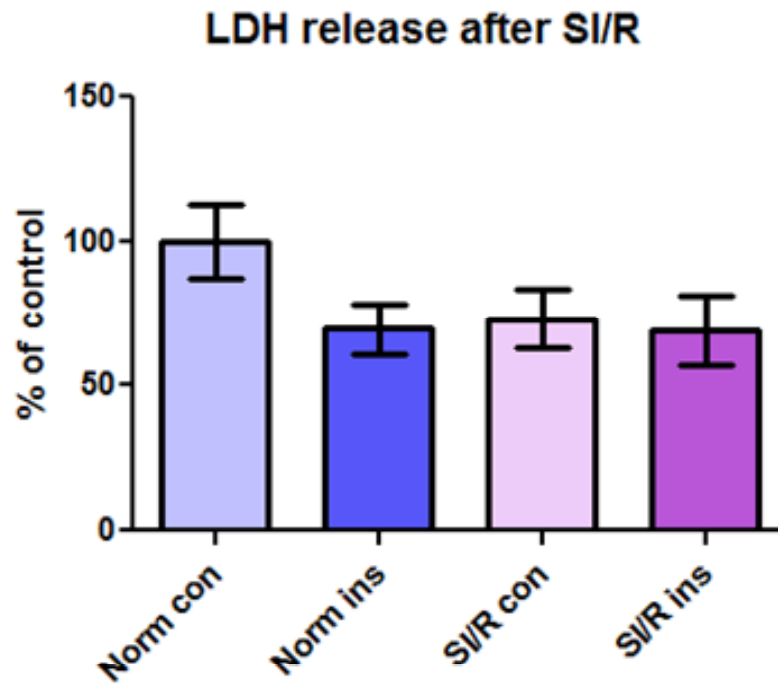


Figure 8.32: Relative viability based on LDH release, showing normoxic control (Norm con), normoxic insulin (Norm ins), simulated ischaemia/reperfusion control (SI/R con) and simulated ischaemia/reperfusion insulin (SI/R Ins). Data expressed as mean±SEM. n>3.

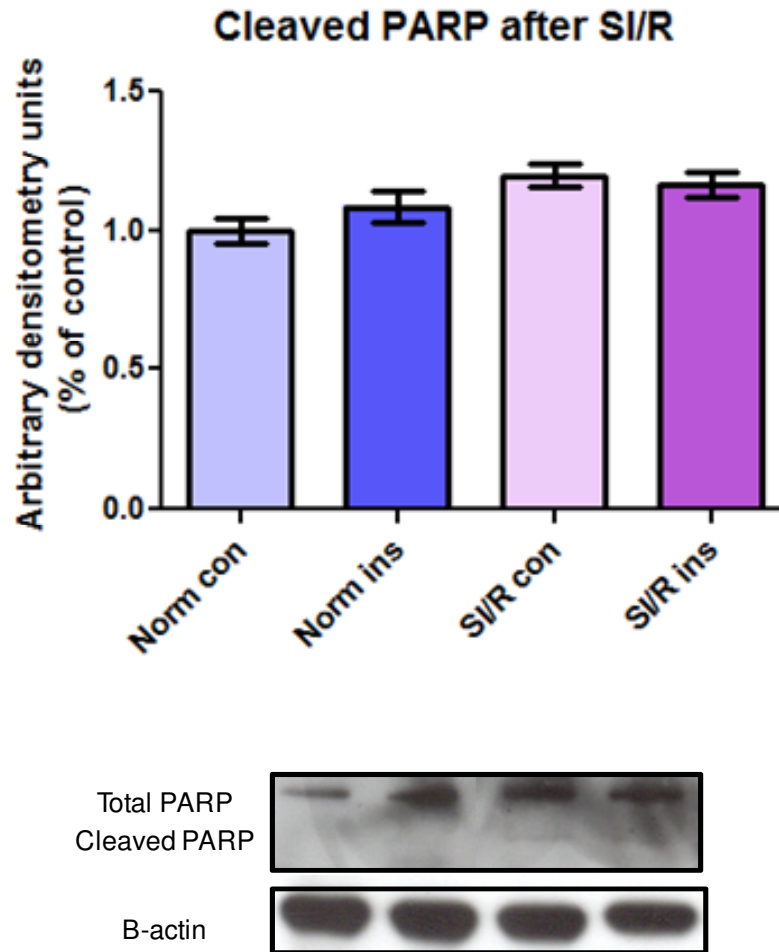


Figure 8.33: PARP cleavage after SI/R, showing normoxic control (Norm con), normoxic insulin (Norm ins), simulated ischaemia/reperfusion control (SI/R con) and simulated ischaemia/reperfusion insulin (SI/R Ins). Data expressed as mean \pm SEM. n>3.

8.4 Investigating insulin induced MKP-1 induction

It was noted that insulin did not result in significant protection from SI/R injury. 2DG was added to the ischaemic buffer to inhibit glycolysis. 2DG is known to be more readily taken up by H9c2 cells in the presence of insulin (Yu *et al.*, 1999). As the modified ischaemic buffer was supplemented with 2DG there was a possibility that the lack of protection in insulin treated groups might have occurred due to increased 2DG uptake caused by insulin.

However, no significant difference in MTT reduction was found between insulin treated groups; normoxic insulin ($107.9 \pm 3.9\%$), SI/R Esumi insulin ($97.9 \pm 3.2\%$) and SI/R Esumi/2DG insulin ($98.54 \pm 3.77\%$) ($p > 0.05$).

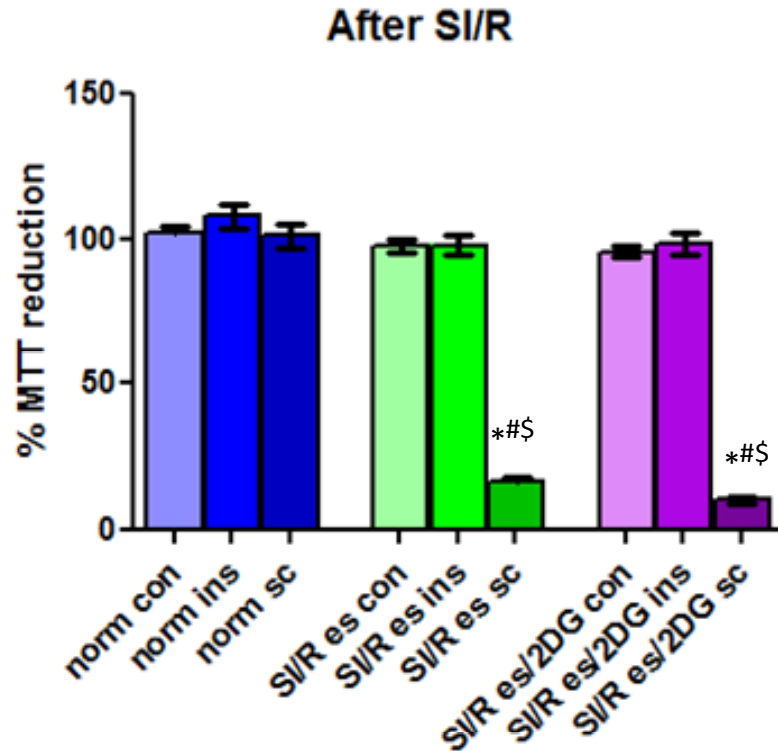


Figure 8.34: Relative viability based of MTT reduction, modified Esumi buffer vs. modified Esumi supplemented with 2DG buffer, showing normoxic control (Norm con), normoxic insulin (Norm ins), normoxic sanguinarine (Norm sc), simulated ischaemia/reperfusion Esumi control (SI/R es con), simulated ischaemia/reperfusion Esumi insulin (SI/R es ins), simulated ischaemia/reperfusion Esumi sanguinarine (SI/R es sc), simulated ischaemia/reperfusion Esumi/2DG control (SI/R es/2DG con), simulated ischaemia/reperfusion Esumi/2DG insulin (SI/R es/2DG ins) and simulated ischaemia/reperfusion Esumi/2DG sanguinarine (SI/R es/2DG sc). Data expressed as mean±SEM. *p<0.001 vs. normoxic groups, #p<0.001 vs. Esumi control and esumi insulin groups, \$p<0.001 vs. Esumi/2DG control and Esumi/2DG insulin groups, n=9.

Carrier mediated (Glut 1 and Glut 4) glucose uptake was then measured by determining uptake of 2-deoxy-D-³[H] glucose in both H9c2 cells used throughout the study and in isolated adult rat cardiac myocytes. Glucose uptake was stimulated by insulin used in previous experiments during this study and also by insulin from another department to investigate whether there are differences between different insulin stocks.

Glucose uptake in H9c2 cardiac myocytes was not stimulated in the presence of insulin, from either source. Glucose uptake that occurred in insulin treated cells can be considered to have occurred via alternate glucose uptake mechanisms. Glucose uptake was however significantly increased, in isolated adult cardiac myocytes, in the presence of insulin from both sources.

H9c2 cells can therefore be considered to be insulin resistant. In contrast to this, previous studies have found glucose uptake by H9c2 cells to be significant (Zorzano *et al.*, 1997; Agnetti *et al.*, 2005). The discrepancy may be because these studies did not use insulin treatment as was done in this study. As insulin was added to experimental groups for up to 4 hrs in this study, it could have resulted in insulin resistance as glucose concentrations in the culture medium are very high. Furthermore, H9c2 cells may also be insulin resistant due to morphological and biochemical differentiation as a result of *in vitro* culturing. As it has been found that H9c2 cells do not express gap junctions, caveolae, myofibrils with organised sarcomeres or T-tubules (Hescheler *et al.*, 1991), it is important to consider that they could also have developed an alternative to Glut mediated glucose uptake.

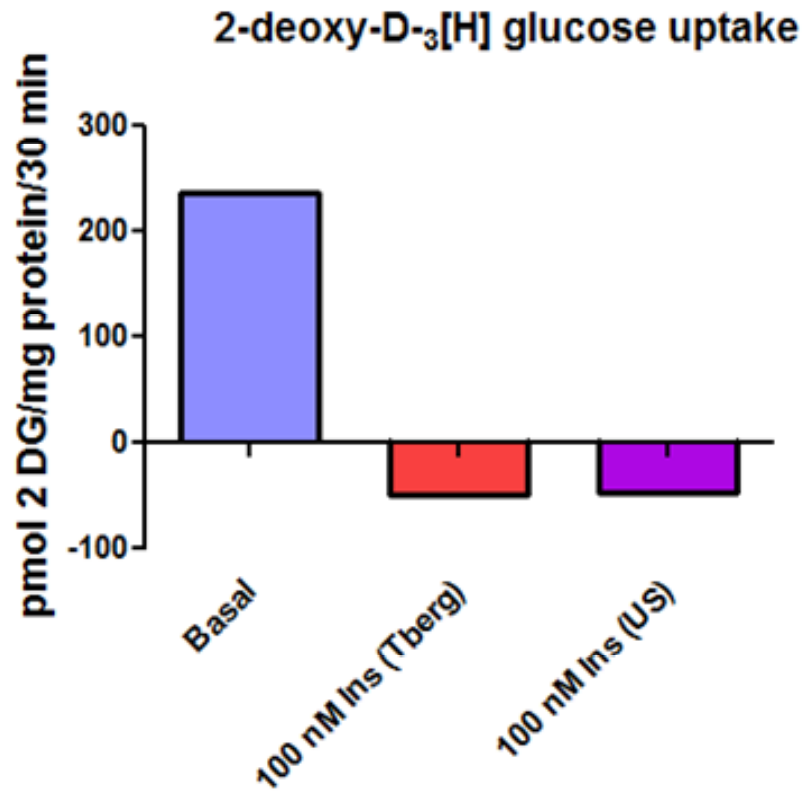


Figure 8.35: Glucose uptake in H9c2 cells, showing basal, insulin from Tygerberg department (Ins Tberg) and insulin from Stellenbosch department (Ins US).

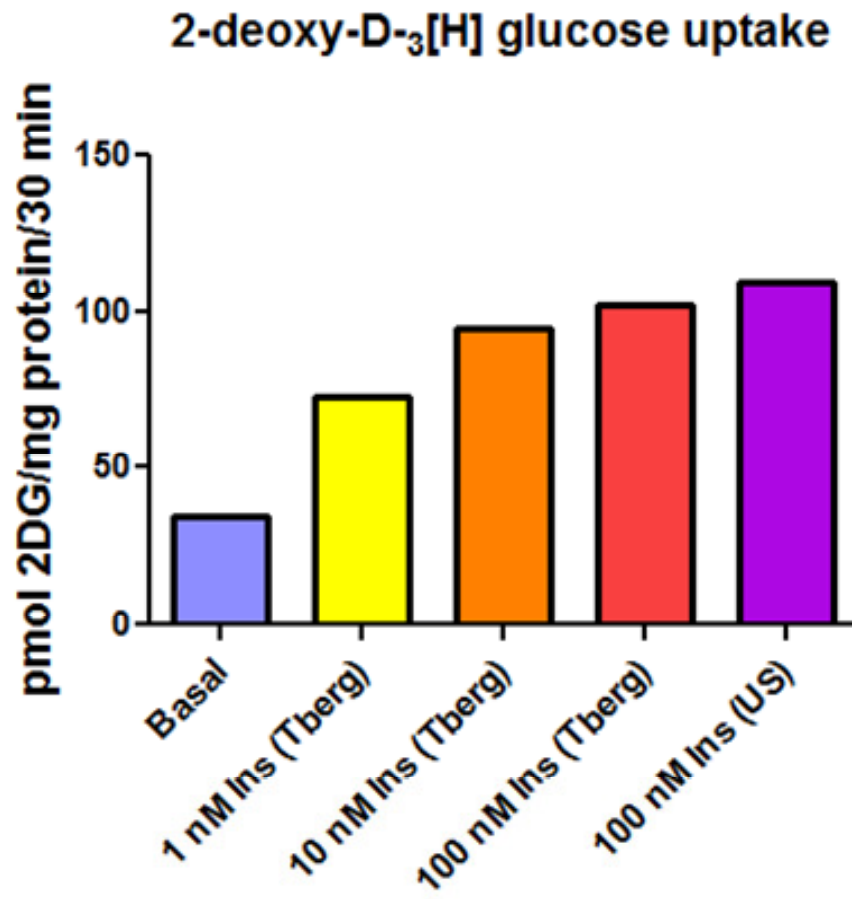


Figure 8.36: Glucose uptake in isolated adult rat myocytes, showing basal, insulin from Tygerberg department (Ins Tberg) and insulin from Stellenbosch department (Ins US).

Insulin did not upregulate MKP-1 and thus did not result in protection from ischaemia/reperfusion injury, as insulin resistance in cardiomyocytes attenuates cytoprotective effects caused by insulin induced MKP-1 expression (Morisco *et al.*, 2007).

8.5 Dexamethasone concentration determination

Attention was then turned to dexamethasone which is also known to result in increased MKP-1 induction (Fan *et al.*, 2009). A western blot was done to investigate dexamethasone induced MKP-1 activity, using three different concentrations (Lasa *et al.*, 2002; Vogt *et al.*, 2008; Fan *et al.*, 2009).

MKP-1 induction was significantly higher in cells treated with 10 μ M dexamethasone (110 ± 1.93) ($p < 0.05$). 10 μ M dexamethasone was therefore decided upon to be used in further analysis, to induce MKP-1 induction.

As significant differences in autophagic activity were more pronounced after reperfusion than after ischaemia, during previous experiments, western blots were done to investigate the role of MKP-1 in autophagy and apoptosis after simulated reperfusion, with the use of dexamethasone and sanguinarine.

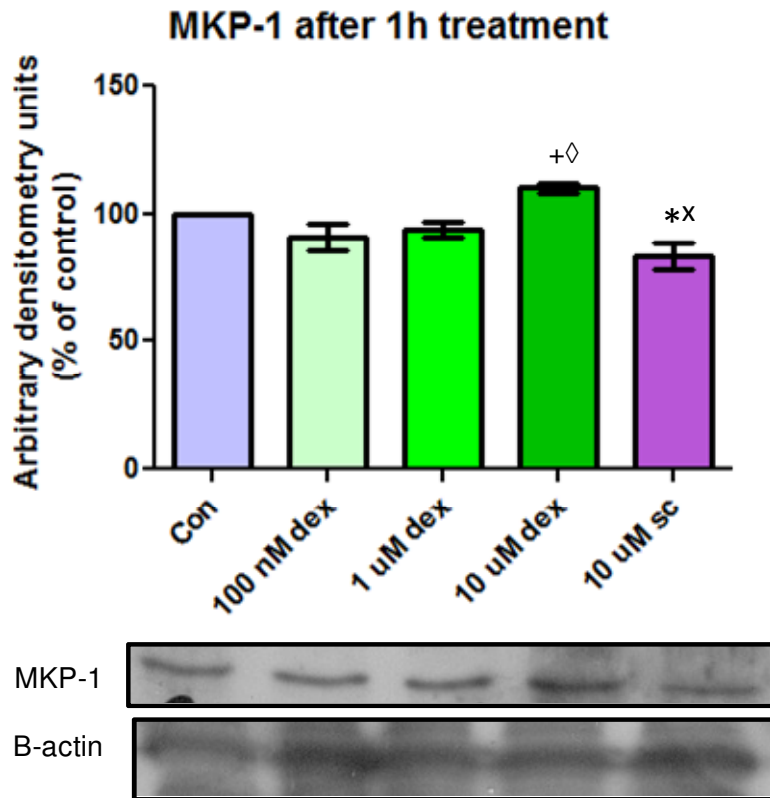


Figure 8.37: MKP-1 induction, showing control (Con), dexamethasone (dex) and sanguinarine (sc). Data expressed as mean \pm SEM. $^{\dagger}p<0.05$ vs. con, $^{\diamond}p<0.01$ vs. 100 nM dex and 1 μ M dex, $^*p<0.05$ vs. con and 1 μ M dex, $^*Xp<0.001$ vs. 10 μ M dex n>3.

REFERENCES

- Abdallah Y & Schafer C (2006) Insulin: an overall cardiovascular protector?
Cardiovasc Res **69**, 4-6.
- Aderem A & Underhill DM (1999) Mechanisms of phagocytosis in
macrophages. *Annu Rev Immunol* **17**, 593-623.
- Agnetti G, Maraldi T, Fiorentini D, Giordano E, Prata C, Hakim G, Muscari C,
Guarnieri C & Caldarera CM (2005) Activation of glucose transport
during simulated ischemia in H9c2 cardiac myoblasts is mediated by
protein kinase C isoforms. *Life Sci* **78**, 264-270.
- Ashkenazi A & Dixit VM (1998) Death receptors: signaling and modulation.
Science **281**, 1305-1308.
- Asoh S, Mori T, Nagai S, Yamagata K, Nishimaki K, Miyato Y, Shidara Y &
Ohta S (2005) Zonal necrosis prevented by transduction of the
artificial anti-death FNK protein. *Cell Death Differ* **12**, 384-394.
- Avitzour M, Diskin R, Raboy B, Askari N, Engelberg D & Livnah O (2007)
Intrinsically active variants of all human p38 isoforms. *FEBS J* **274**,
963-975.
- Bartholomeusz C, Rosen D, Wei C, Kazansky A, Yamasaki F, Takahashi T,
Itamochi H, Kondo S, Liu J & Ueno NT (2008) PEA-15 induces

autophagy in human ovarian cancer cells and is associated with prolonged overall survival. *Cancer Res* **68**, 9302-9310.

Begum N, Ragolia L, Rienzie J, McCarthy M & Duddy N (1998) Regulation of mitogen-activated protein kinase phosphatase-1 induction by insulin in vascular smooth muscle cells. Evaluation of the role of the nitric oxide signaling pathway and potential defects in hypertension. *J Biol Chem* **273**, 25164-25170.

Berger NA, Sims JL, Catino DM & Berger SJ (1983) Poly(ADP-ribose) polymerase mediates the suicide response to massive DNA damage: studies in normal and DNA-repair defective cells. *Princess Takamatsu Symp* **13**, 219-226.

Bergmann A (2007) Autophagy and cell death: no longer at odds. *Cell* **131**, 1032-1034.

Bernaudin M, Tang Y, Reilly M, Petit E & Sharp FR (2002) Brain genomic response following hypoxia and re-oxygenation in the neonatal rat. Identification of genes that might contribute to hypoxia-induced ischemic tolerance. *J Biol Chem* **277**, 39728-39738.

Bogoyevitch MA, Gillespie-Brown J, Ketterman AJ, Fuller SJ, Ben-Levy R, Ashworth A, Marshall CJ & Sugden PH (1996) Stimulation of the stress-activated mitogen-activated protein kinase subfamilies in perfused heart. p38/RK mitogen-activated protein kinases and c-Jun

N-terminal kinases are activated by ischemia/reperfusion. *Circ Res* **79**, 162-173.

Bokemeyer D, Sorokin A & Dunn MJ (1997) Differential regulation of the dual-specificity protein-tyrosine phosphatases CL100, B23, and PAC1 in mesangial cells. *J Am Soc Nephrol* **8**, 40-50.

Bokemeyer D, Sorokin A, Yan M, Ahn NG, Templeton DJ & Dunn MJ (1996) Induction of mitogen-activated protein kinase phosphatase 1 by the stress-activated protein kinase signaling pathway but not by extracellular signal-regulated kinase in fibroblasts. *J Biol Chem* **271**, 639-642.

Boutros T, Chevet E & Metrakos P (2008a) Mitogen-activated protein (MAP) kinase/MAP kinase phosphatase regulation: roles in cell growth, death, and cancer. *Pharmacol Rev* **60**, 261-310.

Boutros T, Nantel A, Emadali A, Tzimas G, Conzen S, Chevet E & Metrakos PP (2008b) The MAP kinase phosphatase-1 MKP-1/DUSP1 is a regulator of human liver response to transplantation. *Am J Transplant* **8**, 2558-2568.

Bradford MM (1976) A rapid and sensitive method for the quantitation of microgram quantities of protein utilizing the principle of protein-dye binding. *Anal Biochem* **72**, 248-254.

- Briddon SJ, Middleton RJ, Cordeaux Y, Flavin FM, Weinstein JA, George MW, Kellam B & Hill SJ (2004) Quantitative analysis of the formation and diffusion of A1-adenosine receptor-antagonist complexes in single living cells. *Proc Natl Acad Sci U S A* **101**, 4673-4678.
- Brondello JM, Brunet A, Pouyssegur J & McKenzie FR (1997) The dual specificity mitogen-activated protein kinase phosphatase-1 and -2 are induced by the p42/p44MAPK cascade. *J Biol Chem* **272**, 1368-1376.
- Brondello JM, Pouyssegur J & McKenzie FR (1999) Reduced MAP kinase phosphatase-1 degradation after p42/p44MAPK-dependent phosphorylation. *Science* **286**, 2514-2517.
- Cagnol S & Chambard JC (2010) ERK and cell death: mechanisms of ERK-induced cell death--apoptosis, autophagy and senescence. *FEBS J* **277**, 2-21.
- Camps M, Nichols A & Arkininstall S (2000) Dual specificity phosphatases: a gene family for control of MAP kinase function. *FASEB J* **14**, 6-16.
- Chang WT, Kang JJ, Lee KY, Wei K, Anderson E, Gotmare S, Ross JA & Rosen GD (2001) Triptolide and chemotherapy cooperate in tumor cell apoptosis. A role for the p53 pathway. *J Biol Chem* **276**, 2221-2227.

- Chinnaiyan AM (1999) The apoptosome: heart and soul of the cell death machine. *Neoplasia* **1**, 5-15.
- Choi BH, Hur EM, Lee JH, Jun DJ & Kim KT (2006) Protein kinase Cdelta-mediated proteasomal degradation of MAP kinase phosphatase-1 contributes to glutamate-induced neuronal cell death. *J Cell Sci* **119**, 1329-1340.
- Chu Y, Solski PA, Khosravi-Far R, Der CJ & Kelly K (1996) The mitogen-activated protein kinase phosphatases PAC1, MKP-1, and MKP-2 have unique substrate specificities and reduced activity in vivo toward the ERK2 sevenmaker mutation. *J Biol Chem* **271**, 6497-6501.
- Clarke PG (1990) Developmental cell death: morphological diversity and multiple mechanisms. *Anat Embryol (Berl)* **181**, 195-213.
- Codogno P & Meijer AJ (2005) Autophagy and signaling: their role in cell survival and cell death. *Cell Death Differ* **12 Suppl 2**, 1509-1518.
- Comes F, Matrone A, Lastella P, Nico B, Susca FC, Bagnulo R, Ingravallo G, Modica S, Lo Sasso G, Moschetta A, Guanti G & Simone C (2007) A novel cell type-specific role of p38alpha in the control of autophagy and cell death in colorectal cancer cells. *Cell Death Differ* **14**, 693-702.

Cory S & Adams JM (2002) The Bcl2 family: regulators of the cellular life-or-death switch. *Nat Rev Cancer* **2**, 647-656.

Cowan KJ & Storey KB (2003) Mitogen-activated protein kinases: new signaling pathways functioning in cellular responses to environmental stress. *J Exp Biol* **206**, 1107-1115.

Crichton D, Wilkinson S, O'Prey J, Syed N, Smith P, Harrison PR, Gasco M, Garrone O, Crook T & Ryan KM (2006) DRAM, a p53-induced modulator of autophagy, is critical for apoptosis. *Cell* **126**, 121-134.

De Duve C & Wattiaux R (1966) Functions of lysosomes. *Annu Rev Physiol* **28**, 435-492.

Dennis SC, Gevers W & Opie LH (1991) Protons in ischemia: where do they come from; where do they go to? *J Mol Cell Cardiol* **23**, 1077-1086.

Devin A, Lin Y & Liu ZG (2003) The role of the death-domain kinase RIP in tumour-necrosis-factor-induced activation of mitogen-activated protein kinases. *EMBO Rep* **4**, 623-627.

Dice JF (2007) Chaperone-mediated autophagy. *Autophagy* **3**, 295-299.

Donthi RV, Huisamen B & Lochner A (2000) Effect of vanadate and insulin on glucose transport in isolated adult rat cardiomyocytes. *Cardiovasc Drugs Ther* **14**, 463-470.

- Elmore S (2007) Apoptosis: a review of programmed cell death. *Toxicol Pathol* **35**, 495-516.
- Engelbrecht AM, Engelbrecht P, Genade S, Niesler C, Page C, Smuts M & Lochner A (2005) Long-chain polyunsaturated fatty acids protect the heart against ischemia/reperfusion-induced injury via a MAPK dependent pathway. *J Mol Cell Cardiol* **39**, 940-954.
- Engelbrecht AM, Niesler C, Page C & Lochner A (2004) p38 and JNK have distinct regulatory functions on the development of apoptosis during simulated ischaemia and reperfusion in neonatal cardiomyocytes. *Basic Res Cardiol* **99**, 338-350.
- Esumi K, Nishida M, Shaw D, Smith TW & Marsh JD (1991) NADH measurements in adult rat myocytes during simulated ischemia. *Am J Physiol* **260**, H1743-1752.
- Fan WJ, Genade S, Genis A, Huisamen B & Lochner A (2009) Dexamethasone-induced cardioprotection: a role for the phosphatase MKP-1? *Life Sci* **84**, 838-846.
- Farooq A & Zhou MM (2004) Structure and regulation of MAPK phosphatases. *Cell Signal* **16**, 769-779.
- Fass E, Shvets E, Degani I, Hirschberg K & Elazar Z (2006) Microtubules support production of starvation-induced autophagosomes but not

their targeting and fusion with lysosomes. *J Biol Chem* **281**, 36303-36316.

Ferraro E & Cecconi F (2007) Autophagic and apoptotic response to stress signals in mammalian cells. *Arch Biochem Biophys* **462**, 210-219.

Festjens N, Vanden Berghe T & Vandenabeele P (2006) Necrosis, a well-orchestrated form of cell demise: signalling cascades, important mediators and concomitant immune response. *Biochim Biophys Acta* **1757**, 1371-1387.

Franklin CC & Kraft AS (1997) Conditional expression of the mitogen-activated protein kinase (MAPK) phosphatase MKP-1 preferentially inhibits p38 MAPK and stress-activated protein kinase in U937 cells. *J Biol Chem* **272**, 16917-16923.

Franklin CC, Srikanth S & Kraft AS (1998) Conditional expression of mitogen-activated protein kinase phosphatase-1, MKP-1, is cytoprotective against UV-induced apoptosis. *Proc Natl Acad Sci U S A* **95**, 3014-3019.

Freude B, Masters TN, Robicsek F, Fokin A, Kostin S, Zimmermann R, Ullmann C, Lorenz-Meyer S & Schaper J (2000) Apoptosis is initiated by myocardial ischemia and executed during reperfusion. *J Mol Cell Cardiol* **32**, 197-208.

Fuglestad BN, Suleman N, Tiron C, Kanhema T, Lacerda L, Andreassen TV, Sack MN, Jonassen AK, Mjos OD, Opie LH & Lecour S (2008) Signal transducer and activator of transcription 3 is involved in the cardioprotective signalling pathway activated by insulin therapy at reperfusion. *Basic Res Cardiol* **103**, 444-453.

Galluzzi L, Morselli E, Vicencio JM, Kepp O, Joza N, Tajeddine N & Kroemer G (2008) Life, death and burial: multifaceted impact of autophagy. *Biochem Soc Trans* **36**, 786-790.

Gao F, Shi DW, Wang XM, Dong L, Wang YM & Ma XL (2003) [Effects of glucose-insulin-potassium cocktail on cardiac myocyte death and post-ischemic recovery cardiac functional recovery: the critical role of insulin]. *Zhonghua Nei Ke Za Zhi* **42**, 148-152.

Garcia VP, Valdes F, Martin R, Luis JC, Afonso AM & Ayala JH (2006) Biosynthesis of antitumoral and bactericidal sanguinarine. *J Biomed Biotechnol* **2006**, 63518.

Golstein P & Kroemer G (2007) Cell death by necrosis: towards a molecular definition. *Trends Biochem Sci* **32**, 37-43.

Gomez LA, Alekseev AE, Aleksandrova LA, Brady PA & Terzic A (1997) Use of the MTT assay in adult ventricular cardiomyocytes to assess viability: effects of adenosine and potassium on cellular survival. *J Mol Cell Cardiol* **29**, 1255-1266.

- Goodwin CJ, Holt SJ, Downes S & Marshall NJ (1995) Microculture tetrazolium assays: a comparison between two new tetrazolium salts, XTT and MTS. *J Immunol Methods* **179**, 95-103.
- Gottlieb RA, Burleson KO, Kloner RA, Babior BM & Engler RL (1994) Reperfusion injury induces apoptosis in rabbit cardiomyocytes. *J Clin Invest* **94**, 1621-1628.
- Gozuacik D & Kimchi A (2007) Autophagy and cell death. *Curr Top Dev Biol* **78**, 217-245.
- Green DR & Chipuk JE (2006) p53 and metabolism: Inside the TIGAR. *Cell* **126**, 30-32.
- Green DR & Reed JC (1998) Mitochondria and apoptosis. *Science* **281**, 1309-1312.
- Hacker G (2000) The morphology of apoptosis. *Cell Tissue Res* **301**, 5-17.
- Hamacher-Brady A, Brady NR & Gottlieb RA (2006) Enhancing macroautophagy protects against ischemia/reperfusion injury in cardiac myocytes. *J Biol Chem* **281**, 29776-29787.
- Hescheler J, Meyer R, Plant S, Krautwurst D, Rosenthal W & Schultz G (1991) Morphological, biochemical, and electrophysiological

characterization of a clonal cell (H9c2) line from rat heart. *Circ Res* **69**, 1476-1486.

Holler N, Zaru R, Micheau O, Thome M, Attinger A, Valitutti S, Bodmer JL, Schneider P, Seed B & Tschopp J (2000) Fas triggers an alternative, caspase-8-independent cell death pathway using the kinase RIP as effector molecule. *Nat Immunol* **1**, 489-495.

Holt JA (1983) Cancer, a disease of defective glucose metabolism. *Med Hypotheses* **10**, 133-150.

Holt KH, Kasson BG & Pessin JE (1996) Insulin stimulation of a MEK-dependent but ERK-independent SOS protein kinase. *Mol Cell Biol* **16**, 577-583.

Hutter D, Chen P, Barnes J & Liu Y (2000) Catalytic activation of mitogen-activated protein (MAP) kinase phosphatase-1 by binding to p38 MAP kinase: critical role of the p38 C-terminal domain in its negative regulation. *Biochem J* **352 Pt 1**, 155-163.

Jacob A, Molkenin JD, Smolenski A, Lohmann SM & Begum N (2002) Insulin inhibits PDGF-directed VSMC migration via NO/ cGMP increase of MKP-1 and its inactivation of MAPKs. *Am J Physiol Cell Physiol* **283**, C704-713.

James TN (1994) Normal and abnormal consequences of apoptosis in the human heart. From postnatal morphogenesis to paroxysmal arrhythmias. *Circulation* **90**, 556-573.

Johnson GL & Lapadat R (2002) Mitogen-activated protein kinase pathways mediated by ERK, JNK, and p38 protein kinases. *Science* **298**, 1911-1912.

Junttila MR, Li SP & Westermarck J (2008) Phosphatase-mediated crosstalk between MAPK signaling pathways in the regulation of cell survival. *FASEB J* **22**, 954-965.

Kaiser RA, Bueno OF, Lips DJ, Doevendans PA, Jones F, Kimball TF & Molkentin JD (2004) Targeted inhibition of p38 mitogen-activated protein kinase antagonizes cardiac injury and cell death following ischemia-reperfusion in vivo. *J Biol Chem* **279**, 15524-15530.

Kajstura J, Cheng W, Reiss K, Clark WA, Sonnenblick EH, Krajewski S, Reed JC, Olivetti G & Anversa P (1996) Apoptotic and necrotic myocyte cell deaths are independent contributing variables of infarct size in rats. *Lab Invest* **74**, 86-107.

Kanduc D, Mittelman A, Serpico R, Sinigaglia E, Sinha AA, Natale C, Santacroce R, Di Corcia MG, Lucchese A, Dini L, Pani P, Santacroce S, Simone S, Bucci R & Farber E (2002) Cell death: apoptosis versus necrosis (review). *Int J Oncol* **21**, 165-170.

- Kassel O, Sancono A, Kratzschmar J, Kreft B, Stassen M & Cato AC (2001) Glucocorticoids inhibit MAP kinase via increased expression and decreased degradation of MKP-1. *EMBO J* **20**, 7108-7116.
- Kerr JF (1971) Shrinkage necrosis: a distinct mode of cellular death. *J Pathol* **105**, 13-20.
- Kerr JF, Wyllie AH & Currie AR (1972) Apoptosis: a basic biological phenomenon with wide-ranging implications in tissue kinetics. *Br J Cancer* **26**, 239-257.
- Keyse SM (2000) Protein phosphatases and the regulation of mitogen-activated protein kinase signalling. *Curr Opin Cell Biol* **12**, 186-192.
- Khan TA, Bianchi C, Ruel M, Voisine P & Sellke FW (2004) Mitogen-activated protein kinase pathways and cardiac surgery. *J Thorac Cardiovasc Surg* **127**, 806-811.
- Kihara A, Kabeya Y, Ohsumi Y & Yoshimori T (2001) Beclin-phosphatidylinositol 3-kinase complex functions at the trans-Golgi network. *EMBO Rep* **2**, 330-335.
- Kim GS, Choi YK, Song SS, Kim WK & Han BH (2005) MKP-1 contributes to oxidative stress-induced apoptosis via inactivation of ERK1/2 in SH-SY5Y cells. *Biochem Biophys Res Commun* **338**, 1732-1738.

Kimes BW & Brandt BL (1976) Properties of a clonal muscle cell line from rat heart. *Exp Cell Res* **98**, 367-381.

Kischkel FC, Hellbardt S, Behrmann I, Germer M, Pawlita M, Krammer PH & Peter ME (1995) Cytotoxicity-dependent APO-1 (Fas/CD95)-associated proteins form a death-inducing signaling complex (DISC) with the receptor. *EMBO J* **14**, 5579-5588.

Klionsky DJ & Emr SD (2000) Autophagy as a regulated pathway of cellular degradation. *Science* **290**, 1717-1721.

Korsmeyer SJ, Wei MC, Saito M, Weiler S, Oh KJ & Schlesinger PH (2000) Pro-apoptotic cascade activates BID, which oligomerizes BAK or BAX into pores that result in the release of cytochrome c. *Cell Death Differ* **7**, 1166-1173.

Kunz JB, Schwarz H & Mayer A (2004) Determination of four sequential stages during microautophagy in vitro. *J Biol Chem* **279**, 9987-9996.

Kurosaka K, Takahashi M, Watanabe N & Kobayashi Y (2003) Silent cleanup of very early apoptotic cells by macrophages. *J Immunol* **171**, 4672-4679.

Kusari AB, Byon J, Bandyopadhyay D, Kenner KA & Kusari J (1997) Insulin-induced mitogen-activated protein (MAP) kinase phosphatase-1 (MKP-1) attenuates insulin-stimulated MAP kinase activity: a

mechanism for the feedback inhibition of insulin signaling. *Mol Endocrinol* **11**, 1532-1543.

Lasa M, Abraham SM, Boucheron C, Saklatvala J & Clark AR (2002) Dexamethasone causes sustained expression of mitogen-activated protein kinase (MAPK) phosphatase 1 and phosphatase-mediated inhibition of MAPK p38. *Mol Cell Biol* **22**, 7802-7811.

Lazo JS, Nunes R, Skoko JJ, Queiroz de Oliveira PE, Vogt A & Wipf P (2006) Novel benzofuran inhibitors of human mitogen-activated protein kinase phosphatase-1. *Bioorg Med Chem* **14**, 5643-5650.

Lee SY, Reichlin A, Santana A, Sokol KA, Nussenzweig MC & Choi Y (1997) TRAF2 is essential for JNK but not NF-kappaB activation and regulates lymphocyte proliferation and survival. *Immunity* **7**, 703-713.

Lee TH, Huang Q, Oikemus S, Shank J, Ventura JJ, Cusson N, Vaillancourt RR, Su B, Davis RJ & Kelliher MA (2003) The death domain kinase RIP1 is essential for tumor necrosis factor alpha signaling to p38 mitogen-activated protein kinase. *Mol Cell Biol* **23**, 8377-8385.

Lee TH, Shank J, Cusson N & Kelliher MA (2004) The kinase activity of Rip1 is not required for tumor necrosis factor-alpha-induced I kappa B kinase or p38 MAP kinase activation or for the ubiquitination of Rip1 by Traf2. *J Biol Chem* **279**, 33185-33191.

- Levine B & Klionsky DJ (2004) Development by self-digestion: molecular mechanisms and biological functions of autophagy. *Dev Cell* **6**, 463-477.
- Li C, Hu Y, Mayr M & Xu Q (1999) Cyclic strain stress-induced mitogen-activated protein kinase (MAPK) phosphatase 1 expression in vascular smooth muscle cells is regulated by Ras/Rac-MAPK pathways. *J Biol Chem* **274**, 25273-25280.
- Li K & Wang S (2005) Fingerprint chromatogram analysis of extracts from the leaves of *Tripterygium wilfordii* Hook. f. by high performance liquid chromatography. *J Sep Sci* **28**, 653-657.
- Li M, Zhou JY, Ge Y, Matherly LH & Wu GS (2003a) The phosphatase MKP1 is a transcriptional target of p53 involved in cell cycle regulation. *J Biol Chem* **278**, 41059-41068.
- Li SP, Junttila MR, Han J, Kahari VM & Westermarck J (2003b) p38 Mitogen-activated protein kinase pathway suppresses cell survival by inducing dephosphorylation of mitogen-activated protein/extracellular signal-regulated kinase kinase1,2. *Cancer Res* **63**, 3473-3477.
- Lin Y, Devin A, Rodriguez Y & Liu ZG (1999) Cleavage of the death domain kinase RIP by caspase-8 prompts TNF-induced apoptosis. *Genes Dev* **13**, 2514-2526.

- Locksley RM, Killeen N & Lenardo MJ (2001) The TNF and TNF receptor superfamilies: integrating mammalian biology. *Cell* **104**, 487-501.
- Lornejad-Schafer M, Schafer C, Richter L, Grune T, Haussinger D & Schliess F (2005) Osmotic regulation of MG-132-induced MAP-kinase phosphatase MKP-1 expression in H4IIE rat hepatoma cells. *Cell Physiol Biochem* **16**, 193-206.
- Lornejad-Schafer MR, Schafer C, Graf D, Haussinger D & Schliess F (2003) Osmotic regulation of insulin-induced mitogen-activated protein kinase phosphatase (MKP-1) expression in H4IIE rat hepatoma cells. *Biochem J* **371**, 609-619.
- Lowry OH, Rosebrough NJ, Farr AL & Randall RJ (1951) Protein measurement with the Folin phenol reagent. *J Biol Chem* **193**, 265-275.
- Lu HH, Kao SY, Liu TY, Liu ST, Huang WP, Chang KW & Lin SC (2010) Areca nut extract induced oxidative stress and upregulated hypoxia inducing factor leading to autophagy in oral cancer cells. *Autophagy* **6**.
- Maiuri MC, Zalckvar E, Kimchi A & Kroemer G (2007) Self-eating and self-killing: crosstalk between autophagy and apoptosis. *Nat Rev Mol Cell Biol* **8**, 741-752.

Majno G & Joris I (1995) Apoptosis, oncosis, and necrosis. An overview of cell death. *Am J Pathol* **146**, 3-15.

Marczin N, El-Habashi N, Hoare GS, Bundy RE & Yacoub M (2003) Antioxidants in myocardial ischemia-reperfusion injury: therapeutic potential and basic mechanisms. *Arch Biochem Biophys* **420**, 222-236.

Marino G & Lopez-Otin C (2004) Autophagy: molecular mechanisms, physiological functions and relevance in human pathology. *Cell Mol Life Sci* **61**, 1439-1454.

Maruyama R, Goto K, Takemura G, Ono K, Nagao K, Horie T, Tsujimoto A, Kanamori H, Miyata S, Ushikoshi H, Nagashima K, Minatoguchi S, Fujiwara T & Fujiwara H (2008) Morphological and biochemical characterization of basal and starvation-induced autophagy in isolated adult rat cardiomyocytes. *Am J Physiol Heart Circ Physiol* **295**, H1599-1607.

Mathers CD & Loncar D (2006) Projections of global mortality and burden of disease from 2002 to 2030. *PLoS Med* **3**, e442.

Matsui Y, Takagi H, Qu X, Abdellatif M, Sakoda H, Asano T, Levine B & Sadoshima J (2007) Distinct roles of autophagy in the heart during ischemia and reperfusion: roles of AMP-activated protein kinase and Beclin 1 in mediating autophagy. *Circ Res* **100**, 914-922.

- Mersmann J, Zacharowski PA, Schmitz I & Zacharowski K (2008) Caspase inhibitor zVAD.fmk reduces infarct size after myocardial ischaemia and reperfusion in rats but not in mice. *Resuscitation* **79**, 468-474.
- Metzler B, Hu Y, Sturm G, Wick G & Xu Q (1998) Induction of mitogen-activated protein kinase phosphatase-1 by arachidonic acid in vascular smooth muscle cells. *J Biol Chem* **273**, 33320-33326.
- Morisco C, Marrone C, Trimarco V, Crispo S, Monti MG, Sadoshima J & Trimarco B (2007) Insulin resistance affects the cytoprotective effect of insulin in cardiomyocytes through an impairment of MAPK phosphatase-1 expression. *Cardiovasc Res* **76**, 453-464.
- Muda M, Theodosiou A, Rodrigues N, Boschert U, Camps M, Gillieron C, Davies K, Ashworth A & Arkininstall S (1996) The dual specificity phosphatases M3/6 and MKP-3 are highly selective for inactivation of distinct mitogen-activated protein kinases. *J Biol Chem* **271**, 27205-27208.
- Murphy E & Steenbergen C (2008) Mechanisms underlying acute protection from cardiac ischemia-reperfusion injury. *Physiol Rev* **88**, 581-609.
- Murry CE, Jennings RB & Reimer KA (1986) Preconditioning with ischemia: a delay of lethal cell injury in ischemic myocardium. *Circulation* **74**, 1124-1136.

- Neufeld TP (2007) Contribution of Atg1-dependent autophagy to TOR-mediated cell growth and survival. *Autophagy* **3**, 477-479.
- Neumar RW (2000) Molecular mechanisms of ischemic neuronal injury. *Ann Emerg Med* **36**, 483-506.
- Nishida K, Kyoji S, Yamaguchi O, Sadoshima J & Otsu K (2009) The role of autophagy in the heart. *Cell Death Differ* **16**, 31-38.
- Nishida K, Yamaguchi O & Otsu K (2008) Crosstalk between autophagy and apoptosis in heart disease. *Circ Res* **103**, 343-351.
- Ogata M, Hino S, Saito A, Morikawa K, Kondo S, Kanemoto S, Murakami T, Taniguchi M, Tani I, Yoshinaga K, Shiosaka S, Hammarback JA, Urano F & Imaizumi K (2006) Autophagy is activated for cell survival after endoplasmic reticulum stress. *Mol Cell Biol* **26**, 9220-9231.
- Ogier-Denis E, Pattingre S, El Benna J & Codogno P (2000) Erk1/2-dependent phosphorylation of Galpha-interacting protein stimulates its GTPase accelerating activity and autophagy in human colon cancer cells. *J Biol Chem* **275**, 39090-39095.
- Okamura T, Miura T, Takemura G, Fujiwara H, Iwamoto H, Kawamura S, Kimura M, Ikeda Y, Iwatate M & Matsuzaki M (2000) Effect of caspase inhibitors on myocardial infarct size and myocyte DNA fragmentation in the ischemia-reperfused rat heart. *Cardiovasc Res* **45**, 642-650.

Olivetti G, Abbi R, Quaini F, Kajstura J, Cheng W, Nitahara JA, Quaini E, Di Loreto C, Beltrami CA, Krajewski S, Reed JC & Anversa P (1997) Apoptosis in the failing human heart. *N Engl J Med* **336**, 1131-1141.

Opie LH (1991) *The heart : physiology and metabolism*, 2nd ed. New York: Raven Press.

Padilla F, Garcia-Dorado D, Agullo L, Barrabes JA, Insete J, Escalona N, Meyer M, Mirabet M, Pina P & Soler-Soler J (2001) Intravenous administration of the natriuretic peptide urodilatin at low doses during coronary reperfusion limits infarct size in anesthetized pigs. *Cardiovasc Res* **51**, 592-600.

Paglin S, Hollister T, Delohery T, Hackett N, McMahon M, Sphicas E, Domingo D & Yahalom J (2001) A novel response of cancer cells to radiation involves autophagy and formation of acidic vesicles. *Cancer Res* **61**, 439-444.

Park KJ, Lee SH, Lee CH, Jang JY, Chung J, Kwon MH & Kim YS (2009) Upregulation of Beclin-1 expression and phosphorylation of Bcl-2 and p53 are involved in the JNK-mediated autophagic cell death. *Biochem Biophys Res Commun* **382**, 726-729.

Pattingre S, Bauvy C & Codogno P (2003) Amino acids interfere with the ERK1/2-dependent control of macroautophagy by controlling the

activation of Raf-1 in human colon cancer HT-29 cells. *J Biol Chem* **278**, 16667-16674.

Pearson G, Robinson F, Beers Gibson T, Xu BE, Karandikar M, Berman K & Cobb MH (2001) Mitogen-activated protein (MAP) kinase pathways: regulation and physiological functions. *Endocr Rev* **22**, 153-183.

Peter C, Waibel M, Radu CG, Yang LV, Witte ON, Schulze-Osthoff K, Wesselborg S & Lauber K (2008) Migration to apoptotic "find-me" signals is mediated via the phagocyte receptor G2A. *J Biol Chem* **283**, 5296-5305.

Robinson MJ & Cobb MH (1997) Mitogen-activated protein kinase pathways. *Curr Opin Cell Biol* **9**, 180-186.

Sack MN & Yellon DM (2003) Insulin therapy as an adjunct to reperfusion after acute coronary ischemia: a proposed direct myocardial cell survival effect independent of metabolic modulation. *J Am Coll Cardiol* **41**, 1404-1407.

Saelens X, Festjens N, Vande Walle L, van Gurp M, van Loo G & Vandenberghe P (2004) Toxic proteins released from mitochondria in cell death. *Oncogene* **23**, 2861-2874.

- Samara C, Syntichaki P & Tavernarakis N (2008) Autophagy is required for necrotic cell death in *Caenorhabditis elegans*. *Cell Death Differ* **15**, 105-112.
- Sandberg EM, Ma X, VonDerLinden D, Godeny MD & Sayeski PP (2004) Jak2 tyrosine kinase mediates angiotensin II-dependent inactivation of ERK2 via induction of mitogen-activated protein kinase phosphatase 1. *J Biol Chem* **279**, 1956-1967.
- Savill J (2000) Apoptosis in resolution of inflammation. *Kidney Blood Press Res* **23**, 173-174.
- Scherz-Shouval R, Shvets E, Fass E, Shorer H, Gil L & Elazar Z (2007) Reactive oxygen species are essential for autophagy and specifically regulate the activity of Atg4. *EMBO J* **26**, 1749-1760.
- Schuler M & Green DR (2001) Mechanisms of p53-dependent apoptosis. *Biochem Soc Trans* **29**, 684-688.
- Seger R & Krebs EG (1995) The MAPK signaling cascade. *FASEB J* **9**, 726-735.
- Silva MT, do Vale A & dos Santos NM (2008) Secondary necrosis in multicellular animals: an outcome of apoptosis with pathogenic implications. *Apoptosis* **13**, 463-482.

Sivaprasad U & Basu A (2008) Inhibition of ERK attenuates autophagy and potentiates tumour necrosis factor-alpha-induced cell death in MCF-7 cells. *J Cell Mol Med* **12**, 1265-1271.

Slee EA, Adrain C & Martin SJ (2001) Executioner caspase-3, -6, and -7 perform distinct, non-redundant roles during the demolition phase of apoptosis. *J Biol Chem* **276**, 7320-7326.

Sodi-Pallares D, Testelli MR, Fishleder BL, Bisteni A, Medrano GA, Friedland C & De Micheli A (1962) Effects of an intravenous infusion of a potassium-glucose-insulin solution on the electrocardiographic signs of myocardial infarction. A preliminary clinical report. *Am J Cardiol* **9**, 166-181.

Stern ST, Zolnik BS, McLeland CB, Clogston J, Zheng J & McNeil SE (2008) Induction of autophagy in porcine kidney cells by quantum dots: a common cellular response to nanomaterials? *Toxicol Sci* **106**, 140-152.

Suzuki K, Kostin S, Person V, Elsasser A & Schaper J (2001) Time course of the apoptotic cascade and effects of caspase inhibitors in adult rat ventricular cardiomyocytes. *J Mol Cell Cardiol* **33**, 983-994.

Takagi H, Matsui Y & Sadoshima J (2007) The role of autophagy in mediating cell survival and death during ischemia and reperfusion in the heart. *Antioxid Redox Signal* **9**, 1373-1381.

- Takano S, Fukuyama H, Fukumoto M, Hirashimizu K, Higuchi T, Takenawa J, Nakayama H, Kimura J & Fujita J (1995) Induction of CL100 protein tyrosine phosphatase following transient forebrain ischemia in the rat brain. *J Cereb Blood Flow Metab* **15**, 33-41.
- Takemura G & Fujiwara H (2006) Morphological aspects of apoptosis in heart diseases. *J Cell Mol Med* **10**, 56-75.
- Tanaka N, Kamanaka M, Enslen H, Dong C, Wysl M, Davis RJ & Flavell RA (2002) Differential involvement of p38 mitogen-activated protein kinase kinases MKK3 and MKK6 in T-cell apoptosis. *EMBO Rep* **3**, 785-791.
- Tartaglia LA, Ayres TM, Wong GH & Goeddel DV (1993) A novel domain within the 55 kd TNF receptor signals cell death. *Cell* **74**, 845-853.
- Thorburn A (2008) Apoptosis and autophagy: regulatory connections between two supposedly different processes. *Apoptosis* **13**, 1-9.
- Tobiume K, Matsuzawa A, Takahashi T, Nishitoh H, Morita K, Takeda K, Minowa O, Miyazono K, Noda T & Ichijo H (2001) ASK1 is required for sustained activations of JNK/p38 MAP kinases and apoptosis. *EMBO Rep* **2**, 222-228.

- Ullman E, Fan Y, Stawowczyk M, Chen HM, Yue Z & Zong WX (2008) Autophagy promotes necrosis in apoptosis-deficient cells in response to ER stress. *Cell Death Differ* **15**, 422-425.
- Vandenabeele P, Declercq W & Berghe TV (2008) Necrotic cell death and 'necrostatins': now we can control cellular explosion. *Trends Biochem Sci* **33**, 352-355.
- Vicencio JM, Galluzzi L, Tajeddine N, Ortiz C, Criollo A, Tasdemir E, Morselli E, Ben Younes A, Maiuri MC, Lavandro S & Kroemer G (2008) Senescence, apoptosis or autophagy? When a damaged cell must decide its path--a mini-review. *Gerontology* **54**, 92-99.
- Virchow RLK (1858) *Die Cellularpathologie in ihrer Begründung auf physiologische und pathologische Gewebelehre*. Berlin,: Hirschwald.
- Vogt A, McDonald PR, Tamewitz A, Sikorski RP, Wipf P, Skoko JJ, 3rd & Lazo JS (2008) A cell-active inhibitor of mitogen-activated protein kinase phosphatases restores paclitaxel-induced apoptosis in dexamethasone-protected cancer cells. *Mol Cancer Ther* **7**, 330-340.
- Vogt A, Tamewitz A, Skoko J, Sikorski RP, Giuliano KA & Lazo JS (2005) The benzo[c]phenanthridine alkaloid, sanguinarine, is a selective, cell-active inhibitor of mitogen-activated protein kinase phosphatase-1. *J Biol Chem* **280**, 19078-19086.

Vollmer W (2006) The prokaryotic cytoskeleton: a putative target for inhibitors and antibiotics? *Appl Microbiol Biotechnol* **73**, 37-47.

vom Dahl S, Dombrowski F, Schmitt M, Schliess F, Pfeifer U & Haussinger D (2001) Cell hydration controls autophagosome formation in rat liver in a microtubule-dependent way downstream from p38MAPK activation. *Biochem J* **354**, 31-36.

Wang G, Liem DA, Vondriska TM, Honda HM, Korge P, Pantaleon DM, Qiao X, Wang Y, Weiss JN & Ping P (2005) Nitric oxide donors protect murine myocardium against infarction via modulation of mitochondrial permeability transition. *Am J Physiol Heart Circ Physiol* **288**, H1290-1295.

Wang SH, Shih YL, Ko WC, Wei YH & Shih CM (2008) Cadmium-induced autophagy and apoptosis are mediated by a calcium signaling pathway. *Cell Mol Life Sci* **65**, 3640-3652.

Wang X, Matta R, Shen G, Nelin LD, Pei D & Liu Y (2006) Mechanism of triptolide-induced apoptosis: Effect on caspase activation and Bid cleavage and essentiality of the hydroxyl group of triptolide. *J Mol Med* **84**, 405-415.

Wei Y, Sinha S & Levine B (2008) Dual role of JNK1-mediated phosphorylation of Bcl-2 in autophagy and apoptosis regulation. *Autophagy* **4**, 949-951.

- Weston CR & Davis RJ (2007) The JNK signal transduction pathway. *Curr Opin Cell Biol* **19**, 142-149.
- Wu GS (2004) The functional interactions between the p53 and MAPK signaling pathways. *Cancer Biol Ther* **3**, 156-161.
- Wu JJ & Bennett AM (2005) Essential role for mitogen-activated protein (MAP) kinase phosphatase-1 in stress-responsive MAP kinase and cell survival signaling. *J Biol Chem* **280**, 16461-16466.
- Wu W, Chaudhuri S, Brickley DR, Pang D, Karrison T & Conzen SD (2004) Microarray analysis reveals glucocorticoid-regulated survival genes that are associated with inhibition of apoptosis in breast epithelial cells. *Cancer Res* **64**, 1757-1764.
- Xu Y, Kim SO, Li Y & Han J (2006) Autophagy contributes to caspase-independent macrophage cell death. *J Biol Chem* **281**, 19179-19187.
- Yamaguchi O, Higuchi Y, Hirotani S, Kashiwase K, Nakayama H, Hikoso S, Takeda T, Watanabe T, Asahi M, Taniike M, Matsumura Y, Tsujimoto I, Hongo K, Kusakari Y, Kurihara S, Nishida K, Ichijo H, Hori M & Otsu K (2003) Targeted deletion of apoptosis signal-regulating kinase 1 attenuates left ventricular remodeling. *Proc Natl Acad Sci U S A* **100**, 15883-15888.

- Yan L, Vatner DE, Kim SJ, Ge H, Masurekar M, Massover WH, Yang G, Matsui Y, Sadoshima J & Vatner SF (2005) Autophagy in chronically ischemic myocardium. *Proc Natl Acad Sci U S A* **102**, 13807-13812.
- Yang H & Wu GS (2004) p53 Transactivates the phosphatase MKP1 through both intronic and exonic p53 responsive elements. *Cancer Biol Ther* **3**, 1277-1282.
- Yang LY, Wu KH, Chiu WT, Wang SH & Shih CM (2009) The cadmium-induced death of mesangial cells results in nephrotoxicity. *Autophagy* **5**, 571-572.
- Yang YP, Liang ZQ, Gu ZL & Qin ZH (2005) Molecular mechanism and regulation of autophagy. *Acta Pharmacol Sin* **26**, 1421-1434.
- Yorimitsu T & Klionsky DJ (2005) Autophagy: molecular machinery for self-eating. *Cell Death Differ* **12 Suppl 2**, 1542-1552.
- Yu B, Poirier LA & Nagy LE (1999) Mobilization of GLUT-4 from intracellular vesicles by insulin and K(+) depolarization in cultured H9c2 myotubes. *Am J Physiol* **277**, E259-267.
- Yu L, Wan F, Dutta S, Welsh S, Liu Z, Freundt E, Baehrecke EH & Lenardo M (2006) Autophagic programmed cell death by selective catalase degradation. *Proc Natl Acad Sci U S A* **103**, 4952-4957.

Yue TL, Wang C, Gu JL, Ma XL, Kumar S, Lee JC, Feuerstein GZ, Thomas H, Maleeff B & Ohlstein EH (2000) Inhibition of extracellular signal-regulated kinase enhances Ischemia/Reoxygenation-induced apoptosis in cultured cardiac myocytes and exaggerates reperfusion injury in isolated perfused heart. *Circ Res* **86**, 692-699.

Zhang W & Liu HT (2002) MAPK signal pathways in the regulation of cell proliferation in mammalian cells. *Cell Res* **12**, 9-18.

Zhu W, Zou Y, Aikawa R, Harada K, Kudoh S, Uozumi H, Hayashi D, Gu Y, Yamazaki T, Nagai R, Yazaki Y & Komuro I (1999) MAPK superfamily plays an important role in daunomycin-induced apoptosis of cardiac myocytes. *Circulation* **100**, 2100-2107.

Zong WX, Ditsworth D, Bauer DE, Wang ZQ & Thompson CB (2004) Alkylating DNA damage stimulates a regulated form of necrotic cell death. *Genes Dev* **18**, 1272-1282.

Zong WX & Thompson CB (2006) Necrotic death as a cell fate. *Genes Dev* **20**, 1-15.

Zordoky BN & El-Kadi AO (2007) H9c2 cell line is a valuable in vitro model to study the drug metabolizing enzymes in the heart. *J Pharmacol Toxicol Methods* **56**, 317-322.

Zorzano A, Sevilla L, Camps M, Becker C, Meyer J, Kammermeier H, Munoz P, Guma A, Testar X, Palacin M, Blasi J & Fischer Y (1997) Regulation of glucose transport, and glucose transporters expression and trafficking in the heart: studies in cardiac myocytes. *Am J Cardiol* **80**, 65A-76A.

Appendix A

Bradford protein determination

Preparation of cells lysates from monolayers:

The entire procedure was done on ice. Eppendorfs were marked and placed on ice.

Treatment medium was removed from the cells. The cells were then washed twice with room temperature sterile PBS. RIPA buffer, pH 7.4 (see appendix B, P207). (60 μ l/3 cm well, 250 μ l/6 cm well, 600 μ l/10 cm well) was added to each well and allowed to stand for 10 minutes at 4°C (on ice). However, when MKP-1 induction was evaluated a phosphatase lysis buffer (see appendix B, P206) was used instead of RIPA buffer.

The cells were then scraped, with a sterile scraper, from the base of the dish. They were transferred to the marked eppendorfs using a micropipette. The wells were washed with RIPA buffer or appropriate lysis buffer again (40 μ l/3 cm well, 125 μ l/6 cm well, 400 μ l/10 cm well) and added to the previously collected lysates.

Pre-Bradford procedure:

The entire procedure was done on ice. Eppendorfs containing lysates were placed on ice. New eppendorfs were marked and placed on ice.

Sonication was performed on the lysates to disrupt cell membranes, so that the cell contents can be released. The sonicator was washed before every sonication. The contents were transferred to the newly marked eppendorfs and placed back on ice.

Eppendorfs were centrifuged in a pre-cooled (0-4°C) centrifuge, at 8000 rpm for 10 minutes. The supernatant containing the cell contents, were decanted into new eppendorfs that have been on ice. The pellet was discarded. The lysates were stored at -80°C or continued with in the Bradford protein quantification preparation immediately.

Bradford protein determination technique:

Protein concentration was determined by the Bradford method (Bradford, 1976).

Bradford reagent stock was prepared from 500 mg Coomassie Brilliant blue G diluted in 250 ml 95% ethanol and 500 ml phosphoric acid. This was mixed thoroughly. This mixture was then made up to 1 litre with distilled water. It was then filtered and stored at 4°C.

A Bradford working solution was made by diluting the stock solution with distilled water in a 1:5 ratio (10 ml Bradford stock/40 ml distilled water). This working solution was filtered through 2 filter papers.

1mg/ml BSA solution was thawed. Lysates were also thawed if they were frozen at -80°C. Lysates were kept on ice. A working solution of 100 µl

BSA:400 μ l distilled water was made up and vortexed. Eppendorfs were marked for standards and for samples.

BSA and distilled water were added to eppendorfs as follows, for the standard curve:

Table A1

Blank:	0 μ l BSA	100 μ l distilled water
2 μl protein:	10 μ l BSA	90 μ l distilled water
4 μl protein:	20 μ l BSA	80 μ l distilled water
8 μl protein:	40 μ l BSA	60 μ l distilled water
12 μl protein:	60 μ l BSA	40 μ l distilled water
16 μl protein:	80 μ l BSA	20 μ l distilled water
20 μl protein:	100 μ l BSA	0 μ l distilled water

5 μ l of each sample was added to 95 μ l distilled water in marked eppendorfs, on ice.

All the tubes were vortexed. 900 μ l Bradford working solution was added to each eppendorf and vortexed again. These were incubated at room temperature for 5 minutes. Absorbencies were read twice for each sample, at 595 nm. If the sample values fell outside the range of the standard curve, the samples had to be diluted with RIPA buffer or appropriate lysis buffer and read again at 595 nm.

A linear plot of the absorbencies was created and this was used to calculate the amount of each sample that had to be added to aliquots for sample preparation.

Sample preparation:

Laemmli sample buffer containing 850 μ l Laemmli sample buffer and 150 μ l mercaptoethanol was prepared and vortexed. This stock solution was added to samples, equal to 1/3 of the final. Appropriate amounts of samples, as calculated in the previous step, were added to the correct eppendorfs.

All samples were then boiled for 5 minutes, vortexed briefly and centrifuged for 5 seconds with a tabletop centrifuge. Samples were then stored at -80°C or used for western blot analysis immediately.

If samples were stored at -80°C they were thawed in boiling water for 5 minutes. Each tube was vortexed and centrifuged for 20 seconds on a tabletop centrifuge. Samples could then be used for western blot analysis.

Western blot analysis

Cell lysates were separated on 10% or 12% polyacrylamide gels, depending on the molecular weight of the protein being probed for, by sodium dodecyl sulphate polyacrylamide gel electrophoresis (SDS-PAGE).

Polyacrylamide gels were made according to the following recipes:

Table A2: **10% gels (2 gels):**

Distilled water	3.85 ml
1.5 M Tris-HCl pH 8.8	2.5 ml
10% SDS (stock)	100 μ l
10% Ammonium persulphate (APS) (Sigma-Aldrich, South Africa) (0.1 g/ml)	20 μ l
Acrylamide 40% (Promega, South Africa)	2.5 ml
N, N, N, N'-Tetramethylethylenediamin (TEMED)	5 μ l

Table A3: **12% gels (2 gels):**

Distilled water	3.35 ml
1.5 M Tris-HCl pH 8.8	2.5 ml
10% SDS (stock)	100 μ l
10% APS (0.1 g/ml)	50 μ l
Acrylamide 40%	3 ml
TEMED	5 μ l

APS and temed were added immediately before gels were poured into gels stands for setting. This is because APS and temed initiate polymerization and allow for the gel to set. Gels were then allowed to set for 1 hour in the glass gel stands with a layer of isobutanol added on top of the gel to ensure the gel set straight. After the gel had set, the isobutanol was washed off with distilled water.

4% stacking gel was made up as follows:

Table A4: 4% stacking gel (2 gels)

Distilled water	3.05 ml
1.5 M Tris-HCl pH 6.8	1.25 ml
10% SDS (stock)	50 μ l
10% APS (0.1 g/ml)	50 μ l
Acrylamide 40%	500 μ l
TEMED	10 μ l

This 4% gel was added to the top of the previously set gels and combs were pushed into the gel to allow for wells to set so that the samples could be loaded. This gel was allowed to set for 30 minutes. After the stacking gel had set, the combs were removed.

The gels were then placed in running buffer. A prestained protein marker (peqGOLD) was loaded in one well on each gel to verify molecular weights of protein bands. Samples were also added to respective wells on the gels. These were then allowed to run through the 4% gel for 10 minutes at 100 V and 400 mA, and thereafter through the 10% or 12% gel at 200 V for 50 minutes (Mini Protean System, Bio-Rad, Hercules), in running buffer*.

After SDS-PAGE proteins were transferred to polyvinylidene fluoride (PVDF) membranes (Immobilon, Millipore, USA) in a semi-dry system (BIORAD PowerPac HCTM), in blotting buffer* for 1 hour at 0.5 A and 15 V.

Thereafter membranes were blocked in 5% (w/v) non-fat dried milk powder in Tris Buffered Saline-Tween20 (TBS-T, 0.05%)* for 1 to 2 hours at room temperature. This prevents non-specific binding of proteins.

Membranes were then washed three times in TBS-T for 5 minutes each, with agitation, before incubation with primary antibodies, against the desired proteins (table A5). Primary antibodies were diluted in TBS-T. Membranes were incubated with primary antibodies overnight at 4°C.

Following 3 wash steps of 5 minutes each, in TBS-T, the membranes were incubated, at room temperature, in anti-rabbit horseradish peroxidase-conjugated secondary antibody (Amersham Life Sciences) for 1 hour. After this incubation period membranes were again washed 3 times (5 minutes each) in TBS-T.

An enhanced chemiluminescence (ECL) kit (Amersham Biosciences) was used to detect antibodies. Protein bands were visualised with x-ray film (Hyperfilm, Amersham Biosciences). Exposure times differed between antibodies used (table A5).

Bands were then quantified with the use of densitometry using the UN-SCAN-IT© program (Silk Scientific Corporation, Utah, USA).

Table A5:Primary antibodies

Primary antibody	Molecular weight (kDa)	Company	Dilution (in TBS-Tween)	ECL exposure time
Beta actin	45	Cell Signaling	1/1000	5 min
Beclin-1	56	Cell Signaling	1/1000	5 min
Caspase-3	35	Cell Signaling	1/1000	5 min
Cleaved caspase-3	17 & 19	Cell Signaling	1/1000	5 min
Cleaved PARP	89	Cell Signaling	1/1000	3 min
ERK	42, 44	Cell Signaling	1/1000	3 min
JNK	46 & 54	Cell Signaling	1/1000	15 min
LC-3	17 & 19	Nano Tools	1/1000	5 min
MKP-1	40	Santa-Cruz Biotechnology	1/500	15 min
PARP	116	Cell Signaling	1/1000	5 min
p-ERK	42, 44	Cell Signaling	1/1000	3 min
p-JNK	46 & 54	Cell Signaling	1/1000	15 min
p-p38 MAPK	38	Cell Signaling	1/1000	5 min
p38 MAPK	38	Cell Signaling	1/1000	5 min

Table A6: secondary antibodies

Secondary antibody	Company	Dilution (in TBS-Tween)
ECL Anti-rabbit IgG, Horseradish peroxidase linked whole antibody	Amersham Life Science	1/4000
Peroxidase labelled anti-mouse antibody	Amersham Life Science	1/4000

MTT assay

A 1% Isopropanol solution containing 1 ml concentrated HCl and 99 ml Isopropanol was made. A 0.1% Triton solution containing 0.1 ml Triton-X-100 was made up to 100 ml with distilled water. A Isopropanol/Triton solution was made in a 50:1 ratio, where 50 ml 1% Isopropanol was added to 1 ml 0.1% Triton. 1% MTT (0.01 g/1 ml PBS) solution was made up just before use. This solution was covered with foil to avoid light exposure. It was then filtered, through a 0.2 µm filter, to remove undissolved granules.

Treatment medium was removed from cells. The cells were not rinsed with PBS as they cells might loosen from the base of the culture dish. 1.5 ml PBS and 500 µl MTT solution was slowly added to each well, so that cells did not loosen. The plate was covered with foil and incubated for 2 hours.

If some cells had loosened the contents of the plates were transferred to 2 ml centrifuge tubes and spun down gently for 2 min at 1000 rpm. The supernatant was discarded and 2 ml Isopropanol/Triton solution was added to each pellet. Cells were then resuspended. The resuspended solution was added back into the original wells.

If no cells had loosened the contents of the wells were removed. 2 ml Isopropanol/Triton solution was added to each well. Plates were then covered in foil.

The plates were then put on a shaker to mix for 5 minutes to allow the cells to loosen from the bottom of the wells. The contents of each wells was transferred to 2 ml eppendorf tubes. These were centrifuged for 2 minutes at 1400 rpm. The absorbance values of the supernatant were read at 540 nm using a spectrophotometer. The Isopropanol/Triton solution was used as a blank.

If any of the absorbance readings was more than 1, the supernatant was diluted with the Isopropanol/Triton solution and read at 540 nm again.

Lowry protein determination

Protein concentrations was determined by the Lowry method (Lowry *et al.*, 1951).

Albumin was used as a standard protein concentration. Working solutions of different concentrations albumin made from a 0.5 M NaOH (20 g NaOH/1000 ml distilled H₂O) as follows:

Table A7

<u>Albumin (0.5 g/10 ml)</u>	<u>0.5 M NaOH</u>	
1 ml	100 ml	=1:100 (Std 3)
0.5 ml	100 ml	=1:200 (Std 2)
0.5 ml	200 ml	=1:400 (Std 1)

Albumin concentrations were then determined by spectrophotometrical reading at 280 nm (UV), with distilled H₂O used as a blank.

A cold NaK-Tartrate-CuSO₄ solution containing: 49ml 2% Na₂CO₃, 0.5 ml 1% CuSO₄.5H₂O and 0.5 ml 2% NaK-Tartrate was made. 1 ml of this solution was added to the following groups in 15 sec intervals:

- 1x 50 µl 0.5 M NaOH as blank
- 3x 50 µl std 1, 2 and 3
- 2x sample lysate

After 10 min 100 µl cold 1:3 Folin Ciocult:distilled H₂O solution was added to the above mentions samples in 15 sec intervals. After 30 min the absorbencies were measured at 750 nm, using 0.5 M NaOH as the blank.

Appendix B

Growth Medium

- 500 ml Dulbecco's Modified Eagles Medium (DMEM)
- 56 ml Fetal Bovine Serum (FBS)
- 5.6 ml Penstrep

X1 Phosphate Buffer Saline (PBS)-2 L

Dissolve the following in 1 L of water

- 16 g NaCl
- 0.4 g KCl
- 2.88 g Na₂HPO₄ (di Sodium hydrogen phosphate)
- 0.48 g KH₂PO₄ (potassium dihydrogen phosphate)

Adjust pH to 7.4, fill up to the 2 L mark with distilled water and sterilize by autoclaving

MKP-1 lysis buffer (pH 7.4)

Table B1

Reagent	Final concentration
Hepes	50 mM
EDTA	10 mM
EGTA	10 mM
PMSF	1 mM
Aprotinin	1 µg/ml
Leupeptin	1 µg/ml
Triton	0.5%

This buffer was made up fresh before use and kept on ice.

RIPA buffer (100 ml)

Prepare 50 mM Tris-HCl: add 790 mg Tris to 75 ml distilled water. Add 900 mg NaCl and stir. Adjust pH to 7.4 using HCl. Pour the prepared Tris-HCl into a 100 ml beaker.

Add the following reagents in the beaker in the following order:

Table B2:

Reagent	Final concentration	Volume
NP-40	1%	10 ml
Na-deoxycholate	0.25%	2.5 ml
EDTA	1 mM	1000 µl
Phenylmethylsulfonyl Fluoride (PMSF)	1 mM	1000 µl
Leupeptin	1 µg/ml	1 µl
SBTI-1	4 µg/ml	80 µl
Benzamidine	1 mM	100 µl
Na₃VO₄	1 mM	1000 µl
NaF	1 mM	500 µl

- Add 1000 µl Triton X-1000 to the solution
- Fill up to 100 ml with distilled water
- Mix thoroughly
- Aliquot 1000 µl of RIPA buffer into eppendorf tubes and store at -20°C

BSA (Bovine serum albumin 1 mg/ml)

- For 1 ml BSA, weight out 1 mg BSA and add 1000 μ l distilled water.
- For use during Western blotting, this BSA needs to be diluted. Pipette 100 μ l from 1 mg/ml BSA in new eppendorf tube and add 400 μ l distilled water
- Vortex

Bradford Reagent (1 L)

- Add 500 mg Coomassie Brilliant Blue G and to 250 ml 95% ethanol
- Add 500 ml phosphoric acid and mix well
- Fill up to 1 L with distilled water and store at 4°C
- For use during Western blotting, this solution needs to be filtered twice and then a 1:5 dilution is made

3X Sample buffer

- Measure 33.3 ml stacking Tris (0.5 M) and place in a beaker
- Add 8.8 g SDS and 20 g glycerol
- Add a pinch of Bromo-phenol blue to the mixture
- Fill up to 75.47 ml with distilled water

Tris pH 8.8 (500 ml)

- Add 68.1 g Tris (1.124 M) and 1.5g SDS (0.3%) to 400 ml distilled water, stir and then adjust pH using HCL
- Add distilled water to make the final volume to 500 ml

Tris pH 6.8 (500 ml)

- Add 30.3 g Tris (0.5 M) and 2 g SDS (0.4%) to 400 ml distilled water, stir and then adjust pH using HCL
- Add distilled water to make the final volume to 500 ml

Tris pH 6.8 (100 ml) for Sample buffer

- Add 6.06 g Tris (0.5M) and 4 ml 10% SDS to 80 ml distilled water, stir and then adjust pH using HCL
- Add distilled water to make the final volume to 100 ml

10% Sodium dodecyl sulphate (SDS 500ml)

- Weight out 50 g SDS and add 500 ml distilled water

10% Ammonium persulphate (1000 µl)

- Weight out 0.1 g APS into an eppendorf tube and add 1000 µl distilled water

Running buffer (1L)

- Add 3.03g Tris, 1.44g Glycine and 1g SDS to 500ml distilled water and stir until dissolved.
- Fill up to 1L with distilled water
- Add 100 ml 100% methanol and fill up to 500 ml with distilled water

10X TBS (5L)

- Add 121 g Tris and 80 g NaCl to 2.5 L distilled water and stir until dissolved.
- Adjust pH to 7.6 using HCl and then fill up to 5 L with distilled water
- For use in Western blotting, take a 1 L measuring cylinder and add 100 ml 10X TBS and dilute with 900ml distilled water
- To make **TBST**, add 1 ml tween to 1 L 1X TBS

Milk blocking solution (100ml)

- Add 5 g non fat dry instant milk powder to 100ml TBST and mix well.

0.2 M NaOH stripping buffer (1 L)

- Weigh out 8 g NaOH. Add 1 L distilled water. Mix well.

Appendix C

Reagent	Catalogue number	Company
Acrylamide	A3699	Sigma
Acridine Orange	212536	Sigma
Ammonium Persulphate (APS)	A3678	Sigma
Aprotinin	A6103	Sigma
Paper (Blotting) Sheets	06-134	Lasec
10X Blotting buffer	161-0771	BioRad
Bovine Serum Albumin (BSA)	A4503	Sigma
Bradford Reagent	B6916	Sigma
Bromophenol Blue	32400A	UnivAR
Coomassie Brilliant Blue	G 27815	Fluka
Cytotoxicity Detection Kit ^{PLUS} (LDH)	04 744 926 001	Roche
Dulbecco's Modified Eagles medium (DMEM)	D5796	Sigma
ECL TM Western Blotting analysis system	RPN2108	Amersham Biosciences
EDTA	2236020	UNIVAR
EGTA	E-4378	Sigma
Fetal Bovine Serum	CN3255	Highveld Biological
Glycerol	G5516	UnivAR

Glycine	G8898	Sigma
Hoechst 33342	B2261	Sigma
Hyperfilm	28-9068-36	Amersham Biosciences
Immobilon™ P transfer membrane (PVDF)	I PVH00010	Millipore
Insulin	I9278	Sigma
Iso-butanol	UN1212	Merck
Isopropanol	31, 461-1	Sigma
Leupeptin	H8511	Sigma
L-glutamine	G7513	Sigma
LysoTracker® Red DND-99	L-7528	Molecular Probes (Invitrogen)
Manual X-ray Developer	9X23018	Axim
Manual X-ray Fixative	9X23013	Axim
Methanol	UN1250	Merck
MTT	M5655-16	Sigma
PeqGold prestained protein marker	27-2110	Peqlab
Penstrep	214	Highveld Biological
Phenol solution	P5447	Sigma
PMSF	10 837 091 001	Roche
Ponceau S solution	P7170	Sigma
Propidium Iodide	P4170	Sigma
Sanguinarine chloride	84480	Sigma

Sodium deoxycholate	D6750	Sigma
Sodium Dodecyl Sulphate (SDS)	L3771	Sigma
Sodium orthovanadate (Na ₃ VO ₄)	S6508	Sigma
Temed	T9281	Sigma
Triptolide	PG490	Pharmagenesis
Triton X-100	X-100	Sigma
Trypsin	T4174	Sigma
Tween 20	P5927	Sigma